UNIVERSIDADE FEDERAL DO CEARÁ
CENTRO DE CIÊNCIAS
DEPARTAMENTO DE BIOQUÍMICA E BIOLOGIA MOLECULAR
PROGRAMA DE PÓS-GRADUAÇÃO EM BIOQUÍMICA

YUGO LIMA-MELO

CONSEQUENCES OF PHOTOINHIBITION OF PHOTOSYSTEM I ON PHOTOSYNTHETIC ELECTRON TRANSPORT AND CARBON METABOLISM

FORTALEZA
2019

YUGO LIMA-MELO

CONSEQUENCES OF PHOTOINHIBITION OF PHOTOSYSTEM I ON PHOTOSYNTHETIC ELECTRON TRANSPORT AND CARBON METABOLISM

Thesis presented to the Graduate Program in Biochemistry of the Federal University of Ceará and to the Doctoral Programme in Molecular Life Sciences of the University of Turku as part of the requirements to obtain the title of Doctor in Biochemistry and Doctor of Philosophy, respectively, as a partnership agreement between both universities covering a program for the joint supervision. Field of research: Plant science.

Supervisors: Prof. Joaquim Albenísio Gomes da Silveira; Prof. Eva-Mari Aro; Dr. Peter Jared Gollan

FORTALEZA

2019

Dados Internacionais de Catalogação na Publicação
Universidade Federal do Ceará
Biblioteca Universitária

L696c Lima-Melo, Yugo.
Consequences of photoinhibition of photosystem I on photosynthetic electron transport and carbon metabolism / Yugo Lima-Melo. – 2019.
117 f. : il. color.

Tese (Doutorado em Bioquímica) - Universidade Federal do Ceará, Centro de Ciências, Programa de Pós-Graduação em Bioquímica, Fortaleza, 2019.
Orientação: Prof. Dr. Joaquim Albenísio Gomes da Silveira, Profa. Dra. Eva-Mari Aro e Dr. Peter Jared Gollan.
A tese é resultado de um acordo de parceria (DOU, seção 3, n. 122, p. 65, 27 de junho 2018, ISSN 1677-7069) entre a University of Turku (Finlândia) e a Universidade Federal do Ceará (Brasil).
Participaram da aprovação da tese no exterior: Prof. Luís Mauro Gonçalves Rosa (Universidade Federal do Rio Grande do Sul) e Dr. Peter Robert Kindgren (University of Copenhagen). Participou da banca de defesa no exterior: Profa. Åsa Strand (Umeå University). Uma versão desta tese foi também publicada pela University of Turku (ISBN 978-951-29-7715-4 / ISSN 2343-3175).

1. Photosynthesis. 2. Photoinhibition. 3. Photosystem. 4. Chloroplasts. I. Título

CDD 572

YUGO LIMA-MELO

CONSEQUENCES OF PHOTOINHIBITION OF PHOTOSYSTEM I ON PHOTOSYNTHETIC ELECTRON TRANSPORT AND CARBON METABOLISM

Thesis presented to the Graduate Program in Biochemistry of the Federal University of Ceará and to the Doctoral Programme in Molecular Life Sciences of the University of Turku as part of the requirements to obtain the title of Doctor in Biochemistry and Doctor of Philosophy, respectively, as a partnership agreement between both universities covering a program for the joint supervision. Field of research: Plant science.

Accepted on 30 Jan. 2019

OPPONENTS

_____
Prof. Dr. Joaquim Albenísio Gomes da Silveira (Orientador)
Universidade Federal do Ceará (UFC)

_____
Dr. Peter Jared Gollan
University of Turku (UTU)

_____
Prof. Dr. Cleverson Diniz Teixeira de Freitas
Universidade Federal do Ceará (UFC)

_____
Prof. Dr. Sérgio Luiz Ferreira da Silva
Universidade Federal Rural de Pernambuco (UFRPE)

_____
Dr. Fabrício Eulálio Leite Carvalho
Universidade Federal do Ceará (UFC)

ACKNOWLEDGMENTS

This study was financed in part by the Coordenação de Aperfeiçoamento de Pessoal de Nível Superior - Brasil (CAPES) - Finance Code 001. This work was also financially supported by the CAPES project BEX10758/14-3 (Brazil) and by *Centre for International Mobility* – CIMO (Finland, project TM-16-10130).

Thanks to the Federal University of Ceará (Universidade Federal do Ceará, UFC), especially to the Graduate Program in Biochemistry and the Department of Biochemistry and Molecular Biology.

Thanks to the University of Turku (UTU), especially to the Molecular Plant Biology group.

More importantly, my thesis was only possible because of the help and participation of friends, colleagues, and other important persons from both sides of the Atlantic Ocean.

I am very grateful of all my supervisors, who had key and specific participation during my PhD studies beyond the duties of a supervisor. I am very lucky for being supported by them.

Thanks to Prof Joaquim Albenísio G Silveira, for encouraging me to continue my academic studies and to look for new scientific adventures abroad; for believing in my potential; for sharing his experience and motivations with me.

Thanks to Prof Eva-Mari Aro, for promptly and kindly accepting me in her group since my very first contact by e-mail; for providing me the chance to work and study in her labs; for giving me the chance of living a dream, which was living in Finland.

Thanks to Dr Peter J Gollan, for being so attentive to my work and to my well-being; for being an excellent teacher and friend; for all the participation in this project, from planning the experiments to the writing process; for being so patient with me; for being the person he is. This work was only possible because of him.

Thanks to Prof Danilo M Daloso and Dr Mikko Tikkanen for their friendship and valuable suggestions, discussions and general participation in the background of my experiments and ideas.

Thanks to Prof Cléverson DT Freitas, Dr Fabrício EL Carvalho and Prof Sérgio LF da Silva, for accepting the role as opponents in my thesis defence in Fortaleza and for the valuable suggestions and corrections. Also, thanks to Dr Ana

Karla M Lobo and Prof José Tadeu A Oliveira for accepting the role as substitute opponents.

Thanks to Prof Åsa Strand for kindly accepting the role as my opponent in my thesis defence in Turku, which I am sure will generate a very fruitful and enjoyable discussion.

Thanks to Prof Luís Mauro G Rosa and Dr Peter R Kindgren for kindly accepting to examine my thesis, which will certainly improve the quality of my dissertation.

Thanks to the people who worked in my *cotutelle* agreement: Prof Cláudio Lucas, Sanna Ranto, Sari Järvi and Tiia Forsström. Special thanks to Prof Eevi Rintamäki, for being so patient with my questions and for taking care of my PhD studies from the Turku side.

Thanks to all the co-authors involved in the publications I participated during my PhD, especially those included in this thesis.

Thanks to all my colleagues in Fortaleza, especially those who spent more time with me and helped me somehow during my PhD: Adilton, Andrielly, Cristiano, Eliezer, Girlaine, Letícia, Marcos, Mateus, Paulo, Rikaely and Valéria. Special thanks to Ana Karla, Fabrício, Rachel, Raissa and Vicente, who had more direct participation in my PhD time and experiments.

Thanks to all my colleagues in Turku, especially those who spent some time by teaching me something or by doing me a favour (or lots of them): Anita, Anniina, Arjun, Azfar, Chus, Eveliina, Fiona, Guido, Hiroaki, Ilaria, Kurt, Maija, Marjaana R, Marjatta, Martina A, Martina J, Mika, Sara, Nagesh, Vipu, Zsófia, and others. Special thanks to Juande for tips on RNA extraction and qPCR; to Julia for tips on electrophoresis and PCR; to Sanna R for tips on Arabidopsis sowing/cultivation and for writing the *tiivistelmä* in this dissertation; to Minna K for tips on my attempt in plant transformation; to Sergey for the support with the O_2 uptake system; to Steffen for the support with Dual-PAM.

Thanks to those who had important roles in my academic career so far or somehow helped me in specific moments of my PhD time: Prof Cristiane M, Prof Josemir M, Prof Eduardo V, Prof Marcia M, Prof Evandro, Seu Roger, Rosana and Raisa Ojala.

Thanks to Tuomas Holopainen and Nightwish for being the starting point of all my adventures in Finland, when these were still a teenage dream, and for composing the soundtracks of my life.

Thanks to my long-time friends Israel, Kel, Leandro, Marvin, Michell, Sedir; Cícera, Luiz, Rassa Corts, Sabs; Fernando and Well.

Last but not least, thanks to my family, the foundation of my life. First, my parents Cristina (*Mãe*) and José Luiz (*Pai*), for being so loving, supportive, and present in my life since always. Also, thanks to all my relatives, especially my nephew Gael, my brother Yuri, my sister Yani, my grandparents *Bá* and *Vovô*, my aunt and third mom *Tia* Ana, my grandmother *Vovó Nanda*, my aunts, uncles, cousins, and brother- and sister-in-law. Finally, thanks to the one who has changed the ways of my life in the best way possible and for putting me on the right track: my beloved Ari (and our little Thor). I love you all.

Yugo

Man, he took his time in the sun,
had a dream to understand
a single grain of sand.
He gave birth to poetry,
but one day'll cease to be.
Greet the last light of the library.
We were here!

Tuomas LJ Holopainen
The Greatest Show on Earth

We are going to die, and that makes us the lucky ones.
Most people are never going to die
because they are never going to be born.
The potential people who could have been here in my place,
but who will in fact never see the light of day,
outnumber the sand grains of *Sahara*.
Certainly those unborn ghosts include greater poets than Keats,
scientists greater than Newton.
We know this because the set of possible people allowed by our DNA
so massively exceeds the set of actual people.
In the teeth of these stupefying odds, it is you and I,
in our ordinariness, that are here.
We privileged few, who won the lottery of birth against all odds.
How dare we whine at our inevitable return to that prior state
from which the vast majority have never stirred?

Richard Dawkins
Unweaving the Rainbow

There is grandeur in this view of life,
with its several powers,
having been originally breathed into a few forms or into one;
and that, whilst this planet has gone cycling
on according to the fixed law of gravity,
from so simple a beginning
endless forms most beautiful and most wonderful have been,
and are being,
evolved.

Charles Darwin
The Origin of Species

RESUMO

A fotossíntese permite que plantas estoquem energia luminosa em compostos orgânicos. Plantas têm um eficiente aparato para coletar fótons da luz solar e usar a energia para fotolisar moléculas de água e transportar elétrons para aceptores de elétrons específicos. O equilíbrio adequado entre as reações de luz e o consumo de elétrons é importante para manter a fotossíntese regulada durante as condições ambientais sob constante mudança. Ao mesmo tempo, componentes fotossintéticos precisam ser protegidos por vários mecanismos regulatórios. Evitar danos ao fotossistema I (PSI) é particularmente importante porque sua recuperação é extremamente lenta comparada à do fotossistema II (PSII). Estudos sobre danos, fotoinibição e recuperação do PSI são mais escassos do que os do fotossistema II. Nesta tese, investigou-se a ocorrência da fotoinibição do PSI e algumas de suas consequências ao metabolismo vegetal. Plantas de *Arabidopsis thaliana* L. deficientes na proteína PROTON GRADIENT REGULATION 5 (mutantes *pgr5*) tratadas em condições de excesso de luz foram utilizadas como um modelo de indução controlada de fotoinibição do PSI. Este modelo foi validado e o impacto da fotoinibição e recuperação do PSI no transporte de elétrons da fotossíntese, no metabolismo primário, na produção de espécies reativas de oxigênio (EROS) e na sinalização retrógrada do cloroplasto foram caracterizados. Os resultados mostram que a fotoinibição do PSI induz graves consequências ao metabolismo primário das plantas, especialmente sob baixas irradiâncias, incluindo danos à assimilação de CO_2, ao acúmulo de amido e à respiração mitocondrial. A recuperação da atividade do PSI após fotoinibição foi dependente das condições luminosas, sendo especialmente deletéria para a fixação do CO_2 sob baixas irradiâncias, suportando a ideia de que um grupo de PSI pode ser recrutado sob condições específicas. Plantas *pgr5* tratadas com alta luz também apresentaram baixa oxidação lipídica associada a menor síntese enzimática de oxilipinas e consequente regulação cloroplástica da expressão gênica nuclear. Este modelo também mostrou que a fotoinibição do PSI previne estresse oxidativo e acúmulo de EROS, evidenciando um papel da inativação do PSI em evitar a super-redução de componentes aceptores de elétrons.

Palavras-chave: Fotossíntese. Dano do PSI. PGR5. Assimilação de CO_2. EROS. Sinalização cloroplástica. Oxirredução do P700.

ABSTRACT

Photosynthesis allows plants to store light energy in organic compounds. Plants have an efficient apparatus to harvest photons from sunlight and use the energy to split water and transport electrons to specific high-energy electron acceptors. A proper balance between light reactions and electron consumption is important to maintain fluent photosynthetic activity during environmental conditions that are constantly changing. At the same time, photosynthetic components are protected through several regulatory mechanisms. The avoidance of damage to photosystem I (PSI) is particularly important because its recovery occurs extremely slowly as compared to that of photosystem II (PSII). Studies on damage, photoinhibition and recovery of PSI are scarcer than those of PSII. In this thesis, the occurrence of photoinhibition of PSI and some of its consequences to the plant metabolism were investigated. *Arabidopsis thaliana* L. plants lacking the PROTON GRADIENT REGULATION 5 protein (*pgr5* mutants) that were treated with excess light were used as a model system for controlled PSI-photoinhibition. This experimental model was validated, and the impact of PSI photoinhibition and recovery on photosynthetic electron transport, primary metabolism, reactive oxygen species (ROS) production and chloroplast retrograde signalling were thoroughly characterised. The results highlight that PSI photoinhibition induces impairment of CO_2 fixation, starch accumulation, and dark respiration. The recovery of PSI function after photoinhibition proved to be dependent on light conditions, being especially deleterious for CO_2 fixation under low irradiances, and supporting the idea that a pool of surplus PSI can be recruited to support photosynthesis under demanding conditions. High light-treated *pgr5* mutants also displayed low occurrence of lipid oxidation associated with attenuated enzymatic oxylipin synthesis and consequent chloroplast regulation of nuclear gene expression. This model also showed that PSI photoinhibition prevents oxidative stress and accumulation of ROS, evidencing a role of PSI inactivation in avoiding over-reduction of downstream redox components.

Keywords: Photosynthesis. PSI damage. PGR5. CO_2 assimilation. ROS. Chloroplast signalling. P700 oxidoreduction.

TIIVISTELMÄ

Fotosynteesissä kasvit muuntavat valoenergiaa kemialliseksi energiaksi, joka varastoituu erilaisiin orgaanisiin yhdisteisiin. Kasvit keräävät tehokkaasti auringon valon fotoneja, hajottavat sen avulla vesimolekyylejä ja kuljettavat elektroneja erityisille vastaanottajamolekyyleille, joiden avulla pystyvät pelkistämään ilmakehän hiilidioksidia. Näiden reaktioiden tasapainottaminen on keskeistä fotosynteettisen aktiivisuuden ylläpitämiseksi jatkuvasti muuttuvissa ympäristöolosuhteissa. Samanaikaisesti on myös suojattava fotosynteettisiä komponentteja ja näistä erityisesti fotosysteemi (PS) I:tä, koska sen palautuminen on hidasta verrattuna PSII:n nopeaan korjauskiertoon. PSI:n vauriota ja palautumista ei ole kuitenkaan tutkittu yhtä paljon kuin PSII:n fotoinhibitiota ja siksi tässä väitöskirjassa kartoitettiin PSI:n fotoinhibition esiintymisen syitä ja sen seurauksia kasvin aineenvaihduntaan. Kokeellisena mallina kontrolloidulle PSI-fotoinhibitiolle käytettiin voimakkaalla valolla käsiteltyjä *Arabidopsis thaliana* L. -kasveja, joista puuttui PROTON GRADIENT REGULATION 5 -proteiini (*pgr5*-mutantti). Malli todettiin toimivaksi ja sen avulla selvitettiin perusteellisesti PSI-fotoinhibition ja siitä palautumisen vaikutuksia fotosynteettiseen elektroninsiirtoon, aineenvaihduntaan, reaktiivisten happilajien muodostumiseen sekä kloroplastin ja tuman väliseen viestintään. Saadut tulokset osoittivat, että PSI:n fotoinhibitio häiritsee vakavasti kasvien aineenvaihduntaa erityisesti heikossa valossa aiheuttaen ongelmia CO_2:n sidontaan, tärkkelyksen kertymiseen ja soluhengitykseen. Lisäksi tutkittiin PSI:n nopeaa fotoinhibitiota ja hidasta palautumista. Tulokset viittaavat siihen, että ylimääräinen PSI, verrattuna PSII:n määrään, ylläpitää fotosynteesiä vaativissa olosuhteissa. Kirkkaalla valolla käsitellyssä *pgr5*-mutantissa lipidien hapettumisen havaittiin vähentyneen ja entsymaattisen oksilipiinisynteesin hidastuneen, minkä seurauksena myös tuman geenienekspression säätely kloroplastissa heikentyi. Malli osoitti myös, että PSI:n fotoinhibitio ei suoraan liity hapettavaan stressiin tai reaktiivisten happilajien kertymiseen, mikä todistaa, että PSI:n inaktivointi suojaa elektroninsiirtoketjun seuraavia komponentteja ylipelkistymiseltä.

Asiasanat: Fotosyntees. PSI:n vaurio. PGR5. Hiilensidonta. Reaktiiviset happilajit. Kloroplastin signalointi. P700:n hapetus-pelkistys.

LIST OF FIGURES

LIST OF ABBREVIATIONS

$^{\bullet}OH$	hydroxyl radical
$^{1}O_2$	singlet oxygen
A	net CO_2 assimilation rate
A/C_i	maximum carboxylation efficiency
ADP	adenosine diphosphate
AOX	alternative oxidase
APX	ascorbate peroxidase
ASC	ascorbate
ATP	adenosine triphosphate
bp	nucleotide base pair
CAT	catalase
C_i	internal CO_2 concentration
CSD	Cu/Zn-superoxide dismutase
Col-0	*Arabidopsis thaliana* L. ecotype Columbia-0
Cyt *b6f*	cytochrome *b6f* complex
DAB	3,3-diaminobenzidine
DHA	dehydroascorbate
DHAR	dehydroascorbate reductase
E	transpiration rate
EDTA	ethylenediaminetetraacetic acid
ETC	electron transport chain
FED	ferredoxin 2
FeS	iron-sulphur
Fd	ferredoxin
Fdm, Fdxm	maximal reduction state of ferredoxin
FL	fluctuating light
Fm	maximum chlorophyll *a* fluorescence
FNR	ferredoxin:$NADP^+$ oxidoreductase
Fo	minimum chlorophyll *a* fluorescence
FSD	Fe-superoxide dismutase
FTR	ferredoxin:thioredoxin reductase
Fv/Fm	maximum efficiency of PSII

GL	growth light (120 or 125 µmol photons m^{-2} s^{-1})
gl1	*Arabidopsis thaliana* L. ecotype Columbia glabra-1
GO	Gene Ontology
GO-BP	Gene Ontology Biological Process
GPX	glutathione peroxidase
GR	glutathione reductase
GRX	glutaredoxin
g_s	stomatal conductance rate
GSH	glutathione
GSSG	glutathione disulphide
H_2O_2	hydrogen peroxide
HL	high light (1000 µmol photons m^{-2} s^{-1})
IRGA	infra-red gas analyser
JA	jasmonic acid
KLAS	kinetic LED-array spectrophotometer
LHCI	light harvesting complex I
LHCII	light harvesting complex II
LOX	lipoxygenase
LOX-C	chloroplast lipoxygenase
MDHAR, MDAR	monodehydroascorbate reductase
MSD	Mn-superoxide dismutase
$NADP^+$	oxidised nicotinamide adenine dinucleotide phosphate
NADPH	reduced nicotinamide adenine dinucleotide phosphate
NBT	nitro-blue tetrazolium
NDH	NADH dehydrogenase-like complex
NPQ	non-photochemical quenching
$O_2^{\bullet-}$	superoxide radical
OEC	oxygen evolving process
OPDA	12-oxophytodienoic acid
P680	photosystem II reaction centre
P700	photosystem I reaction centre
PC	plastocyanin
PCm	maximum oxidation state plastocyanin
PGR5	proton gradient regulation 5

PGRL1	PGR5-like 1
Pi	inorganic phosphate
Pm	maximum oxidizable P700
pmf	proton motive force
PPFD	photosynthetic photon flux density
PQ	plastoquinone
PRX	peroxiredoxin
PSI	photosystem I
PSII	photosystem II
PTOX	plastid terminal oxidase
PVDF	polyvinylidene difluoride
qE	energy-dependent quenching
ROS	reactive oxygen species
RuBisCO	ribulose-1,5-biphosphate carboxylase/oxygenase
sAPX	stromal ascorbate peroxidase
SDS-PAGE	Na-dodecyl sulfate-polyacrylamide gel electrophoresis
SOD	superoxide dismutase
tAPX	thylakoidal ascorbate peroxidase
TBARS	thiobarbituric acid reactive substances
TRX	thioredoxin
TRX_{ox}	oxidised thioredoxin
TRX_{red}	reduced thioredoxin
WUE	water use efficiency
ΔpH	proton gradient
ΔΨ	membrane potential

TABLE OF CONTENTS

1 INTRODUCTION

1.1 Photosynthesis

Photosynthesis is vital for life as we know it, being the main source of organic compounds on Earth. Water-splitting photosynthesis also releases oxygen (O_2), making this process crucial for all aerobic life. Photosynthesis is intrinsically associated with plant productivity (RAINES, 2011) through biomass yield and allocation of assimilated carbon. Therefore, efficient photosynthesis is essential to maintain the growth and productivity of crops (SUN et al., 2009; FOYER; RUBAN; NIXON, 2017). Several studies have provided evidence to support an increase in photosynthetic capacity as a viable route to increase the yield of crop plants (LONG; MARSHALL-COLON; ZHU, 2015; CAEMMERER; FURBANK, 2016; KROMDIJK et al., 2016; SIMKIN et al., 2017; SALESSE-SMITH et al., 2018). The importance of these studies for the development of higher-yielding crop varieties is also related to the panorama of increasing food and fuel demands by the growing world population (FISCHER; EDMEADES, 2010; RAY et al., 2012; LONG; MARSHALL-COLON; ZHU, 2015; SIMKIN et al., 2017).

Photosynthesis is the process prevailing in plants and algae to convert light energy into chemical energy, which is stored as carbohydrates molecules synthesised from carbon dioxide (CO_2) and water. In plants, photosynthesis encompasses two steps: photochemistry and carbon assimilation/fixation. In the first step, chlorophyll and other photosynthetic pigments of the cell absorb light energy to produce the energy-carrier molecules ATP and NADPH. In the second step, ATP and NADPH generated from the photochemical phase are used to reduce CO_2 molecules to produce carbohydrates and their derivative products. Both steps are detailed in the following sections.

1.1.1 The photosynthetic electron transport chain

The photochemical phase of photosynthesis, also known as “light-dependent reactions” or simply “light reactions”, allows the synthesis of ATP and NADPH molecules by using energy from light. This step involves a linear electron flux, or a cyclic electron flux under specific conditions (explained in section 1.3), through a

succession of redox cofactors, most of which are housed in integral or peripheral protein complexes of the thylakoid membrane (Figure 1). First, the photons are harvested by light-harvesting pigment-protein antennae. The harvested photons excite chlorophyll pools and other accessory pigments, which transfer the energy to reaction centres in photosystem I and II (PSI and PSII, respectively). Light-harvesting complex I (LHCI) delivers excitation specifically to PSI, while light-harvesting complex II (LHCII) serves both PSII and PSI. After being excited, each photosystem reaction centre induces separation of electric charge, producing a strong electron donor and a strong electron acceptor (GOVINDJEE; SHEVELA; BJÖRN, 2017).

After photon-induced excitation through the LHCII, the PSII reaction centre chlorophyll P680 transfers electrons through a series of PSII cofactors to a plastoquinone (PQ) pool, filling the electron hole at P680 with electrons extracted from molecules of water through an oxygen-evolving complex (OEC), which also liberates O_2 and protons into the thylakoid lumen (Vinyard et al. 2013). Reduced PQ transfers electrons to the cytochrome *b6f* complex (cyt *b6f*) and becomes oxidised and available to be reduced by PSII again. The reduced cyt *b6f* donates electrons to a soluble electron carrier located in the thylakoid lumen named plastocyanin (PC). Similar to PSII, the PSI reaction centre (P700) chlorophyll is excited by light through both LHCI and LHCII (GRIECO et al., 2012, 2015; WIENTJES; VAN AMERONGEN; CROCE, 2013; RANTALA; TIKKANEN, 2018). In the case of PSI, the electrons are donated to the stromal ferredoxin (Fd) and replaced by electrons provided by the PC pool. Considering the linear electron flow, the Fd pool transfers electrons to ferredoxin-$NADP^+$ reductase, which finally allows the regeneration of $NADP^+$ to NADPH (VINYARD; ANANYEV; CHARLES DISMUKES, 2013; RUBAN, 2015; GOVINDJEE; SHEVELA; BJÖRN, 2017). The Fd pool can also donate electrons to ferredoxin-thioredoxin reductase (FTR), which allows the maintenance of the ferredoxin-dependent thioredoxin system. This system is also important for the CO_2 assimilation step by activating essential enzymes of the Calvin-Benson-Bassham (CBB) cycle (BUCHANAN, 2016; NIKKANEN; TOIVOLA; RINTAMÄKI, 2016).

In addition to the reduction of $NADP^+$, the electron flow through the thylakoid membrane is essential for the synthesis of ATP to feed the reactions of CO_2 fixation (explained in the following section). The synthesis of ATP during the light reactions is possible because of the formation of a transmembrane proton motive force (*pmf*), which is made up of the proton gradient (ΔpH) across the thylakoid membrane and the

membrane potential (ΔΨ). In the linear electron flow, the most important steps in which protons are concentrated in the thylakoid lumen in relation to the stromal side of the membrane are the splitting reaction of H_2O occurring in the PSII by its water-oxidising complex, and the electron transfer from the PQ pool to the cyt *b6f*. The chloroplastic ATP synthase makes use of the *pmf* to translocate protons from the lumen to the stroma, using the derived energy to produce ATP from ADP and inorganic phosphate.

Figure 1 – A simplified scheme of the photosynthetic electron transport chain in the thylakoid membrane and its interaction with CO_2 assimilation in the Calvin-Benson-Bassham cycle.

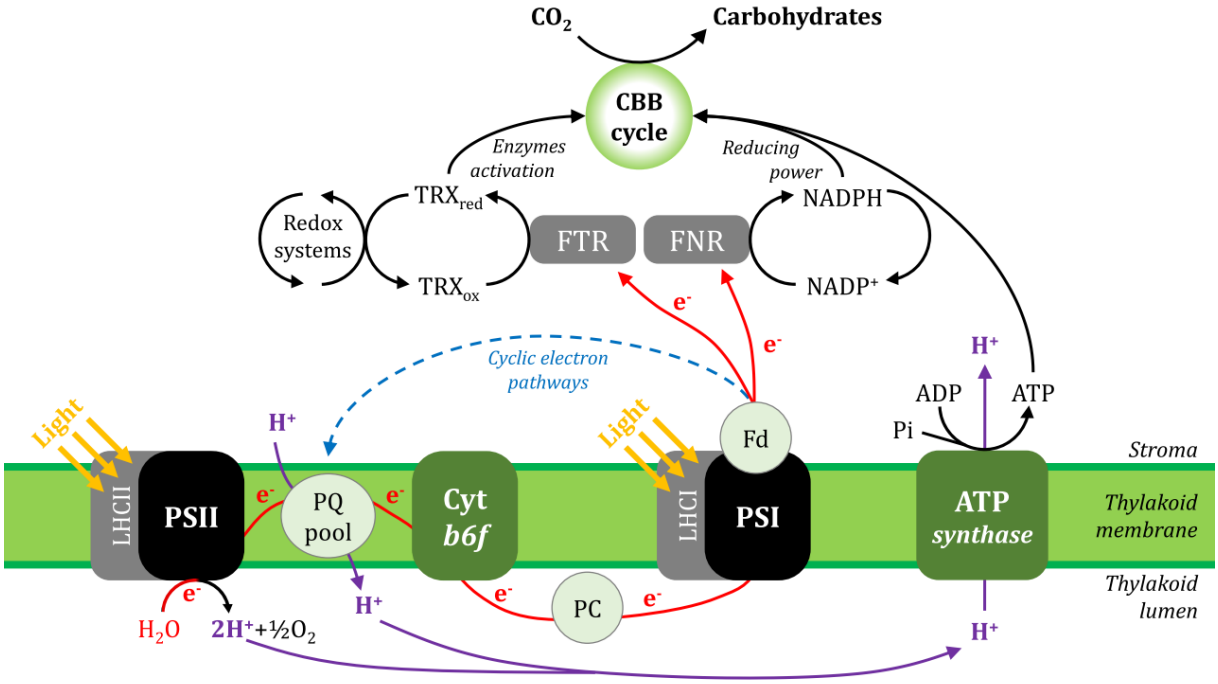

Source: the author.
Linear electron (e^-) transport is shown in red lines and cyclic electron transport is represented in a blue dashed line. The proton (H^+) fluxes are represented in purple lines. ADP = adenosine diphosphate; ATP = adenosine triphosphate; CBB cycle = Calvin-Benson-Bassham cycle; Cyt *b6f* = cytochrome *b6f*; Fd = ferredoxin; FNR = ferredoxin:$NADP^+$ oxidoreductase; FTR = ferredoxin:thioredoxin reductase; LHCI = light-harvesting complex I; LHCII = light-harvesting complex II; $NADP^+$ = oxidised nicotinamide adenine dinucleotide phosphate; NADPH = reduced nicotinamide adenine dinucleotide phosphate; PC = plastocyanin; Pi = inorganic phosphate; PQ = plastoquinone; PSI = photosystem I; PSII = photosystem II; TRX_{ox} = oxidised thioredoxin; TRX_{red} = reduced thioredoxin.

1.1.2 CO_2 assimilation and the Calvin-Benson-Bassham cycle

The diffusion of CO_2 into plant leaves is regulated by stomata. Stomatal resistance and aperture are the major limiting factors for CO_2 uptake by plants and thus for photosynthesis and plant growth (LAWSON; BLATT, 2014; WANG et al., 2014). Stomatal regulation is very sensitive to the environment, mainly in response to changes in light and relative humidity, and involves highly coordinated and dynamic signalling processes (DALOSO et al., 2017; DEVIREDDY et al., 2018). After passing through stomata, CO_2 molecules concentrate in the intercellular air space, before passing across the cell wall, plasmalemma, cytosol, and chloroplast envelope and finally reaching the stroma, where they are available to be used as a substrate for the CBB cycle (EVANS; VON CAEMMERER, 1996; EVANS et al., 2009).

ATP and NADPH molecules synthesised at the photochemical phase are used to reduce CO_2 into phosphate trioses (BENSON et al., 1950) through three steps of the CBB cycle: (1) CO_2 fixation, which is catalysed by ribulose-1,5-bisphosphate carboxylase/oxygenase (RuBisCO); (2) reduction of 3-phosphoglycerate to glyceraldehyde-3-phosphate; and (3) regeneration of ribulose-1,5-bisphosphate, which is a substrate for RuBisCO in addition to CO_2, from triose phosphate sugars. The glyceraldehyde-3-phosphate molecules generated during the second step of the cycle can be used to directly provide energy via glycolysis or serve as a substrate for synthesis of other carbohydrates with different functions, including stored energy (e.g. starch), sources of energy that are transported throughout plant tissues (e.g. sucrose), structural carbohydrates (e.g. cellulose), and signalling compounds (PAUL; FOYER, 2001; KÖLLING et al., 2015; WINGLER, 2018). For each molecule of glyceraldehyde-3-phosphate, three molecules of CO_2 are assimilated and nine molecules of ATP plus six of NADPH are consumed during each round of the cycle (BENSON et al., 1950; RAINES, 2003).

1.2 Photo-oxidative stress, photoinhibition and photoprotection

Although light energy is vital for photosynthesizing organisms, this same energy can also damage the photosynthetic apparatus in a condition named photo-oxidative stress. This condition occurs when the electron pressure in the photosynthetic electron transport chain exceeds the capacity of electron consumption

by electron sink pathways and regulation mechanisms provide insufficient protection (photoprotection is discussed in section 1.3). As a result, transient or sustained production of reactive oxygen species (ROS) develops, leading to photo-oxidation processes. Photo-oxidative conditions are usually triggered by changes in environmental conditions and lead to a phenomenon known as “photoinhibition”, which is characterised as the inactivation of the photosystems (POWLES, 1984; ARO; VIRGIN; ANDERSSON, 1993; GURURANI; VENKATESH; TRAN, 2015).

Photoinhibition negatively affects photosynthetic capacity and thus is deleterious for plant growth and crop yield (TAKAHASHI; MURATA, 2008; KATO et al., 2012; SIMKIN et al., 2017). Among the photoinhibitory conditions, light intensity is especially important since it is directly related to photon incidence on leaves. For example, high electron pressure conditions, like high light intensity and fluctuating light conditions, induce damage to the photosynthetic apparatus, leading to a photoinhibitory condition (POWLES, 1984; ARO; VIRGIN; ANDERSSON, 1993; GURURANI; VENKATESH; TRAN, 2015). In addition, photoinhibition is exacerbated by other environmental stresses (e.g. low and high temperatures, drought, salinity) through the limitation of the photosynthetic fixation of CO_2 (TAKAHASHI; MURATA, 2008). The following sections will approach the harmful and signalling properties of ROS, the occurrence of photoinhibition and mechanisms of photoprotection.

1.2.1 Reactive oxygen species as both harmful and beneficial components

ROS, including singlet oxygen ($^1O_2$), superoxide radicals ($O_2^{\bullet-}$), hydrogen peroxide (H_2O_2) and hydroxyl radicals ($^{\bullet}OH$), are reactive derivatives of molecular oxygen that are capable of oxidation of various cellular components and can cause oxidative destruction in the cell (MITTLER, 2002; APEL; HIRT, 2004; MUNNS, 2005; CZARNOCKA; KARPIŃSKI, 2018; MHAMDI; VAN BREUSEGEM, 2018). More precisely, the term “ROS” has been defined as any oxygen derivative that is more reactive than an oxygen molecule (O_2) (FOYER; NOCTOR, 2009; MITTLER, 2017; MHAMDI; VAN BREUSEGEM, 2018). Formation of ROS occurs when electrons or excitation are transferred to molecular oxygen (O_2), which takes place constantly as a by-product of metabolic pathways in almost all cells (MHAMDI; VAN BREUSEGEM, 2018). However, excessive ROS concentrations cause oxidative stress, which implicates ROS in the impairment of metabolic homeostasis through oxidative damage

to lipids, proteins, and nucleic acids because of the high affinity between ROS and these molecules (reviewed in: Sharma et al., 2012; Soares et al., 2018).

Increased generation of ROS occurs when metabolic pathways are mismatched, which is usually associated with biotic and abiotic stress conditions. This occurs, for example, when photosynthetic electron carriers become highly reduced (SONOIKE; TERASHIMA, 1994; TERASHIMA; FUNAYAMA; SONOIKE, 1994; GRIECO et al., 2012; SUORSA et al., 2012; TAKAGI et al., 2016a). Although ROS are produced in all compartments within the cell, chloroplasts, mitochondria, and peroxisomes are recognised as the metabolic ROS powerhouses of leaf cells (FOYER; NOCTOR, 2003; NOCTOR; FOYER, 2016).

While ROS are harmful under high concentrations, these chemical compounds also act as signalling molecules, regulating important biological processes in both animal and plant cells (DAT et al., 2000; MITTLER, 2002; HALLIWELL, 2006). Although ROS-dependent signalling is still poorly understood, studies have shown its importance for several biological processes including cellular proliferation and differentiation, plant development, as well as for activation of responses to stresses and metabolic defence pathways (SUZUKI et al., 2012; EXPOSITO-RODRIGUEZ et al., 2017; MITTLER, 2017; LOCATO; CIMINI; DE GARA, 2018; MHAMDI; VAN BREUSEGEM, 2018; NOCTOR; REICHHELD; FOYER, 2018). Because it has a relatively long half-life compared to other ROS and the ability to cross membranes via aquaporins (BIENERT et al., 2007), H_2O_2 has special importance for signalling and stress-sensing events, being among the most studied ROS-signalling molecules (MARINHO et al., 2014; ČERNÝ et al., 2018; SMIRNOFF; ARNAUD, 2019). Specifically, H_2O_2 can drive redox changes leading to (in)activation of signalling networks (EXPOSITO-RODRIGUEZ et al., 2017; NOCTOR; REICHHELD; FOYER, 2018).

The precise control of different ROS concentrations in cells is critical for metabolic homeostasis. Accordingly, aerobic organisms have developed several non-enzymatic and enzymatic ROS-scavenging systems to prevent oxidative damage and to control the concentration of these species in cells (DAT et al., 2000). Enzymatic and non-enzymatic ROS-scavenging systems are present in all cellular compartments, demonstrating the importance of the control of the ROS concentrations for cell homeostasis (MITTLER et al., 2004; SHARMA et al., 2012; SOUZA et al., 2018), Together, both systems, which are interdependent, are part of a complex metabolic

network which involves, for example, more than 150 genes in *Arabidopsis thaliana* (MITTLER et al., 2004; SOUZA et al., 2018).

Among the non-enzymatic components, the redox balance between the reduced and oxidised forms of ascorbate (reduced ascorbate/dehydroascorbate; ASC/DHA) and glutathione (reduced glutathione/glutathione disulphide; GSH/GSSG) are probably the most studied systems in terms of antioxidant metabolism. Tocopherols, flavonoids, anthocyanins, and carotenoids also make part of the non-enzymatic scavengers. These molecules are antioxidants of low molecular weight that work as redox buffers, interacting with ROS and acting as a molecular interface to modulate proper acclimation responses or programmed cell death. The enzymatic ROS-scavenging system includes several isoforms of superoxide dismutases (SOD), catalases (CAT), peroxiredoxins (PRX), ascorbate peroxidases (APX), monodehydroascorbate reductases (MDAR), dehydroascorbate reductases (DHAR), glutathione peroxidases (GPX), glutathione reductases (GR), glutaredoxins (GRX) and other peripheral enzymes. These enzymes are important not only for scavenging excessive ROS but also for regulating the redox balance of ascorbate and glutathione (SOUZA et al., 2018).

Additionally, subsequent products of reactions involving ROS are central to photosynthesis signalling and regulation (PINTÓ-MARIJUAN; MUNNÉ-BOSCH, 2014; MULLINEAUX et al., 2018). For example, $^1O_2$ generated in the thylakoid electron transport chain can be primarily quenched by carotenoids and α-tocopherol, generating products that can act as molecular signals (RAMEL et al., 2012a, 2012b; SHUMBE; BOTT; HAVAUX, 2014). Similarly, oxidation products of lipids, such as oxylipins, have been shown to act as signalling compounds (MOSBLECH; FEUSSNER; HEILMANN, 2009; LÓPEZ et al., 2011; SATOH et al., 2014). Lipid oxidation is associated with the metabolism of jasmonates, which are essential phytohormones involved with regulation of plant development and environmental adaptation (MOSBLECH; FEUSSNER; HEILMANN, 2009; CHINI et al., 2016).

1.2.2 Photosystem II and its photoinhibition

PSII is a dimer complex and each monomer is composed of 20 to 23 subunits, depending on the organism (BEZOUWEN et al., 2017; SU et al., 2017). Most of these subunits are membrane-intrinsic proteins, including the PSII reaction centre

core proteins D1 (PsbA) and D2 (PsbD) and inner antennae proteins CP43 (PsbB) and CP47 (PsbC), which bind several chlorophylls (SHEN, 2015; BEZOUWEN et al., 2017; SU et al., 2017). The light-harvesting complex II (LHCII) contains three major trimeric light-harvesting chlorophyll a/b-binding proteins (LHCB1, LHCB2 and LHCB3), while three minor monomeric LHCB pigment-proteins are associated with PSII (LHCB4, LHCB5 and LHCB6) (LU, 2016; BEZOUWEN et al., 2017). The PSII core also binds to the OEC proteins (PsbO, PsbP, PsbQ), which are located at the lumenal side (BRICKER et al., 2012; SU et al., 2017). Several other subunits are involved with PSII complex assembly, stability, and repair (NIXON et al., 2010; NICKELSEN; RENGSTL, 2013; JÄRVI; SUORSA; ARO, 2015; LU, 2016).

PSII is particularly susceptible to photoinhibition because of the very strong oxidative potential of its reaction centre, which is required to oxidise water (RUBAN, 2015), making PSII a significant source of ROS in plants (NOCTOR; REICHHELD; FOYER, 2018). For example, $^1O_2$ production can occur when active PSII absorbs excitation through its surrounding chlorophylls, and the pool of PQ is highly reduced (KRIEGER-LISZKAY, 2005; ZAVAFER et al., 2017). ROS around PSII can also be generated from two-electron oxidations of water or one-electron reductions of O_2 on the PSII electron donor and acceptor sides of the OEC, respectively (KALE et al., 2017). These conditions lead to the formation of triplet chlorophylls in the PSII reaction centre (P680) by charge recombination, which readily react with O_2, producing $^1O_2$ (Zavafer et al., 2017; Vass et al., 1992; Telfer et al., 1994).

The ROS generated around PSII can cause PSII photoinhibition mainly by oxidising the D1 and D2 proteins at the PSII reaction centre (ARO; VIRGIN; ANDERSSON, 1993; KALE et al., 2017). The damaged PSII proteins, mainly D1, are replaced by newly synthesized versions after PSII complex disassembly and degradation in an event called the PSII repair cycle (ARO; VIRGIN; ANDERSSON, 1993; KATO et al., 2012; LI; ARO; MILLAR, 2018). The PSII repair rate depends on light, although it is saturated at low light intensities (TYYSTJÄRVI; ARO, 1996; ALLAKHVERDIEV; MURATA, 2004). Also, exposure to environmental stresses (such as high light, salt, cold, moderate heat and oxidative stress) inhibits the PSII turnover as a consequence of the inhibition of the *de novo* D1 protein synthesis at translation level, which also characterises a photoinhibitory condition (ALLAKHVERDIEV; MURATA, 2004; TAKAHASHI; MURATA, 2008).

1.2.3 Photosystem I and its photoinhibition

In plants, the PSI-LHCI supercomplex comprises the PSI core (composed of the membrane-embedded subunits PsaA, PsaB, PsaF, PsaG, PsaH, PsaI, PsaJ, PsaK, PsaL, and the stromal subunits PsaC, PsaD and PsaE) and the peripheral light-harvesting complex I (LHCI) dimers (LHCA1/4 and LHACA2/3) (QIN et al., 2015; SUGA et al., 2016; MAZOR et al., 2017). Under normal light and normal CBB cycle functioning, electrons are transported from plastocyanin (PC) to Fd through PSI by cofactors P700 and A_0 chlorophylls, phylloquinone A_1, and the iron-sulphur (FeS) centres F_X, F_A, and F_B (Figure 2) (AMUNTS; DRORY; NELSON, 2007; KOZULEVA; IVANOV, 2016). P700, A_0, A_1 and F_x are held by subunits PsaA and/or PsaB, which form the central heterodimer of PSI and are bound to the majority of the components of the PSI core and antenna (GOLBECK, 1992; BEN-SHEM; FROLOW; NELSON, 2003; AMUNTS; NELSON, 2009; QIN et al., 2015; MAZOR et al., 2017). The PSI subunit PsaC binds the FeS centres F_A, and F_B and, together with PsaD and PsaE, has a central role for reduction of Fd (GOLBECK, 1992; CASHMAN et al., 2014; MARCO et al., 2018). While PsaC establishes close protein contact required for fast electron transfer between the iron-sulfur clusters of PSI and Fd, PsaD and PsaE are responsible for the electrostatic guidance of Fd into the PSI binding pocket (BUSCH; HIPPLER, 2011; MARCO et al., 2018). There is a consensus that PsaD protein has a central role in the docking of Fd (BARTH; LAGOUTTE; SÉTIF, 1998; PIERRE et al., 2002; CASHMAN et al., 2014; KAPOOR et al., 2018). The specific functions of the other PSI subunits are less known, but many of them have been shown to be involved with maintenance and stabilisation of the PSI complex structure (CHITNIS, 2001; JENSEN et al., 2007; QIN et al., 2015; MAZOR et al., 2017).

PSI photoinhibition, similar to that of PSII, is associated with the generation of ROS when electron carriers at the photosynthetic transport chain become highly reduced (SONOIKE; TERASHIMA, 1994; TERASHIMA; FUNAYAMA; SONOIKE, 1994; GRIECO et al., 2012; SUORSA et al., 2012; TAKAGI et al., 2016a). This phenomenon has been reported, for example, under low temperatures (INOUE; SAKURAI; HIYAMA, 1986; TERASHIMA; FUNAYAMA; SONOIKE, 1994; TJUS; MØLLER; SCHELLER, 1998) and under high and fluctuating light (MUNEKAGE; GENTY; PELTIER, 2008; SUORSA et al., 2012; KONO; TERASHIMA, 2016; TIWARI et al., 2016). Such over-reduction promotes the generation of ROS when the electron-

accepting capacity of the PSI acceptors are saturated and molecular oxygen functions as an alternative acceptor. Reduction of O_2 is thought to occur at the acceptor side of PSI or at the phylloquinone A_1 site, in both cases producing $O_2^{\bullet-}$ (MEHLER, 1951; ASADA; KISO; YOSHIKAWA, 1974; TAKAGI et al., 2016a). $O_2^{\bullet-}$ produced can react with FeS centres, generating $^{\bullet}OH$ via the Fenton reaction, which can also attack PSI components and induce its photoinhibition (INOUE; SAKURAI; HIYAMA, 1986; TAKAHASHI; ASADA, 1988; SONOIKE et al., 1995). Recent findings have shown that not only $O_2^{\bullet-}$ and $^{\bullet}OH$, but $^1O_2$ produced from the reaction between P700 triplet-state (^{3}P700) and O_2, also causes PSI photoinhibition (TAKAGI et al., 2016a). Photoinhibition of PSI is usually associated with the degradation of PSI core proteins subunits like PsaA and mainly PsaB (SONOIKE et al., 1995, 1997; SONOIKE, 1996; KUDOH; SONOIKE, 2002). Degradation of PSI subunits has been recently argued to be a consequence, and not the first step, of PSI damage (TAKAGI et al., 2016a). Although the knowledge on PSI photoinhibition is expanding, its exact molecular mechanism is still unknown. Studies usually tend to unify the understanding of the mechanism of PSI photoinhibition in higher plants, but this phenomenon can occur differently in different species (KONO; TERASHIMA, 2016; TAKAGI et al., 2016a; HUANG et al., 2017; YANG et al., 2017; HUANG; TIKKANEN; ZHANG, 2018). Thus, the relation among PSI photoinhibition, ROS production in PSI and oxidative stress should be interpreted with caution.

Little is still known about PSI recovery from photoinhibition and the consequences on primary metabolism. Also, only a few studies explore aspects of the recovery phase after PSI photoinhibition. Recent studies have shown that PSI photoinhibition severely affects net carbon assimilation, photoprotection, and plant growth (BRESTIC et al., 2015; ZIVCAK et al., 2015; YAMORI; SHIKANAI, 2016). However, while PSI is highly resistant to photoinhibition in comparison to PSII (BARTH; KRAUSE; WINTER, 2001; HUANG; ZHANG; CAO, 2010), PSII recovery occurs faster than PSI (LI et al., 2004; ZHANG; SCHELLER, 2004; ZHANG et al., 2011; TIKKANEN; GREBE, 2018). For this reason, PSI photoinhibition is believed to have more severe consequences on plant metabolism than PSII photoinhibition under environmental stresses (SONOIKE, 2011; TAKAGI et al., 2016a; HUANG et al., 2017).

Figure 2 – A simplified scheme of the arrangement of the main cofactors and subunits involved in linear electron transport through PSI.

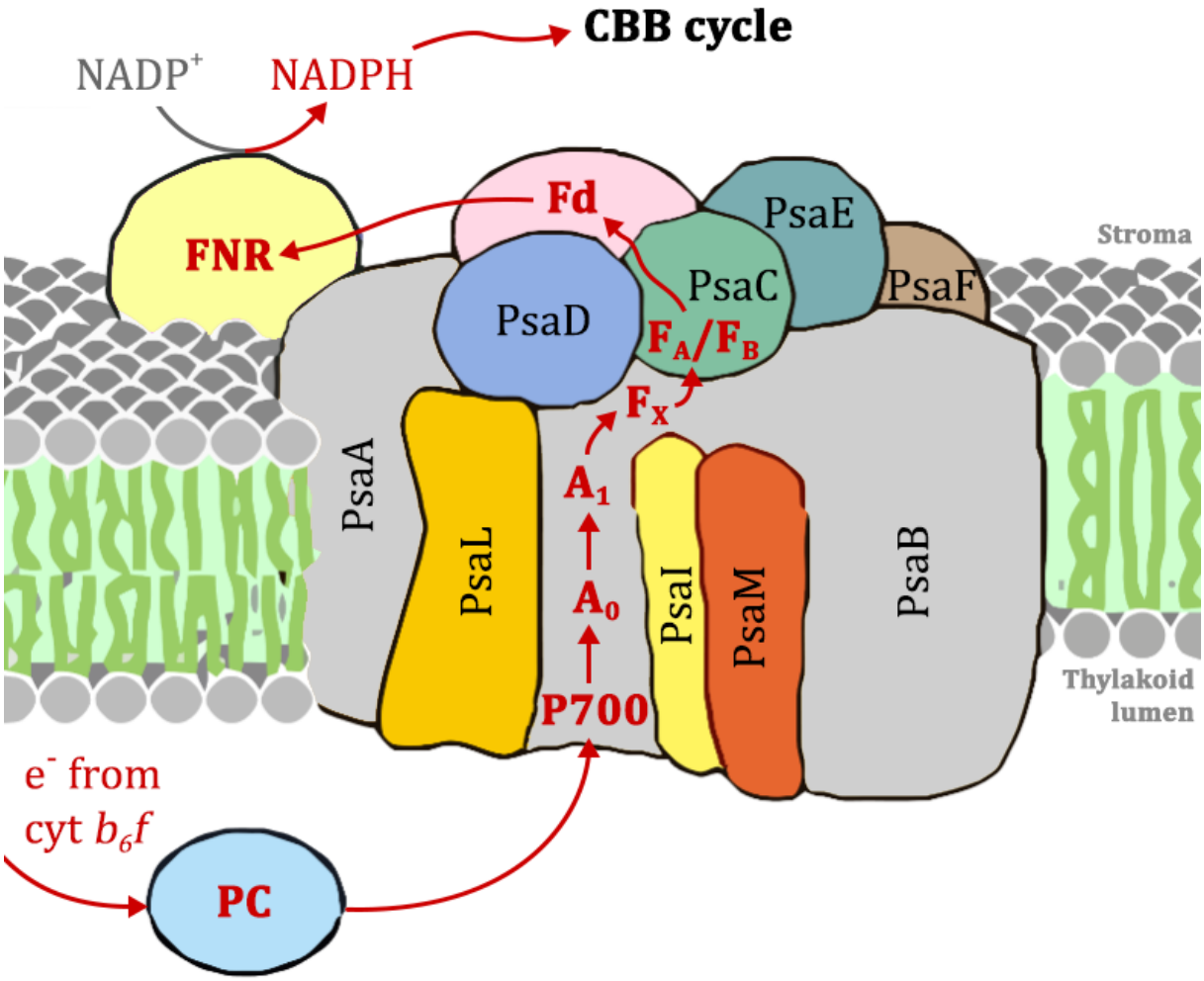

Source: the author.
CBB cycle = Calvin-Benson-Bassham cycle; Cyt *b6f* = cytochrome *b6f*; Fd = ferredoxin; FNR = ferredoxin:$NADP^+$ oxidoreductase; $NADP^+$ = oxidised nicotinamide adenine dinucleotide phosphate; NADPH = reduced nicotinamide adenine dinucleotide phosphate; PC = plastocyanin. Adapted from the Kyoto Encyclopedia of Genes and Genomes (KEGG) pathway map image map00195 (KANEHISA; GOTO, 2000) with kind permission.

1.3 Photoprotection

Plants have developed several photoprotective mechanisms to avoid photoinhibition of both photosystems or repair photodamage, which include protection of the photosynthetic apparatus and plant metabolism by regulating light absorption, dissipating absorbed light, balancing photosynthetic electron transport, effectively consuming the excess of electrons produced from light absorption, and scavenging

ROS (DEMMIG-ADAMS; ADAMS, 1992; TAKAHASHI; BADGER, 2011; CAZZANIGA et al., 2013). The front-line photoprotective mechanism is naturally the avoidance of excessive light absorption, which means physically blocking light from reaching chloroplasts. This includes, for example, the avoidance of light exposure by leaf and chloroplast movement (KASAHARA et al., 2002) or by light and/or ultraviolet radiation screening through specific molecules (e.g. phenolic compounds) at the leaf epidermis (BOOIJ-JAMES et al., 2000; HOLUB et al., 2019).

In case excess light is not avoided, absorbed energy can be dissipated via nonphotochemical quenching (NPQ) of chlorophyll excitation (RUBAN et al., 2007). NPQ is a multi-component process, mainly related to its major component, the energy-dependent quenching (qE), which is a consequence of conformational changes within the LHCII proteins that cause the formation of energy traps (RUBAN, 2016). The LHCII antenna rearrangement is dependent on protonation of antenna components, mainly the PsbS subunit of PSII, which is involved in the triggering of the dissipation of excess excitation energy as heat (RUBAN, 2016; SACHARZ et al., 2017). In addition, qE has been shown to be associated with the xanthophyll cycle, in which epoxy groups from xanthophylls (e.g. violaxanthin and antheraxanthin) are enzymatically removed to create zeaxanthin that carries out energy dissipation as heat within LHCII antenna proteins (GOSS; JAKOB, 2010; RUBAN; JOHNSON; DUFFY, 2012; SACHARZ et al., 2017).

Balancing the electron flow through the photosynthetic electron transport in conditions of excessive light absorption is also important to avoid photodamage. Several mechanisms, functioning at different levels of photosynthetic energy conversion, are involved in this balance (reviewed in Tikkanen and Aro 2014). Examples of these mechanisms are (1) the control of the proton gradient between the thylakoid lumen and stroma (ΔpH), which is mostly dependent on the activities of the water-splitting complex in PSII, of cyt *b6f*, and of ATP synthase; (2) the excitation balance between PSII and PSI via LHCII phosphorylation; (3) PSII inactivation; and (4) cyclic electron flow. These mechanisms are interconnected and have an important role in the regulation of plant metabolism to acclimate to diverse environmental changes (TIKKANEN; ARO, 2014).

Another important mechanism to avoid or alleviate photoinhibition consists of increasing the capacity for electron consumption by strengthening transitory electron sinks (PADMASREE; PADMAVATHI; RAGHAVENDRA, 2002; ALRIC; JOHNSON,

2017; WADA et al., 2018). The strongest sink is naturally CO_2 assimilation in the CBB cycle, which uses reducing power produced in the thylakoid electron transport chain for the synthesis of carbohydrates, meaning that this pathway also contributes to avoidance of photoinhibition caused by excessive electron pressure. For example, starch synthesis can serve as a transient sink to allocate excess energy, such as under high light conditions (PAUL; FOYER, 2001). In accordance, the excessive accumulation of starch has long been speculated as a negative regulator of photosynthetic activity (PAUL; FOYER, 2001; ADAMS et al., 2013). However, while some studies explore the consequences of PSII photoinhibition in carbohydrate metabolism or source-sink regulation, these subjects are neglected in terms of PSI photoinhibition (ADAMS et al., 2013). Although the CBB and carbohydrate metabolism probably account for the strongest photosynthetic electron sink, alternative electron transport pathways have been proven to protect plants from photoinhibition (reviewed in Alric and Johnson 2017). The most studied pathways known to be involved in photoinhibition avoidance by electron consumption in plants are photorespiration, mitochondrial respiration (including the alternative oxidase (AOX) pathway), the Mehler reaction within the water-water cycle, and chlororespiration by the plastid terminal oxidase (PTOX).

As previously explained, plants possess a complex antioxidant system which controls their levels of ROS. In case all above-mentioned photoprotective mechanisms are not able to alleviate the electron pressure in the transport chain, ROS can be produced in large quantity and lead to oxidative destruction of cellular components (as detailed in section 1.2.1). Thus, the reinforcement of the ROS-scavenging system is also considered an important photoprotective mechanism (DEMMIG-ADAMS; ADAMS, 1992; TAKAHASHI; BADGER, 2011).

1.3.1 Mechanisms for PSI photoprotection

As mentioned above, PSI photoinhibition is harmful to plant fitness because of the slow recovery of PSI, differently from PSII (TAKAGI et al., 2016a; HUANG et al., 2017). This highlights the importance of protecting this photosystem, which indeed features some specific photoprotective mechanisms. PSI fitness is essentially dependent on the balance between the redox states of its donor side (PC pool) and its acceptor side (Fd pool) (detailed in section 1.2.3).

A key mechanism for PSI protection at the PSI donor side is the establishment of a proton gradient across the thylakoid membrane (ΔpH), which slows the rate of electron transfer from PSII to PSI through acidification of the thylakoid lumen (JOLIOT; JOHNSON, 2011; TIKKANEN; RANTALA; ARO, 2015; SHIKANAI, 2016). The downregulation of electron transfer from PSII to PSI by acidification of the thylakoid lumen is achieved through two different mechanisms. One of them is the activation of the thermal dissipation of excessively absorbed light energy from PSII antennae (usually monitored through the NPQ component qE), which is dependent on xanthophyll quenching and on the interaction between the PsbS protein and the LHCII, as detailed in section 1.3 (reviewed in Ruban 2016). The other mechanism, also known as “photosynthetic control”, is the downregulation of cyt *b6f* complex activity (STIEHL; WITT, 1969; TIKHONOV, 2014).

The control of electron flow through the cyt *b6f* complex is especially important for protecting PSI from over-reduction under high electron pressure conditions like fluctuating light and high light (SUORSA et al., 2012; KONO; NOGUCHI; TERASHIMA, 2014; TIKKANEN; RANTALA; ARO, 2015; TAKAGI; MIYAKE, 2018). A ΔpH is generated as a consequence of the photosynthetic electron flow, both linear and cyclic, which generates a proton motive force (*pmf*) and allows the production of ATP by ATP synthase (section 1.1.1). The thylakoid lumen acidification is therefore coupled with two important mechanisms, the electron flow and the activity of ATP synthase.

In cyclic electron flow (CEF), electrons are recycled around photosystem I by re-routing them from Fd to PQ. As a result, ΔpH is formed across the thylakoid membrane, leading to the production of ATP without concomitant production of NADPH, thus increasing the ATP:NADPH ratio within the chloroplast (YAMORI; SHIKANAI, 2016). At least two routes for CEF are widely accepted: the PGR pathway, involving PGR5 (PROTON GRADIENT REGULATION 5) and PGRL1 (PGR5-like1); and the NADH dehydrogenase-like complex (NDH)-mediated pathway (BURROWS et al., 1998; MUNEKAGE et al., 2002, 2004; SHIKANAI, 2007; SUORSA, 2015). However, although PGR5 has been proven to control ΔpH across the thylakoid membrane, the direct involvement of PGR5 in electron transport to PQ, and therefore the existence of a PGR5/PGRL1-dependent pathway, is currently under debate (NANDHA et al., 2007; SUORSA et al., 2012; TIKKANEN et al., 2012a; TAKAGI; MIYAKE, 2018).

Arabidopsis PGR5 is the product of the gene At2g05620. Mature PGR5 is a 10-kDa protein located in the chloroplast thylakoid membrane, sharing high homology with correspondent PGR5 proteins in other photosynthetic organisms (e.g. rice, soybean, algae and cyanobacteria) (MUNEKAGE et al., 2002; OKEGAWA et al., 2007). Several studies have shown that PGR5 is indeed necessary for lumen acidification (MUNEKAGE et al., 2002), and, in accordance, for protecting PSI functionality by downregulating the electron flow through the cyt *b6f* complex (TIKKANEN et al., 2012b; TIKKANEN; RANTALA; ARO, 2015; MOSEBACH et al., 2017; TAKAGI; MIYAKE, 2018). As a consequence, PGR5 has been reported as an important modulator of the linear electron flow, and this has been attributed as its major role in plants (DALCORSO et al., 2008; SUORSA et al., 2016; TAKAGI; MIYAKE, 2018). Thus, PGR5 has been shown to be vital for plant viability during environmental acclimation (SUORSA, 2015; YAMORI; SHIKANAI, 2016) although its exact molecular function is unknown.

PSI photoinhibition has been shown to occur in Arabidopsis and rice *pgr5* mutants under high luminosity and fluctuating light conditions because of the excessive accumulation of electrons in the photosynthetic electron chain (MUNEKAGE et al., 2002; KONO; NOGUCHI; TERASHIMA, 2014; KONO; TERASHIMA, 2016; YAMORI; MAKINO; SHIKANAI, 2016). The difference between the WT and the *pgr5* mutant in controlling the electron flow through the cyt *b6f* for PSI photoprotection is illustrated in Figure 3.

Figure 3 – Simplified scheme of the ΔpH-dependent control of the electron pressure through the cytochrome *b6f* (cyt *b6f*) complex in wild-type plants (WT) and the *pgr5* mutant immediately upon transition from growth light (GL) to high light (HL).

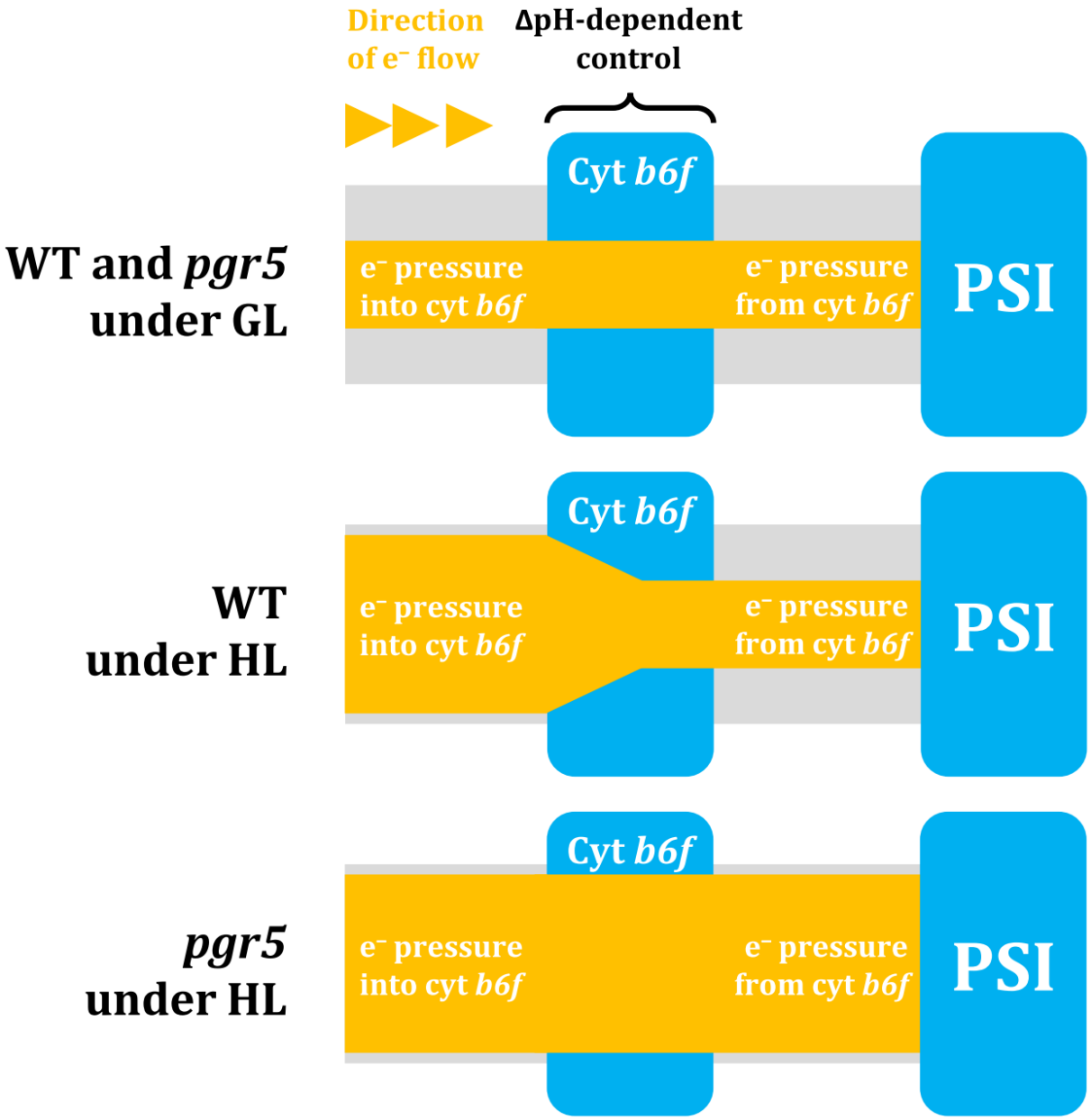

Source: the author.
Under GL, the ΔpH-dependent control of the cyt *b6f* is not engaged. In WT under HL, electron flow through the cyt *b6f* is controlled because the activity of PGR5 protein ensures ΔpH formation across the thylakoid membrane, thus protecting PSI from photoinhibition. However, the *pgr5* mutant is unable to control electron flow through the cyt *b6f* and thus the high electron pressure at PSI induces PSI photoinhibition.

In addition to the regulation of electron flow at the PSI donor side, the CBB cycle and alternative reduction pathways work as electron sinks to alleviate the electron pressure in the electron transport chain and avoid PSI photoinhibition. Several

PSI-acceptor-side mechanisms have been proposed to specifically avoid PSI over-reduction, like increases in the electron sink of photosynthesis (i.e. CO_2 assimilation and photorespiration), the water-water cycle, and mitochondrial alternative oxidase activity (HODGES et al., 2016; KONO; TERASHIMA, 2016; TAKAGI et al., 2016b; ALRIC; JOHNSON, 2017). Although the photoprotective role of photorespiration and mitochondrial metabolism as electron sinks has been gaining attention in the last years, their importance specifically in avoiding PSI photoinhibition has been neglected.

The water-water cycle is believed to be important for protection from photoinhibition by playing a dual function, as ROS scavenger as well as participating in the dissipation of excess photons and electrons as an alternative electron flux (ASADA, 1999, 2000). However, some studies have questioned the role of the water-water cycle as an excess energy dissipator (DRIEVER; BAKER, 2011). As defined by Asada (2000), “the water-water cycle in chloroplasts is the photoreduction of dioxygen to water in photosystem I by the electrons generated in photosystem II from water”. A key reaction for this process is the Mehler reaction (MEHLER, 1951), which occurs when the photoreduction of O_2 in PSI generates $O_2^{\bullet -}$ (as commented in section 1.2.3) followed by its dismutation to H_2O_2 mainly by SOD. The water-water cycle is a consequence of this reaction and includes the reduction of H_2O_2 to water by the thylakoid APX using ascorbate as an electron donor (ASADA, 1999; FOYER; SHIGEOKA, 2011). A broader version of the water-water cycle, named Foyer-Halliwell-Asada cycle, includes the glutathione-dependent ascorbate regenerating system, also known as the ascorbate-glutathione cycle (FOYER; HALLIWELL, 1976; FOYER; SHIGEOKA, 2011). Moreover, because the water-water cycle is directly related to the ROS levels and redox balance within the chloroplasts, it can be an important signal trigger specifically related to the photoinhibition of PSI.

2 AIMS OF THE STUDY

Photosystem I (PSI) inhibition has been shown to significantly suppress photosynthesis and growth, which are essential for plant fitness. Additionally, PSI inhibition has been shown to occur under conditions of high light, fluctuating light and chilling in different species, demonstrating the importance of understanding PSI damage, regulation, and protection also for plant improvement under field conditions. However, PSI photoinhibition and recovery has received little attention, especially compared to PSII photoinhibition and recovery. The central hypothesis of this thesis is that PSI damage and photoinhibition induce strong changes to plant metabolism, mainly to PSI downstream components. Therefore, the main aim of this study was to determine and understand the effects of PSI photoinhibition in plant metabolism by investigating its occurrence in *Arabidopsis thaliana* L. mutant lacking the PGR5 protein, treated with excess light conditions. Specific aims of this thesis were:

1. To develop high light-treated *pgr5* mutant as a model system for induction and study of PSI photoinhibition;

2. To investigate the consequences of PSI inhibition on photosynthetic electron transport, gas exchange, carbon assimilation processes and mitochondrial respiration;

3. To detail the dynamics of PSI inhibition, and to characterise the recovery of PSI function after its photoinhibition;

4. To investigate the impact of PSI photoinhibition on chloroplast retrograde signalling, production, and turnover of reactive oxygen species, and induction of oxidative stress.

3 METHODOLOGY

3.1 Plant material and treatments

Arabidopsis thaliana (L.) Heynh. ecotypes Columbia glabra-1 (*gl1*) and Columbia-0 (Col-0) were used as wild-type controls (WT) for the *pgr5* (MUNEKAGE et al., 2002) and *npq4* (LI; GILMORE; NIYOGI, 2002) mutants, respectively. The *npq4* mutant lacks the PsbS protein and thus NPQ, but the control of cyt *b6f* is retained. Therefore, *npq4* was used as a control for *pgr5* wherein both NPQ and cyt *b6f* control are missing (TIKKANEN; RANTALA; ARO, 2015). Plants were grown for six weeks in a phytotron at 23 °C, relative humidity of 60%, 8 h photoperiod under constant white growth light (GL) of 120 or 125 µmol photons m^{-2} s^{-1}. High-light treatments (HL) involved shifting plants from GL to 1000 µmol photons m^{-2} s^{-1} in temperature-controlled growth chambers set at 23 °C. Time of HL treatment lasted 1 h (Annex A and Annex C) or 4 h (Annex B) for most of the experiments, or as described in the figure legends. For the fluctuating light treatment, the plants were exposed to 50 µmol photons m^{-2} s^{-1} for 5 min and to 500 µmol m^{-2} s^{-1} for 1 min, controlled by an automatic shading system over a photoperiod of 8 h/16 h (light/dark), similarly to previous experiments (TIKKANEN et al., 2010; GRIECO et al., 2012; SUORSA et al., 2013). Recovery treatments involved returning plants treated with HL or fluctuating light to GL. Other treatments used in this thesis were performed as explained in the figure legends. All the experiments were repeated at least twice and at least three biological replicates were used in every experiment.

3.2 Photochemistry

Photochemistry analyses are detailed in Annexes A, B and C. The photochemical parameters of PSI and PSII were simultaneously measured based on chlorophyll *a* fluorescence (SCHREIBER; BILGER; NEUBAUER, 1995) and the P700 absorbance (KLUGHAMMER; SCHREIBER, 1998), using a WALZ Dual-PAM-100 system (Annexes A and C) or a WALZ Kinetic LED-Array Spectrophotometer (KLAS) (Annex B). Pm and Fm measurements were taken from detached leaves after 30 min of dark acclimation. Light-dependent measurements (Fo, F', Y(NA), Y(ND), and NPQ) were taken after 5 min exposure to each tested actinic light intensity after the dark

acclimation. Changes in redox states of ferredoxin (Fdm) and plastocyanin (PCm) were measured in intact leaves with a KLAS, through the deconvolution of their respective absorbance signals (KLUGHAMMER; SCHREIBER, 2016). Measurements were performed as previously described (SCHREIBER; KLUGHAMMER, 2016; SCHREIBER, 2017)

3.3 Gas exchange parameters

Evaluation of gas exchange parameters is detailed in Annexes A, B and C. Leaves were acclimated in the dark for 15 min and leaf gas exchange parameters were measured in 400 ppm CO_2 (Annexes A, B and C) and 2000 ppm CO_2 (Annex A) at 23 °C, using the LI-COR LI-6400XL Portable Infrared Gas Analyzer system (IRGA). Photosynthetic photon flux density (PPFD) values inside IRGA's chamber were set as shown in each figure. Data were taken after IRGA parameters reached a steady-state value following the onset of the respective PPFD (usually around 120 s).

3.4 Mitochondrial respiration

Day respiration was estimated using the data obtained with 0 PPFD from IRGA measurements, as described in section 3.3 and detailed in Annex B. O_2 uptake was measured for 5 min in darkness at 23 °C using an Unisense 'OX-NP' oxygen microsensor, from three detached leaves submerged in 50 mM sodium phosphate buffer (pH 7.2), as detailed in Annex B. Leaves were dark acclimated for at least 15 min prior to each O_2 consumption rate measurement.

3.5 Carbohydrate quantification

Frozen leaves were oven dried at 60 °C for 72 h for the determination of starch, glucose, and fructose contents, as detailed in Annexes A and B. Starch content was measured using a total starch assay kit (Megazyme K-TSTA assay kit). After ethanolic extraction (80% v/v) at 99 °C for 15 min, glucose and fructose contents were determined using the Sucrose/Fructose/D-Glucose test kit (Megazyme K-SUFRG assay kit). All assays were performed according to the manufacturer's protocol. Leaves

from the same plants were fixed with glutaraldehyde and starch accumulation was analysed through transmission electron microscopy (TEM) imaging.

3.6 Leaf membrane damage

Leaf membrane damage (MD) was estimated through the electrolyte leakage method (BLUM; EBERCON, 1981), as shown in Annex C. Detached leaves were placed in tubes containing deionized water and incubated in a shaking water bath at 25 °C for 24 h. After measuring the first electric conductivity (L1), the solution was heated at 95 °C for 1 h and then cooled to 25 °C, after which the second electric conductivity (L2) was measured. Membrane damage was calculated as MD = (L1/L2) × 100.

3.7 12-Oxo-phytodienoic acid, H_2O_2 and singlet oxygen quantifications

12-Oxo-phytodienoic acid (OPDA) abundance was quantified by ultra-performance liquid chromatography-tandem mass spectrometry (UPLC-MS) in frozen leaves after extraction in methanol, as described in Annex A. H_2O_2 content was quantified using the Amplex Red Hydrogen Peroxide/Peroxidase Assay Kit (Life Technologies) according to the manufacturer's protocol, as detailed in Annex C. Singlet oxygen ($^1O_2$) trapping was performed in isolated thylakoids as previously described (YADAV et al., 2010) using a Miniscope (MS5000) electron paramagnetic resonance (EPR)-spectrometer equipped with a variable temperature controller (TC-HO4) and Hamamatsu light source (LC8), as shown in Annex A.

3.8 Histochemical detection of superoxide and hydrogen peroxide

Nitroblue tetrazolium (NBT) and diaminobenzidine (DAB) staining, as detailed in Annex C, were performed in leaves after the light treatments for detection of superoxide ($O_2^{\bullet-}$) and hydrogen peroxide (H_2O_2), respectively, as previously described (Ogawa et al., 1997; Thordal-Christensen et al., 1997). After staining, leaves were treated with ethanol-chloroform bleaching solutions and results were compared through their photographs.

3.9 Lipid peroxidation imaging and quantification

Lipid peroxidation, as detailed in Annexes A and C, was evaluated through autoluminescence imaging and quantification of thiobarbituric acid-reactive substances (TBARS). Autoluminescence analyses were performed in detached leaves and rosettes after 2 h of dark incubation according to the method described in Birtic et al. (2011). The luminescence signal was collected for 20 min using an IVIS Lumina II system (Caliper Life Sciences) containing an electrically-cooled charged-couple device (CCD) camera, which allowed obtaining autoluminescence images for evaluation. TBARS were extracted from frozen leaves in TCA acid and supernatants were evaluated based on the formation of thiobarbituric acid-malondialdehyde complex, as previously described (HEATH; PACKER, 1968).

3.10 Enzymatic activity assays

Enzymatic activity assays are detailed in Annex C. Total protein was extracted from whole leaves in a potassium phosphate buffer (final concentration of 100 mM; pH 7.0) containing EDTA (final concentration of 1 mM) and used for enzymatic activity assays. Superoxide dismutase (SOD; EC 1.15.1.1) activity was determined based on inhibition of nitro blue tetrazolium chloride (NBT) photoreduction (GIANNOPOLITIS; REIS, 1977). Catalase (CAT; EC 1.11.1.6) activity was based on the reduction of H_2O_2 (BEERS; SIZER, 1952; HAVIR; MCHALE, 1987). Ascorbate peroxidase (APX; EC 1.11.1.11) activity was measured based on the oxidation of ascorbate (ASC) (NAKANO; ASADA, 1981). Monodehydroascorbate reductase (MDHAR; EC 1.6.5.4) activity was assayed based on the generation of monodehydroascorbate (MDHA) free radicals by ascorbate oxidase (AO; 1.10.3.3) and following oxidation of NADH (HOSSAIN; NAKANO; ASADA, 1984). Dehydroascorbate reductase (DHAR; EC 1.8.5.1) activity was assayed based on the oxidation of glutathione (GSH) (NAKANO; ASADA, 1981).

3.11 Western blotting

Western blotting procedures are detailed in Annexes B and C. Thylakoids were isolated from mature leaves as previously described (JÄRVI et al., 2011). Total

thylakoid proteins (Annex B) or total leaf proteins (Annex C) were separated by SDS-PAGE, transferred to polyvinylidene difluoride (PVDF) membranes and blotted with polyclonal antibodies against PsaB, PsaC, PsaD and LOX-C.

3.12 RNA isolation and transcriptome analysis

Transcriptomics-related methods are detailed in Annexes A and C. Total RNA was isolated from frozen leaves using TRIsure (Bioline) according to the protocol supplied, with an additional final purification in 2.5 M LiCl overnight at -20 °C, and used for RNAseq library construction. Libraries were sequenced in 50 bp single-end reads using Illumina Hiseq 2500 technology (BGI Tech Solutions). Reads were aligned to the reference genome build *Arabidopsis thaliana* TAIR 10 and quantified using the DESeq R package. Gene expression fold changes were calculated using a two-way ANOVA test with Benjamini-Hochberg *p*-value correction. Analyses of enriched Gene Ontology for Biological Process (GO-BP) terms were performed using the enrichment analysis tool of the Gene Ontology Consortium.

4 OVERVIEW OF THE RESULTS

4.1 Characterization of PSI photoinhibition in high light-treated *pgr5* mutants

In order to evaluate PSI photoinhibition, the maximum oxidation capacity of P700 at the PSI reaction centre (Pm) was monitored as an indicator of PSI functionality. The results showed that *pgr5* mutants have levels of oxidisable PSI (Pm) around 25% lower in normal growth light conditions (GL; 125 µmol photons m^{-2} s^{-1}) when compared to wild-type plants (WT) (Figure 1 in Annex A; Figure 1b in Annex B; Figure 1a in Annex C). However, Pm values in *pgr5* mutants decreased to lower than 25% of the WT value within only 1 h of high light (HL; 1000 µmol photons m^{-2} s^{-1}), while Pm in WT was almost unaffected (Figure 1 in Annex A; Figure 1b in Annex B; Figure 1a in Annex C). Pm seemed to reach its minimum value in PSI-photoinhibited plants within only 1 h of HL, and remained this low for at least the next 5 h of the excess light treatment (Figure 1 in Annex A; Figure 1b in Annex B; Figure 1a in Annex C). In accordance, HL-induced weaker PSI donor side limitation (Y(ND)) and stronger PSI acceptor side limitation (Y(NA)) in *pgr5* mutants compared to WT, illustrating unregulated electron transport to PSI in excess of the capacity of stromal electron acceptors from PSI (Figure 2a and 2b in Annex A). The recovery of Pm in HL-treated *pgr5* plants occurred over a period of 4 days, after which time the Pm value of *pgr5* plants was restored to a similar level to that of untreated plants (Figure 1b in Annex B). Similar results were obtained in an experiment using a fluctuating light (FL) treatment, in which FL-treated *pgr5* took more than 5 days to recover to the values observed in the GL treatment (Figure 4). No significant difference was observed between GL- and HL-treated WT plants during the recovery experiment (Figure 1b in Annex B). Furthermore, PSI photoinhibition correlated with the depletion of the PsaB subunit, but not PsaC nor PsaD, of the PSI complex after HL as well as during PSI recovery (Figure 2 in Annex B).

Figure 4 – The impact of fluctuating light (FL) treatment on PSI in the *pgr5* mutant.

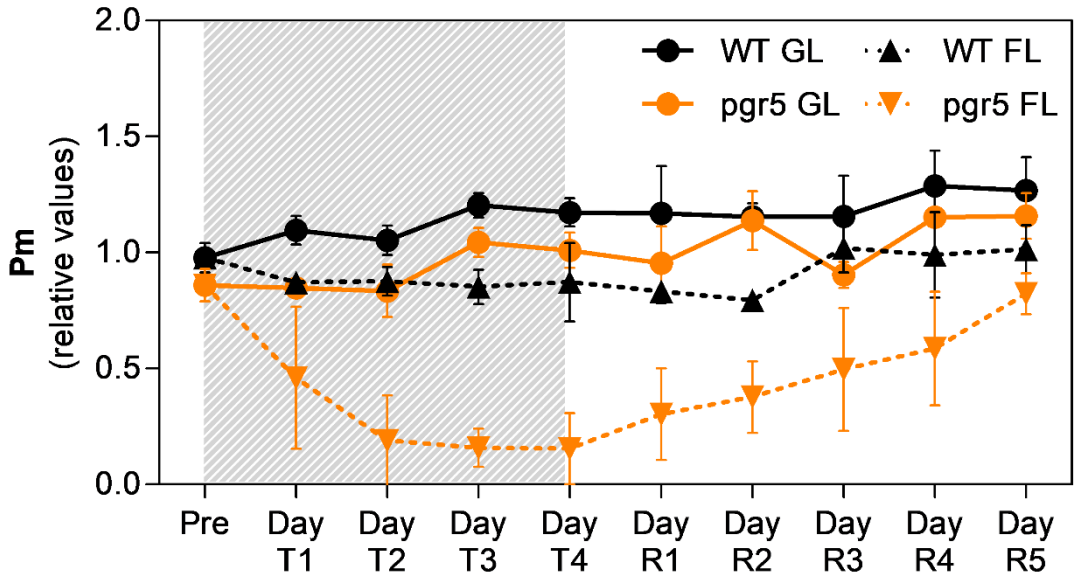

Source: the author.
The maximum amount of oxidisable P700 (Pm) in WT and *pgr5* plants treated with growth light (GL, 125 µmol photons m^{-2} s^{-1}) or FL (50 µmol photons m^{-2} s^{-1} for 5 min, 500 µmol m^{-2} s^{-1} for 1 min), controlled by an automatic shading system over a photoperiod of 8 h/16 h (light/dark). Error bars show standard deviation among replicates (n = 4). Significant differences between treatments and between genotypes occurred when error bars do not overlap (Student's t-test, $p < 0.05$). The shaded area represents the time during which the fluctuating light treatment was applied to the FL-treated plants. Measurements of FL-treated plants occurred from day T1 to day T4, whereas measurements with plants in the recovery phase occurred from day R1 to day R5.

4.2 Effects of high light on the photosynthetic electron transport chain of *pgr5* mutants

Photoinhibition of PSI induced malfunction in several components of the photosynthetic electron transport chain (Figure 2 in Annex A; Figure 1 in Annex B; Figure 1 in Annex C). A strong decrease of the maximal reduction state of Fd (Fdm) was observed in *pgr5* mutants, but not in WT, after a 4-h HL treatment (Figure 1c in Annex B). This decrease in Fdm, as well as its recovery, were correlated to the Pm values in HL-treated *pgr5* mutants (Figures 1c and 1e in Annex B), suggesting that PSI photoinhibition led to relative oxidation of the Fd pool, which is the first PSI electron acceptor in linear electron flow. However, no significant changes were observed in the maximum oxidation state of plastocyanin (PCm) after the HL treatment or during the

recovery phase (Figure 1d in Annex B), suggesting no correlation between PSI photoinhibition and the redox state of the plastocyanin pool, the PSI electron donor (Figure 1f in Annex B).

To assess PSII function , the parameters F'/Fm and Fm were used to avoid the confounding effect of PSI photoinhibition on fluorescence, which influences the Fv/Fm parameter because of the effect of PSI status on Fo values (TIKKANEN et al., 2017) (Figure S1b in Annex B; Figure 1c and 1d in Annex C). F'/Fm increased in GL-treated *pgr5* that were subjected to HL, demonstrating an increase in the number of closed PSII reaction centres, while this was not observed in the WT (Figure 2c in Annex A). The effects of HL in the F'/Fm parameter measured in *pgr5* mutants may be a consequence of the lack of ΔpH-dependent NPQ in these plants, as observed by measuring NPQ (Figure 2d in Annex A). However, HL-treated *pgr5* mutants showed high values for F'/Fm even when measured under low light, which may be due to limited PSI activity and consequent over-reduction of the electron transport chain (Figure 2c in Annex A). This idea is supported by Fm values measured in WT and *pgr5* mutants after 4 h HL treatment (Figure 1a in Annex B) and from 1-5 h (Figure 1b in Annex C), which in *pgr5* mutants were much lower than those of the GL treatment. Together, these results show that, while PSI photoinhibition occurred only in HL-treated *pgr5* mutants, HL induced PSII photoinhibition in both the WT and the *pgr5* mutant. However, the photoinhibition of PSI (measured through Pm) in *pgr5* mutants was clearly much stronger and more rapid than of PSII (measured through Fm) (Figures 1a and 1b in Annex B; Figures 1a and 1b in Annex C). The recovery of PSII function was also more rapid than that of PSI (Figures 1a and 1b in Annex B).

4.3 Effects of PSI photoinhibition on CO_2 assimilation and gas exchange

High light treatments induced impaired CO_2 assimilation rate (*A*) in *pgr5* mutants compared to WT in all experiments (Figure 3 in Annex A; Figure 3 in Annex B; Figures 2 and 3 in Annex C). Light curves (*A*-PPFD curves) under 400 ppm CO_2 showed that HL-treated *pgr5* mutants have lower *A* compared to WT under all irradiances used in the curve, although the difference between the genotypes was most pronounced under lower irradiances. However, no differences between GL-pre-treated *pgr5* and WT were observed (Figure 3 in Annex A; Figure 3 in Annex C). The effect of HL on CO_2 assimilation was detailed using a time-course experiment of PSI

photoinhibition (Figure 2 in Annex C). This experiment clearly showed the negative impact of HL-induced PSI photoinhibition on *A* in *pgr5* mutants, mainly within the first 30 minutes of the light stress. During illumination with GL directly after 1 h of HL treatment, *A* in *pgr5* mutants was approximately 0, whereas WT exhibited the same *A* rates as before undergoing the HL treatment. In a second HL treatment after 1 h recovery in GL, *A* values were approximately equivalent to the rates observed before the end of the previous HL treatment for both genotypes, which was 35% lower in *pgr5* than in WT. In comparison to the first HL treatment, the rate of increase in *A* during the second HL treatment was slower in both WT and *pgr5*. The rate of *A* decline was similar between WT and *pgr5*, and smaller when compared to the first HL treatment for both genotypes (Figure 2 in Annex C).

To better understand the consequences of PSI damage and recovery on CO_2 assimilation and its relevance under different light intensities, *A* of HL-pretreated *pgr5* mutants and WT were assessed under low (50 µmol photons m^{-2} s^{-1}), growth (125 µmol photons m^{-2} s^{-1}) and high (1000 µmol photons m^{-2} s^{-1}) irradiances (Figure 3 in Annex B). In each case, *pgr5* showed a distinct inhibition of *A* immediately after the HL treatment; however, the magnitude of the decrease depended on the intensity of the light used for the measurement. The impact of PSI photoinhibition on *A* in *pgr5* mutants was greater under lower irradiances. For example, *A* in HL-treated *pgr5* mutants was restored to the pre-treatment level after only 1 day of recovery when measured under high irradiance, while 3 days of recovery was required to restore normal *A* in the same plants when measured under low irradiance (Figure 3 in Annex B).

HL-treated *pgr5* exhibited higher internal CO_2 concentration (C_i), mainly under the lowest irradiances of the *A*-PPFD curve (Figure 3b in Annex C). In accordance, lower *A* in HL-treated *pgr5*, compared to HL-treated WT, was also observed under high CO_2 concentrations (2000 ppm) (Figure 3b in Annex A). These results show that lower assimilation rates in *pgr5* mutants compared to the WT, both after HL, was not associated with CO_2 limitation. In addition, the stomatal conductance (g_s) and the transpiration rates (*E*) of HL-treated *pgr5* and WT were similar, showing that the lower *A* in HL-treated *pgr5*, compared to HL-treated WT, is also not associated with stomatal limitation (Figures 3c and 3d in Annex C). As a consequence of these results, lower maximum carboxylation efficiency (A/C_i) and water use efficiency (WUE) were observed in HL-treated *pgr5* in comparison to HL-treated WT.

4.4 Effects of PSI photoinhibition on carbohydrate accumulation and mitochondrial respiration

The effects of PSI photoinhibition on carbohydrate accumulation was studied through the evaluation of starch, fructose and glucose contents (Figure 4 in Annex A; Figure 4 in Annex B). The results show that HL induced a strong accumulation of starch in the WT, while only slight accumulation occurred in *pgr5* mutants, both compared to the GL treated controls (Figure 4 in Annex A; Figure 4a in Annex B). During the first day of recovery under GL after the HL treatment, the starch content strongly decreased in *pgr5*, reaching less than half of the content observed in untreated plants, while in the WT the starch content was slightly higher compared to GL-treated WT (Figure 4 in Annex A; Figure 4a in Annex B). The starch content in *pgr5* gradually recovered over a period of 3 days, until it reached GL levels (Figure 4a in Annex B). The HL treatment induced substantial increases in glucose and fructose concentrations in both WT and *pgr5* leaves, but the increase in *pgr5* was approximately half of that in the WT for both sugars (Figure 4b and 4c in Annex B). Glucose content in WT and *pgr5*, which was similar during the whole recovery phase, was slightly lower during the initial 2 days of recovery than in GL-treated controls (Figure 4b in Annex B). No differences between genotypes nor between light treatments were observed for the fructose content during the recovery phase (Figure 4c in Annex B).

As the mitochondrial respiration is directly related to photosynthetic energy production, day and night respiration rates were evaluated in leaves of GL- and HL-treated WT and *pgr5* plants (Figure 5 in Annex B). Day respiration was much higher in HL-treated WT plants than in HL-treated *pgr5*, in relation to their respective GL, but no differences between the genotypes or between the light treatment were observed during the recovery phase (Figure 5a in Annex B). O_2 uptake measurements were performed for 4 h in the dark in order to evaluate the importance of night respiration during the first night after the HL treatment (Figure 5b in Annex B). While the rate of decrease in O_2 uptake was equivalent in both GL-treated genotypes, HL-treated WT had a three-fold slower decrease in O_2 uptake rate compared to HL-treated *pgr5*, which in turn was similar to that of GL-treated plants (Figure 5b in Annex B). Additionally, night respiration was assessed to investigate possible differences in comparison to the day respiration (Figure 5c and 5d in Annex B). O_2 uptake during night-time respiration showed no significant changes for HL-treated WT throughout the experiment, whereas

in the *pgr5* mutants night-time respiration decreased in the second night after the HL treatment and was restored to the level of GL-treated plants by the following night (Figure 5d in Annex B).

4.5 Reactive oxygen species accumulation and oxidative stress in *pgr5* mutants after PSI photoinhibition

The relationship between PSI photoinhibition and oxidative stress was evaluated after GL and 1 h HL treatments of WT and *pgr5* mutant plants through several different approaches described below, which showed no major differences between the genotypes (Figure 7 in Annex A; Figures 4, 5, 6 and 7 in Annex C). The HL treatment induced membrane damage, which is a consistent marker of oxidative stress, in both genotypes; however, no differences were observed between the genotypes in either light treatment (Figure 4a in Annex C). H_2O_2 content showed no differences between genotypes or light treatments (Figure 4b in Annex C), and histochemical analysis showed similar accumulations of H_2O_2 (Figure 4c in Annex C) and superoxide (Figure 4d in Annex C) in both HL-treated WT and the HL-treated *pgr5* mutant. HL induced $^1O_2$ production, but no differences were observed between the WT and the *pgr5* mutant under both light conditions (Figure 7 in Annex A).

Total activities of Foyer-Halliwell-Asada cycle enzymes like superoxide dismutase (SOD), catalase (CAT), ascorbate peroxidase (APX), monodehydroascorbate reductase (MDHAR) and dehydroascorbate reductase (DHAR) were quantified. The only significant differences were increased MDHAR activity in the HL-treated WT, compared to *pgr5*, and increased DHAR activity in the HL-treated *pgr5* mutant, compared to WT. Additionally, higher CAT activity was detected in the *pgr5* mutant compared to the WT (Figures 5b, 5d and 5e in Annex C). The abundance of transcripts encoding enzymes in the Foyer-Halliwell-Asada cycle was also evaluated in WT and *pgr5* prior to HL treatment, as well as after 15 min and 1 h HL exposure. Most genes were upregulated by HL treatment in both WT and *pgr5* plants but, similarly to the enzyme activities, there were no strong differences between gene expression of the analysed enzymes in the two genotypes (Figure 6 in Annex C).

Lipid oxidation was also measured as a marker to evaluate the occurrence of oxidative stress. The results clearly show that 1 h HL treatment induces a decrease in the lipid oxidation levels of *pgr5* mutants (Figure 7 in Annex C). For example, the

content of thiobarbituric acid reactive substances (TBARS) was similar between the WT and the *pgr5* mutant under GL, but decreased only in the *pgr5* mutant after 1 h HL treatment (Figure 7a in Annex C). Similarly, the increased autoluminescence signal induced by HL occurred in the WT (Figure 7b and 7c in Annex C), while there was no corresponding increase in lipid peroxidation signal in HL-treated *pgr5*. Finally, the abundance of the chloroplast lipoxygenase (LOX-C) was shown to be lower in *pgr5* compared to the WT in both light treatments (Figure 7d in Annex C).

4.6 Chloroplast retrograde signalling in PSI-photoinhibited *pgr5* mutants

The effects of PSI photoinhibition on chloroplast retrograde signalling is closely related to results on ROS and lipid oxidation described above. The transcriptome profiles of *pgr5* mutants were shown to be severely altered during light stress and recovery. The low occurrence of oxidative stress in HL-treated *pgr5* plants were supported by an analysis of enriched Gene Ontology for Biological Process (GO-BP) terms in lists of genes differentially expressed in the mutants (Figure 5; Table 1 in Annex A). The results show that several GO-BP terms related to signalling and/or oxidative stress are downregulated in *pgr5* compared with WT under GL and even more after 1 h HL (Figure 5A; Table 1 in Annex A). Some of the 31 enriched GO-BP terms of downregulated genes in *pgr5* compared with WT under GL are “response to hydrogen peroxide” (GO:0042542), “response to reactive oxygen species” (GO:0000302), and “response to oxidative stress“ (GO:0006979), in addition to several other GO-BP terms related to stressful conditions and signalling (Figure 5A; Table 1 in Annex A). 62 GO-BP terms were enriched in downregulated genes in *pgr5* after 1 h HL treatment, compared with HL-treated WT. These include several terms related to lipid peroxidation and jasmonic acid metabolism. For example, 6 GO-BP terms directly related to jasmonic acid (JA) metabolism are present in the top 10 most enriched GO-BP terms of the list (Figure 5B; Table 1 in Annex A). Upregulated genes in GL-treated *pgr5* compared with WT contained no enriched GO-BP terms, and only five GO-BP terms were classified as statistically enriched genes upregulated in *pgr5* after HL treatment ("intracellular sequestrating of iron ion", "sequestrating of iron ion", “hormone metabolic process", "regulation of hormone levels", and "regulation of biological quality") using the criteria selected for this study (Figure 5C; Table 1 in Annex A).

In accordance with the analysis of enriched GO-BP terms, several specific genes related with oxylipin biosynthesis and signalling (e.g. lipoxygenases and JA signalling regulation factors), and abiotic stress response (e.g. heat shock protein chaperones and the cytosolic APX2) were strongly downregulated in *pgr5* mutants in comparison to the WT after 1 h HL (Table 2 in Annex A). Interestingly, even more genes in the list were further downregulated during the recovery treatment (1 h under GL after the 1 h of HL) in comparison to the 1 h HL treatment (Table 2 in Annex A). Additionally, a clustered heatmap of HL-responsive genes showed that approximately 400 genes induced by 12-oxophytodienoic acid (OPDA), which is an oxylipin hormone and chloroplast precursor for JA, were downregulated in *pgr5* compared to WT in the 1-h HL treatment and in the recovery (1 h of GL after 1 h HL) (Figure 5 in Annex A). In accordance, the relative quantification of OPDA showed that *pgr5* mutants indeed have a lower abundance than the WT before and after HL, as well as after 1 h recovery in GL (Figure 6 in Annex A). Transcriptomics analysis also revealed that H_2O_2-responsive genes were upregulated in both genotypes after 1 h HL treatment, but were under-expressed in *pgr5* compared to the WT. This is in accordance with results showing that PSI damage limits the occurrence of oxidative stress, suggesting compromised chloroplast retrograde signalling.

Figure 5 – Enriched Gene Ontology for Biological Process (GO-BP) terms in lists of genes differentially expressed in *pgr5* mutants.

Source: the author.

Genes in *pgr5* mutants treated with growth light (GL; 125 µmol m^{-2} s^{-1}; A) and high light (HL; 1000 µmol m^{-2} s^{-1}; B and C) for 1 h with expression values lower than 0.5 (downregulated; A and B) and higher than 2 (upregulated; C) compared to WT under the respective light treatments were submitted to the enrichment analysis tool of the Gene Ontology Consortium (http://geneontology.org) using Fisher's exact test with FDR correction (≤0.05). Only GO terms with fold enrichment values higher than 2.0 are shown.

5 DISCUSSION

The proper balance between light reactions and electron consumption is important to maintain fluent photosynthetic activity during environmental conditions that are constantly changing. When photosynthetic electron transport exceeds the capacity of electron acceptors, saturation of electron carriers in the photosynthetic electron transport chain can lead to the photoinhibition of photosystem II (PSII) and photosystem I (PSI). Both conditions are limiting for plant fitness and crop yield (BARBER; ANDERSSON, 1992; ADAMS et al., 2013; KROMDIJK et al., 2016; KAISER; MORALES; HARBINSON, 2018; SLATTERY et al., 2018), but much less is known about PSI photoinhibition in comparison to PSII photoinhibition. Although PSI has been considered to be more stable than PSII for most of the species and environmental conditions (BARTH; KRAUSE; WINTER, 2001; HUANG; ZHANG; CAO, 2010), PSI can be very sensitive to photodamage under certain conditions such as fluctuating light and chilling stress under moderate light, which are typical conditions in nature (SONOIKE, 1996, 2011; SCHELLER; HALDRUP, 2005). In this thesis, high light-treatments of Arabidopsis *pgr5* mutants were used to investigate the dynamics of PSI photoinhibition, and its consequences on photosynthetic electron transport, primary metabolism, ROS production and chloroplast retrograde signalling of plants during stress and recovery.

5.1 The role of PROTON GRADIENT REGULATION 5

Thanks to studies using the *pgr5* mutant, the importance of PGR5 in PSI protection has been slowly revealed over recent years. The role of PGR5 in limiting the overreduction of the acceptor side of PSI, thus preventing PSI photoinhibition, has been known for more than 17 years (MUNEKAGE et al., 2002). This function has been credited to the existence of a PGR5-mediated cyclic electron flow (CEF) around PSI (MUNEKAGE et al., 2002, 2004), which may be compared to the NADH dehydrogenase-like (NDH)-mediated CEF pathway (BURROWS et al., 1998; SHIKANAI et al., 1998). Despite this, there has been no direct demonstration that PGR5 is involved in electron transport to plastoquinone. Although the exact mechanism of PGR5 photoprotection of PSI is not known and the molecular function of this protein has not been fully resolved to date, there is a consensus about the role

of PGR5 in the establishment of the proton gradient (ΔpH) across the thylakoid membrane through lumen acidification. As a consequence, PGR5 has an essential role in preventing overreduction of the photosynthetic electron transport chain, and thus avoiding photoinhibition, by regulating the activation of NPQ and downregulation of electron flow through the cytochrome *b6f* complex (TIKHONOV, 2014; TIKKANEN; ARO, 2014). The exact function of PGR5 has been intensively investigated in many recent studies of rice and Arabidopsis *pgr5* mutants (SUORSA et al., 2012; TIWARI et al., 2016; YAMORI; MAKINO; SHIKANAI, 2016; KAWASHIMA et al., 2017; WADA et al., 2018; WANG; TAKAHASHI; SHIKANAI, 2018; YAMAMOTO; SHIKANAI, 2019). The current study did not aim at determining the mechanism of action of PGR5. Instead, the work in this thesis aimed to exploit the effect of PGR5 in photoprotection of PSI, using Arabidopsis *pgr5* mutants as an experimental tool to better understand the consequences of PSI photoinhibition. Nonetheless, the results presented here clearly show that PGR5 has an essential function in controlling the electron pressure at the donor side of PSI and in avoiding PSI photoinhibition.

5.2 PSI is rapidly photoinhibited and recovers slowly in high light-treated *pgr5* mutants

PSI photoinhibition has been previously reported under high irradiance and fluctuating light conditions in Arabidopsis and rice *pgr5* mutants (MUNEKAGE et al., 2002; SUORSA et al., 2012; KONO; NOGUCHI; TERASHIMA, 2014; KONO; TERASHIMA, 2016; TIWARI et al., 2016; YAMORI; MAKINO; SHIKANAI, 2016). In the current work, PSI photoinhibition was shown to occur rapidly under conditions of a severe imbalance between photosynthetic electron transport and acceptor capacity, as is the case for HL-treated *pgr5* mutant (Annex C). Indeed, several results in this thesis show that an exposure of *pgr5* mutants to HL (1000 μmol photons m^{-2} s^{-1}) for 15 min is enough to induce strong PSI photoinhibition followed by severe impairments on plant metabolism (Annexes A and C). Rapid inhibition of PSI in *pgr5* presumably occurred due to a rapid increase in the production of ROS that subsequently inactivated the PSI FeS clusters (SONOIKE, 2011). This result demonstrates the susceptibility of PSI to photoinhibition, in spite of the fully operational ROS detoxification network including SOD and ascorbate cycle enzymes in *pgr5* (Annex C).

Previous studies with plants of different species treated with chilling stress under moderate light showed that PSI damage takes much more time to fully recover its activity when compared to PSII (LI et al., 2004; ZHANG; SCHELLER, 2004; ZHANG et al., 2011). For this reason, PSI photoinhibition is believed to have more severe consequences than PSII photoinhibition in higher plants (TAKAGI et al., 2016a; HUANG et al., 2017). The results in the current study highlight the importance of PGR5-dependent regulation of the ΔpH across the thylakoid membrane to avoid PSI photoinhibition under natural environmental conditions by showing that PSI recovers very slowly in Arabidopsis *pgr5* mutants treated with high light or fluctuating light (Figure 4; Annexes A and B). Gradual recovery of Pm in PSI-photoinhibited plants (HL-treated *pgr5* plants) was accompanied by gradual recovery of CO_2 assimilation measured under low light, which was restored to the pre-treatment level after 3 days of recovery (Annex B). This demonstrates that, although the PSI pool of HL-treated *pgr5* mutants experienced severe photoinhibition, CO_2 assimilation was still possible, which allowed plants to recover (Annex B). PSI functionality despite severe photoinhibition was probably partly enabled by LHCII phosphorylation, which increases the quantity of excitation directed towards PSI (WIENTJES; VAN AMERONGEN; CROCE, 2013; GRIECO et al., 2015), improving the efficiency of PSI (TIWARI et al., 2016). These observations may also suggest recruitment of a hypothetical reserve of PSI in order to support electron transport under conditions of damaged PSI that was evident in HL-treated *pgr5* mutants (Annex B). Indeed, a stable intermediate in PSI assembly named PSI*, that contains only a specific subset of the PSI core subunits, (OZAWA; ONISHI; TAKAHASHI, 2010; WITTENBERG et al., 2017; MARCO et al., 2018) is a candidate to restore PSI function by renewing the damaged PSI pool. However, further experiments are necessary to test this hypothesis.

5.3 PSI photoinhibition and recovery affects photosynthetic electron transport and limits electron flow to PSI acceptor side

The results obtained here show that PSI photoinhibition was accompanied by changes in other components of the photosynthetic electron transport chain. For example, HL clearly induced photoinhibition not only of PSI but also of PSII in *pgr5* as measured by maximum chlorophyll *a* fluorescence (Fm). However, these results were expected because the effects of HL on PSII photoinhibition has been known for a long

time (reviewed in Aro et al., 1993; Gururani et al., 2015). Indeed, not only *pgr5* mutants but also the WT experienced some level of PSII damage in all HL-treatments. The photoinhibition of PSII was however much less severe than PSI photoinhibition in HL-treated *pgr5*, as shown by the relative difference between PSII and PSI parameters after HL. This is due to over-reduction of the intersystem when PSI is inactivated.

Several results in this thesis provide strong evidence that PSI photoinhibition limits electron flow to its acceptors. For example, ferredoxin (Fd) capacity was strongly decreased in HL-treated *pgr5* plants and followed the same recovery pattern as for PSI capacity, as shown by a strong positive correlation between the maximal reduction state of Fd (Fdm) and Pm. However, no changes were observed for the plastocyanin (PC) capacity during PSI photoinhibition or during its recovery (Annex B). Interestingly, the oxidation of Fd pool was not associated with any changes in thylakoid Fd abundance (Figure S2 in Annex B), rather suggesting that inhibited PSI was unable to reduce its primary electron acceptor Fd. The low capacity for reduction of the Fd pool, and the normal capacity of oxidation of the PC pool, which directly donates electrons to PSI, both under conditions of PSI photoinhibition (Annex B), are key evidences that PSI photoinhibition limits electron flow to PSI acceptors. These observations were supported by the findings of low limitation of electron transfer to the donor (lumenal) side of PSI (Y(ND)) and high limitation of electron transfer from the acceptor (stromal) side of PSI (Y(NA)) in *pgr5* mutants under HL. This means that, under conditions of PSI photoinhibition, electrons are delivered to PSI but do not efficiently flow to downstream pathways. Indeed, the metabolic events downstream of PSI presented as results in this study were clearly downregulated in the PSI-photoinhibited plants used in this thesis. For example, CO_2 assimilation was clearly negatively affected by PSI inhibition in HL-treated *pgr5* leaves in the current study (Annexes A, B and C). Consequently, other downstream pathways dependent on CO_2 assimilation were also downregulated in HL-treated *pgr5* mutants. This is the case, for example, for sugar and starch accumulation, and mitochondrial respiration. Low PSI-dependent ROS production were also observed in *pgr5* mutants under HL (Annexes A and C), indicating that the O_2 reduction rate was also downregulated as a consequence of PSI inhibition, similarly to the other PSI downstream pathways. Furthermore, low lipid oxidation and attenuated chloroplast signalling mediated by oxylipins in HL-treated *pgr5* may also be effects of limited PSI electron transport. These events are summarised as a hypothetical scheme showing the limitation in electron flow to the

PSI acceptor side and the dependent metabolism involved (Figure 6), which are discussed in the following sections.

Figure 6 – Causes and consequences of PSI photoinhibition on plant metabolism observed in this thesis.

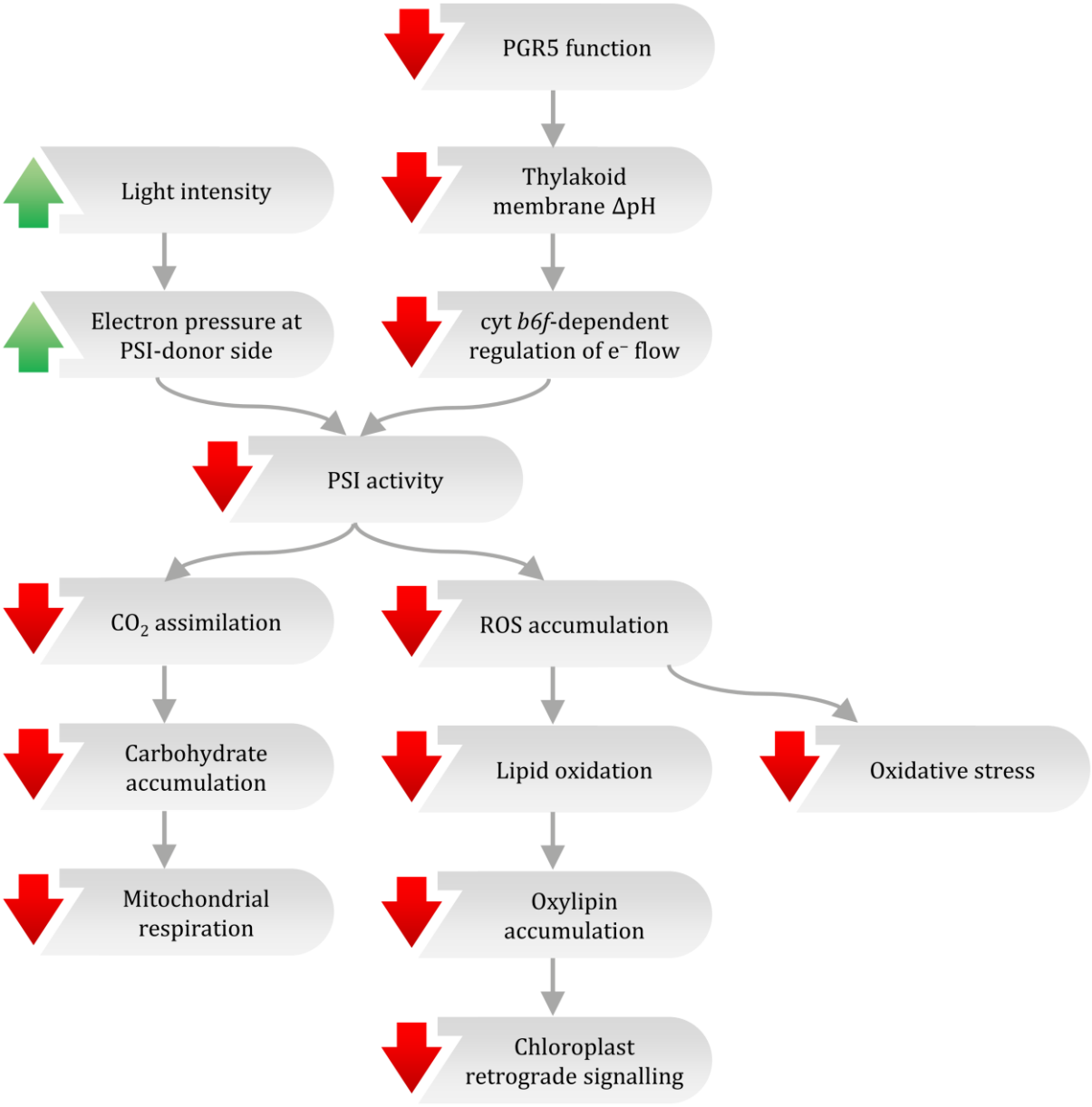

Source: the author.

5.4 PSI photoinhibition induces a strong metabolic penalty

The current studies highlight the sustained negative impact of PSI photoinhibition on plant metabolism, including metabolic processes directly related to

crop production like CO_2 assimilation, carbohydrates accumulation and mitochondrial respiration. The current results show that HL-treated *pgr5* mutants have low CO_2 assimilation rates, as previously reported (MUNEKAGE; GENTY; PELTIER, 2008; NISHIKAWA et al., 2012). The primary reason for the low CO_2 assimilation in HL-treated *pgr5* mutants was probably the effect of severe PSI photoinhibition on limiting the stromal content of NADPH to supply the CBB cycle. A secondary reason may have been the low reduction levels of the stromal thioredoxin network mediated by the ferredoxin-thioredoxin reductase (FTR), resulting in an impaired redox activation of the CBB cycle enzymes under non-saturating light conditions (HALDRUP; LUNDE; SCHELLER, 2003; NIKKANEN; TOIVOLA; RINTAMÄKI, 2016; SOUZA et al., 2018).

PSI photoinhibition also induced altered carbohydrate metabolism. The data show diminished starch accumulation during HL treatment of *pgr5* mutants, as well as during recovery under GL conditions (Annexes A and B). Starch synthesis can serve as a transient sink to allocate excess reducing power, like under HL conditions (PAUL; FOYER, 2001), suggesting a lack of excess reductants after PSI photoinhibition that is consistent with diminished PSI activity. Although *pgr5* mutants were able to synthesize D-glucose and D-fructose, the concentration increases for these sugars were half of those observed for WT leaves. Changes in leaf starch concentration could also be correlated with lower accumulations of D-glucose and D-fructose in *pgr5* during HL treatments, as starch synthesis has been linked to soluble sugar concentrations (PAUL; FOYER, 2001). The fact that the sugar concentrations quickly decreased after the HL treatment mainly in *pgr5* mutants may be related to the plant's demand for energy to recover from HL stress. This would be in agreement with results observed during the recovery phase, in which HL-treated plants, mainly the *pgr5* mutants, slowly recover their starch concentration to the GL levels (Annex B). In addition, the lower starch concentration was an expected result in HL-treated *pgr5* mutants because CO_2 assimilation decreased as a consequence of PSI photoinhibition.

The data presented here demonstrate that PSI damage in HL-treated *pgr5* mutants also limits mitochondrial respiration during both day and night (Annex C), in accordance with other recently published data (FLOREZ-SARASA et al., 2016). Although the regulatory link between mitochondria and photosynthesis has been demonstrated through different pathways and mechanisms, many fundamental questions regarding this cross-talk are unanswered. For example, little is known about the consequences of PSI photoinhibition on plant respiration and the role of

mitochondria, an important source of energy in the cell, on PSI recovery. It is well accepted that reducing equivalents generated in the chloroplasts can be transported to other locations in the cell, including mitochondria, via shuttle machineries such as the malate/oxaloacetate shuttle (HEINEKE et al., 1991; RAGHAVENDRA; PADMASREE, 2003; SCHEIBE, 2004; VISHWAKARMA et al., 2015; ALRIC; JOHNSON, 2017). Specifically, carbohydrates produced from photosynthesis can generate respiratory substrates for the mitochondria like malate and pyruvate through cytosolic glycolysis (O'LEARY; PLAXTON, 2016; O'LEARY et al., 2017), making mitochondria important electron sinks during conditions of high electron pressure in the chloroplast transport electron chain. Recently, night-time leaf respiration rate has been shown to correlate with stored carbon substrates, including starch, in Arabidopsis (O'Leary et al. 2017). These observations are in agreement with the lower mitochondrial respiration caused by lower carbohydrate synthesis in PSI-photoinhibited *pgr5* mutants, which in turn was a consequence of low CO_2 assimilation. Indeed, the plant mitochondrial respiration is mostly dependent on carbohydrates (PLAXTON; PODESTÁ, 2006). Thus, the low mitochondrial activity in HL-treated *pgr5* mutants may be a consequence of low malate/oxaloacetate shuttle activity and low carbohydrate availability, both being consequences of low PSI activity.

5.5 PSI photoinhibition prevents oxidative stress

Photosynthetic electron transport generally occurs in an oxygen-rich environment, and the transfer of electrons or energy to oxygen is a frequent occurrence. Thus, the photosynthetic electron transport chain is associated with the generation of ROS which, although important in plant signalling, can cause oxidative stress when accumulated in cells (CZARNOCKA; KARPIŃSKI, 2018; FOYER, 2018; MULLINEAUX et al., 2018). The results presented here show no greater occurrence of oxidative stress in PSI-photoinhibited plants, compared with control plants, with the exception of PSI photoinhibition itself that is thought to occur through oxidative inactivation of FeS clusters. Additionally, the data clearly show lower lipid oxidation in HL-treated *pgr5* compared to HL-treated WT, which is attributed to lower oxidative stress (MUELLER, 2004; MOSBLECH; FEUSSNER; HEILMANN, 2009; WASTERNACK; HAUSE, 2013) (Annex: Annex C) and under-expression of genes associated with H_2O_2 signalling (Annex A). The absence of any abnormally high

accumulation of ROS or oxidative stress in HL-treated *pgr5* could be the result of an efficient scavenging and antioxidant system. However, no substantial increase in ROS scavenging capacity was observed in the PSI-photoinhibited plants (Annex C). Instead, the results shown here suggest that the rapid occurrence of PSI photoinhibition stops the transfer of electrons to O_2, thus preventing excess production of ROS. In accordance, a recent study showed that the production rate and the accumulation of ROS is probably not related to PSI photoinhibition (TAKAGI et al., 2016a). Furthermore, the same study suggests that the ROS production site, rather than the quantity of ROS, is critical for PSI photoinhibition (TAKAGI et al., 2016a), which is in accordance with the results presented here. Therefore, PSI photoinhibition seems to prevent oxidative stress by downregulating ROS production because the inactivated PSI pool is probably unable to donate electrons to molecular oxygen. This hypothesis is in line with the other results of this thesis which show that photoinhibition of PSI blocks the electron flow to its electron acceptors, impairing their downstream events.

ROS and their oxidation products generated in chloroplasts can also serve as important signalling mechanisms for plant reprogramming, which is required to face changes in the environment (GEIGENBERGER; FERNIE, 2014; GOLLAN; TIKKANEN; ARO, 2015; DIETZ; TURKAN; KRIEGER-LISZKAY, 2016). The results presented here clearly show that oxylipin signalling, which is a chloroplast retrograde signalling pathway dependent on lipid peroxidation (PINTÓ-MARIJUAN; MUNNÉ-BOSCH, 2014; SATOH et al., 2014; GOLLAN; TIKKANEN; ARO, 2015; SAVCHENKO et al., 2017), was severely affected in the *pgr5* mutant, being more evident under HL, when this pathway is activated in WT plants (Figure 3; Annex A). The oxylipin metabolic pathway includes the 12-oxophytodienoic acid (OPDA), which is produced in the chloroplast from polyunsaturated fatty acids, after enzymatic peroxidation by lipoxygenase (LOX) (HOWE, 2018). Both, OPDA and chloroplastic LOX, were shown to be downregulated in *pgr5* mutants under GL and HL (Annexes A and C), in line with the disrupted oxylipin-dependent chloroplast signalling observed in the mutant. The lower levels of lipid peroxidation observed in HL-treated *pgr5* (Annex C) are also in line with its downregulated oxylipin-dependent chloroplast signalling since lipid peroxidation is an early step in enzymatic oxylipin synthesis and provides the material for oxylipin production (MUELLER, 2004; MOSBLECH; FEUSSNER; HEILMANN, 2009; WASTERNACK; HAUSE, 2013). These findings, in addition to the consistent results about the photoinhibition of PSI in the HL-treated *pgr5* mutants, suggest that

PSI activity is important for chloroplast retrograde signalling through both the oxylipin-dependent and H_2O_2-dependent pathways.

6 CONCLUDING REMARKS AND FUTURE PERSPECTIVES

This thesis investigated the detrimental impact of photosynthetic imbalance on PSI and revealed important details about the depletion and restoration of photosynthesis and primary metabolism after severe PSI photoinhibition. The data presented here show new insights into the occurrence of PSI photoinhibition and its negative consequences on plant metabolism and chloroplast retrograde signalling. Highlight findings of this thesis were:

1. High light treatment of the *pgr5* mutants is a valuable model for the study of PSI photoinhibition and recovery, as well as the study of related phenomena including the reduction state of photosynthetic electron carriers;

2. PSI photoinhibition is rapidly induced under conditions of reduction-pressure imbalance between PSI donor and acceptor sides, which severely inhibits CO_2 fixation, carbohydrate accumulation and mitochondrial respiration;

3. Plants are able to rapidly recover their CO_2 fixation despite PSI inhibition, by improving PSI efficiency through LHCII phosphorylation and activation of “reserve” PSI;

4. Chloroplast regulation of nuclear gene expression is dependent on PSI activity under high light stress through enzymatic oxylipin synthesis and H_2O_2 production;

5. Inactivation of PSI can be a protective mechanism against oxidative stress in the chloroplast stroma and in the wider cell by preventing ROS over-production.

Although the use of *pgr5* mutant combined with high light treatments has been shown in this thesis and in literature as a very good model for studying PSI photoinhibition, future work on this topic involving other model systems could strengthen the conclusions obtained here. For example, the use of other mutants with

compromised PSI activity and/or protection, or other methods for inducing PSI photoinhibition (SEJIMA et al., 2014; TIKKANEN; GREBE, 2018), are promising perspective for deepening the knowledge on PSI photoinhibition. In addition, ongoing work to determine the exact function of the PGR5 protein opens a vast field for exploration and should receive more research attention.

This study strengthens the importance of regulation of balance between the photosynthetic light reactions and CO_2 fixation, which is vital for normal photosynthesis, carbon metabolism and chloroplast signalling, thus contributing to plant fitness. Some attempts for plant improvement focusing on upregulation of photosynthetic electron transfer have neglected the importance of developing strong electron sinks, including the maintenance of CO_2 assimilation and carbohydrate metabolism. Findings in this thesis show that strong electron sinks and protection of the stromal components of photosynthesis are ultimately important. In addition, these events are essential for the maintenance and protection of the electron transport chain at the thylakoid membrane. Therefore, this thesis highlights the importance of considering the prospect of damage and recovery of PSI, and the consequent impact on plant metabolism, as well as the importance of balancing photosynthetic electron transfer in thylakoids with stromal sink strength, during development of bioengineering strategies designed to improve yield in crop plants.

REFERENCES

ADAMS, W. W. et al. May photoinhibition be a consequence, rather than a cause, of limited plant productivity? **Photosynthesis Research**, Dordrecht, v. 117, p. 31–44, 2013.

ALLAKHVERDIEV, S. I.; MURATA, N. Environmental stress inhibits the synthesis de novo of proteins involved in the photodamage-repair cycle of Photosystem II in Synechocystis sp. PCC 6803. **Biochimica et Biophysica Acta**, Amsterdam, v. 1657, p. 23–32, 2004.

ALRIC, J.; JOHNSON, X. Alternative electron transport pathways in photosynthesis: a confluence of regulation. **Current Opinion in Plant Biology**, Oxford, v. 37, p. 78–86, 2017.

AMUNTS, A.; DRORY, O.; NELSON, N. The structure of a plant photosystem I supercomplex at 3.4 Å resolution. **Nature**, London, v. 447, p. 58–63, 2007.

AMUNTS, A.; NELSON, N. Plant photosystem I design in the light of evolution. **Structure**, Oxford, v. 17, p. 637–650, 2009.

APEL, K.; HIRT, H. Reactive oxygen species: metabolism, oxidative stress, and signal transduction. **Annual Review of Plant Biology**, Palo Alto, v. 55, p. 373–399, 2004.

ARO, E. M.; VIRGIN, I.; ANDERSSON, B. Photoinhibition of photosystem II. Inactivation, protein damage and turnover. **Biochimica et Biophysica Acta**, Amsterdam, v. 1143, p. 113–134, 1993.

ASADA, K. The water-water cycle in chloroplasts: scavenging of active oxygens and dissipation of excess photons. **Annual Review of Plant Physiology and Plant Molecular Biology**, Palo Alto, v. 50, p. 601–639, 1999.

ASADA, K. The water-water cycle as alternative photon and electron sinks. **Philosophical Transactions of the Royal Society B: Biological Sciences**, London, v. 355, p. 1419–1431, 2000.

ASADA, K.; KISO, K.; YOSHIKAWA, K. Univalent reduction of molecular oxygen by spinach chloroplasts on illumination. **The Journal of Biological Chemistry**, Baltimore, v. 249, p. 2175–2181, 1974.

BARBER, J.; ANDERSSON, B. Too much of a good thing : light can be bad for photosynthesis. **Trends in Biochemical Sciences**, Amsterdam, v. 17, p. 61–66, 1992.

BARTH, C.; KRAUSE, G. H.; WINTER, K. Responses of photosystem I compared with photosystem II to high-light stress in tropical shade and sun leaves. **Plant, Cell and Environment**, Oxford, v. 24, p. 163–176, 2001.

BARTH, P.; LAGOUTTE, B.; SÉTIF, P. Ferredoxin reduction by photosystem I from Synechocystis sp. PCC 6803: toward an understanding of the respective roles of

subunits PsaD and PsaE in ferredoxin binding. **Biochemistry**, Washington, v. 37, p. 16233–16241, 1998.

BEERS, R. F.; SIZER, I. W. A spectrophotometric method for measuring the breakdown of hydrogen peroxide by catalase. **The Journal of Biological Chemistry**, Baltimore, v. 195, p. 133–140, 1952.

BEN-SHEM, A.; FROLOW, F.; NELSON, N. Crystal structure of plant photosystem I. **Nature**, London, v. 426, p. 630–635, 2003.

BENSON, A. A. et al. The path of carbon in photosynthesis. V. Paper chromatography and radioautography of the products. **Journal of the American Chemical Society**, Washington, v. 72, p. 1710–1718, 1950.

BEZOUWEN, L. S. Van et al. Subunit and chlorophyll organization of the plant photosystem II supercomplex. **Nature Plants**, London, v. 3, p. 17080, 2017.

BIENERT, G. P. et al. Specific aquaporins facilitate the diffusion of hydrogen peroxide across membranes. **The Journal of Biological Chemistry**, Baltimore, v. 282, p. 1183–1192, 2007.

BIRTIC, S. et al. Using spontaneous photon emission to image lipid oxidation patterns in plant tissues. **The Plant Journal**, Oxford, v. 67, p. 1103–1115, 2011.

BLUM, A.; EBERCON, A. Cell membrane stability as a measure of drought and heat tolerance in wheat. **Crop Science**, Madison, v. 21, p. 43–47, 1981.

BOOIJ-JAMES, I. S. et al. Ultraviolet-B radiation impacts light-mediated turnover of the photosystem II reaction center heterodimer in Arabidopsis mutants altered in phenolic metabolism. **Plant Physiology**, Rockville, v. 124, p. 1275–1283, 2000.

BRESTIC, M. et al. Low PSI content limits the photoprotection of PSI and PSII in early growth stages of chlorophyll b -deficient wheat mutant lines. **Photosynthesis Research**, Dordrecht, v. 125, p. 151–166, 2015.

BRICKER, T. M. et al. The extrinsic proteins of photosystem II. **Biochimica et Biophysica Acta**, Amsterdam, v. 1817, p. 121–142, 2012.

BUCHANAN, B. B. The path to thioredoxin and redox regulation beyond chloroplasts. **Annual Review of Plant Biology**, Palo Alto, v. 67, p. 1–24, 2016.

BURROWS, P. A. et al. Identification of a functional respiratory complex in chloroplasts through analysis of tobacco mutants containing disrupted plastid ndh genes. **The EMBO Journal**, Heidelberg, v. 17, p. 868–876, 1998.

BUSCH, A.; HIPPLER, M. The structure and function of eukaryotic photosystem I. **Biochimica et Biophysica Acta**, Amsterdam, v. 1807, p. 864–877, 2011.

CASHMAN, D. J. et al. Molecular interactions between photosystem I and ferredoxin: an integrated energy frustration and experimental model. **Journal of Molecular Recognition**, New York, v. 27, p. 597–608, 2014.

CAZZANIGA, S. et al. Interaction between avoidance of photo absroption, excess energy dissipation and zeaxanthin synthesis against photooxidative stress in Arabidopsis. **The Plant Journal**, Oxford, v. 76, p. 568–579, 2013.

ČERNÝ, M. et al. Hydrogen peroxide: its role in plant biology and crosstalk with signalling networks. **International Journal of Molecular Sciences**, Basel, v. 19, p. 2812, 2018.

CHINI, A. et al. Redundancy and specificity in jasmonate signalling. **Current Opinion in Plant Biology**, Oxford, v. 33, p. 147–156, 2016.

CHITNIS, P. R. Photosystem I: function and physiology. **Annual Review of Plant Physiology and Plant Molecular Biology**, Palo Alto, v. 52, p. 593–626, 2001.

CZARNOCKA, W.; KARPIŃSKI, S. Friend or foe? Reactive oxygen species production, scavenging and signaling in plant response to environmental stresses. **Free Radical Biology and Medicine**, New York, v. 122, p. 4–20, 2018.

DALCORSO, G. et al. A complex containing PGRL1 and PGR5 is involved in the switch between linear and cyclic electron flow in Arabidopsis. **Cell**, New York, v. 132, p. 273–285, 2008.

DALOSO, D. M. et al. Metabolism within the specialized guard cells of plants. **New Phytologist**, Cambridge, v. 216, p. 1018–1033, 2017.

DAT, J. et al. Dual action of the active oxygen species during plant stress responses. **Cellular and Molecular Life Sciences**, Basel, v. 57, p. 779–795, 2000.

DEMMIG-ADAMS, B.; ADAMS, W. W. Photoprotection and other responses of plants to high light stress. **Annual Review of Plant Physiology and Plant Molecular Biology**, Palo Alto, v. 43, p. 599–626, 1992.

DEVIREDDY, A. R. et al. Coordinating the overall stomatal response of plants: rapid leaf-to-leaf communication during light stress. **Science Signaling**, Washington, v. 11, p. eaam9514, 2018.

DIETZ, K.-J.; TURKAN, I.; KRIEGER-LISZKAY, A. Redox- and reactive oxygen species-dependent signaling into and out of the photosynthesizing chloroplast. **Plant Physiology**, Rockville, v. 171, p. 1541–1550, 2016.

DRIEVER, S. M.; BAKER, N. R. The water-water cycle in leaves is not a major alternative electron sink for dissipation of excess excitation energy when CO2 assimilation is restricted. **Plant, Cell and Environment**, Oxford, v. 34, p. 837–846, 2011.

EVANS, J. R. et al. Resistances along the CO2 diffusion pathway inside leaves. **Journal of Experimental Botany**, Oxford, v. 60, p. 2235–2248, 2009.

EVANS, J. R.; VON CAEMMERER, S. Carbon Dioxide Diffusion inside Leaves. **Plant Physiology**, Rockville, v. 110, p. 339–346, 1996.

EXPOSITO-RODRIGUEZ, M. et al. Photosynthesis-dependent H2O2 transfer from

chloroplasts to nuclei provides a high-light signalling mechanism. **Nature Communications**, London, v. 8, p. 1–10, 2017.

FISCHER, R. A. T.; EDMEADES, G. O. Breeding and cereal yield progress. **Crop Science**, Madison, v. 50, p. S85–S98, 2010.

FLOREZ-SARASA, I. et al. Impaired cyclic electron flow around photosystem I disturbs high-light respiratory metabolism. **Plant Physiology**, Rockville, v. 172, p. 2176–2189, 2016.

FOYER, C. H. Reactive oxygen species, oxidative signaling and the regulation of photosynthesis. **Environmental and Experimental Botany**, New York, v. 154, p. 134–142, 2018.

FOYER, C. H.; HALLIWELL, B. The presence of glutathione and glutathione reductase in chloroplasts: a proposed role in ascorbic acid metabolism. **Planta**, Berlin, v. 133, p. 21–25, 1976.

FOYER, C. H.; NOCTOR, G. Redox sensing and signalling associated with reactive oxygen in chloroplasts, peroxisomes and mitochondria. **Physiologia Plantarum**, Oxford, v. 119, p. 355–364, 2003.

FOYER, C. H.; NOCTOR, G. Redox regulation in photosynthetic organisms: signaling, acclimation, and practical implications. **Antioxidants & Redox Signaling**, New Rochelle, v. 11, p. 861–905, 2009.

FOYER, C. H.; RUBAN, A. V.; NIXON, P. J. Photosynthesis solutions to enhance productivity. **Philosophical Transactions of the Royal Society B: Biological Sciences**, London, v. 372, p. 3–6, 2017.

FOYER, C. H.; SHIGEOKA, S. Understanding oxidative stress and antioxidant functions to enhance photosynthesis. **Plant Physiology**, Rockville, v. 155, p. 93–100, 2011.

GEIGENBERGER, P.; FERNIE, A. R. Metabolic control of redox and redox control of metabolism in plants. **Antioxidants & Redox Signaling**, New Rochelle, v. 21, p. 1389–1421, 2014.

GIANNOPOLITIS, C. N.; REIS, S. K. Superoxide dismutases. I. Occurrence in higher plants. **Plant Physiology**, Rockville, v. 59, p. 309–314, 1977.

GOLBECK, J. H. Structure and function of photosystem I. **Annual Review of Plant Physiology and Plant Molecular Biology**, Palo Alto, v. 43, p. 293–324, 1992.

GOLLAN, P. J.; TIKKANEN, M.; ARO, E.-M. Photosynthetic light reactions: integral to chloroplast retrograde signalling. **Current Opinion in Plant Biology**, Oxford, v. 27, p. 180–191, 2015.

GOSS, R.; JAKOB, T. Regulation and function of xanthophyll cycle-dependent photoprotection in algae. **Photosynthesis Research**, Dordrecht, v. 106, p. 103–122, 2010.

GOVINDJEE; SHEVELA, D.; BJÖRN, L. O. Evolution of the Z-scheme of photosynthesis: a perspective. **Photosynthesis Research**, Dordrecht, v. 133, p. 5–15, 2017.

GRIECO, M. et al. Steady-state phosphorylation of light-harvesting complex II proteins preserves photosystem I under fluctuating white light. **Plant Physiology**, Rockville, v. 160, p. 1896–1910, 2012.

GRIECO, M. et al. Light-harvesting II antenna trimers connect energetically the entire photosynthetic machinery - including both photosystems II and I. **Biochimica et Biophysica Acta**, Amsterdam, v. 1847, p. 607–619, 2015.

GURURANI, M. A.; VENKATESH, J.; TRAN, L.-S. P. Regulation of photosynthesis during abiotic stress-induced photoinhibition. **Molecular Plant**, Oxford, v. 8, p. 1304–1320, 2015.

HALDRUP, A.; LUNDE, C.; SCHELLER, H. V. Arabidopsis thaliana plants lacking the PSI-D subunit of photosystem I suffer severe photoinhibition, have unstable photosystem I complexes, and altered redox homeostasis in the chloroplast stroma. **The Journal of Biological Chemistry**, Baltimore, v. 278, p. 33276–33283, 2003.

HALLIWELL, B. Reactive species and antioxidants. Redox biology is a fundamental theme of aerobic life. **Plant Physiology**, Rockville, v. 141, p. 312–322, 2006.

HAVIR, E. A.; MCHALE, N. A. Biochemical and Developmental Characterization of Multiple Forms of Catalase in Tobacco Leaves. **Plant Physiology**, Rockville, v. 84, p. 450–455, 1987.

HEATH, R. L.; PACKER, L. Photoperoxidation in isolated chloroplasts. I. Kinects and stoichiometry of fatty acid peroxidation. **Archives of Biochemistry and Biophysics**, Amsterdam, v. 125, p. 189–198, 1968.

HEINEKE, D. et al. Redox transfer across the inner chloroplast envelope membrane. **Plant Physiology**, Rockville, v. 95, p. 1131–1137, 1991.

HODGES, M. et al. Perspectives for a better understanding of the metabolic integration of photorespiration within a complex plant primary metabolism network. **Journal of Experimental Botany**, Oxford, v. 67, p. 3015–3026, 2016.

HOLUB, P. et al. Induction of phenolic compounds by UV and PAR is modulated by leaf ontogeny and barley genotype. **Plant Physiology and Biochemistry**, Amsterdam, v. 134, p. 81–93, 2019.

HOSSAIN, M. A.; NAKANO, Y.; ASADA, K. Monodehydroascorbate reductase in spinach chloroplasts and its participation in regeneration of ascorbate for scavenging hydrogen peroxide. **Plant and Cell Physiology**, Oxford, v. 25, p. 385–395, 1984.

HOWE, G. A. Metabolic end run to jasmonate. **Nature Chemical Biology**, London, v. 14, p. 109–110, 2018.

HUANG, W. et al. Superoxide generated in the chloroplast stroma causes photoinhibition of photosystem I in the shade-establishing tree species Psychotria

henryi. **Photosynthesis Research**, Dordrecht, v. 132, p. 293–303, 2017.

HUANG, W.; TIKKANEN, M.; ZHANG, S.-B. Photoinhibition of photosystem I in Nephrolepis falciformis depends on reactive oxygen species generated in the chloroplast stroma. **Photosynthesis Research**, Dordrecht, v. 137, p. 129–140, 2018.

HUANG, W.; ZHANG, S.-B.; CAO, K.-F. The different effects of chilling stress under moderate light intensity on photosystem II compared with photosystem I and subsequent recovery in tropical tree species. **Photosynthesis Research**, Dordrecht, v. 103, p. 175–182, 2010.

INOUE, K.; SAKURAI, H.; HIYAMA, T. Photoinactivation sites of photosystem I in isolated chloroplasts. **Plant and Cell Physiology**, Oxford, v. 27, p. 961–968, 1986.

JÄRVI, S. et al. Optimized native gel systems for separation of thylakoid protein complexes: novel super- and mega-complexes. **Biochemical Journal**, London, v. 439, p. 207–214, 2011.

JÄRVI, S.; SUORSA, M.; ARO, E.-M. Photosystem II repair in plant chloroplasts - Regulation, assisting proteins and shared components with photosystem II biogenesis. **Biochimica et Biophysica Acta**, Amsterdam, v. 1847, p. 900–909, 2015.

JENSEN, P. E. et al. Structure, function and regulation of plant photosystem I. **Biochimica et Biophysica Acta**, Amsterdam, v. 1767, p. 335–352, 2007.

JOLIOT, P.; JOHNSON, G. N. Regulation of cyclic and linear electron flow in higher plants. **Proceedings of the National Academy of Sciences of the United States of America**, Washington, v. 108, p. 13317–13322, 2011.

KAISER, E.; MORALES, A.; HARBINSON, J. Fluctuating light takes crop photosynthesis on a rollercoaster ride. **Plant Physiology**, Rockville, v. 176, p. 977–989, 2018.

KALE, R. et al. Amino acid oxidation of the D1 and D2 proteins by oxygen radicals during photoinhibition of Photosystem II. **Proceedings of the National Academy of Sciences of the United States of America**, Washington, v. 201618922, p. 1–6, 2017.

KANEHISA, M.; GOTO, S. KEGG: Kyoto Encyclopedia of Genes and Genomes. **Nucleic Acids Research**, Oxford, v. 28, p. 27–30, 2000.

KAPOOR, K. et al. Binding Mechanisms of Electron Transport Proteins with Cyanobacterial Photosystem I: An Integrated Computational and Experimental Model. **The Journal of Physical Chemistry B**, Washington, v. 122, p. 1026–1036, 2018.

KASAHARA, M. et al. Chloroplast avoidance movement reduces photodamage in plants. **Nature**, London, v. 420, p. 829–832, 2002.

KATO, Y. et al. Cooperative D1 Degradation in the Photosystem II Repair Mediated

by Chloroplastic Proteases in Arabidopsis. **Plant Physiology**, Rockville, v. 159, p. 1428–1439, 2012.

KAWASHIMA, R. et al. Relative contributions of PGR5- and NDH-dependent photosystem I cyclic electron flow in the generation of a proton gradient in Arabidopsis chloroplasts. **Planta**, Berlin, v. 246, p. 1045–1050, 2017.

KLUGHAMMER, C.; SCHREIBER, U. Measuring P700 absorbance changes in the near infrared spectral region with a dual wavelength pulse modulation system. In: GARAB, G. (Ed.). **Photosynthesis: Mechanisms and Effects**. Dordrecht: Springer Netherlands, 1998. p. 4357–4360.

KLUGHAMMER, C.; SCHREIBER, U. Deconvolution of ferredoxin, plastocyanin, and P700 transmittance changes in intact leaves with a new type of kinetic LED array spectrophotometer. **Photosynthesis Research**, Dordrecht, v. 128, p. 195–214, 2016.

KÖLLING, K. et al. Carbon partitioning in Arabidopsis thaliana is a dynamic process controlled by the plants metabolic status and its circadian clock. **Plant, Cell and Environment**, Oxford, v. 38, p. 1965–1979, 2015.

KONO, M.; NOGUCHI, K.; TERASHIMA, I. Roles of the cyclic electron flow around PSI (CEF-PSI) and O2-dependent alternative pathways in regulation of the photosynthetic electron flow in short-term fluctuating light in Arabidopsis thaliana. **Plant and Cell Physiology**, Oxford, v. 55, p. 990–1004, 2014.

KONO, M.; TERASHIMA, I. Elucidation of photoprotective mechanisms of PSI against fluctuating light photoinhibition. **Plant and Cell Physiology**, Oxford, v. 57, p. 1405–1414, 2016.

KOZULEVA, M. A.; IVANOV, B. N. The mechanisms of oxygen reduction in the terminal reducing segment of the chloroplast photosynthetic electron transport chain. **Plant and Cell Physiology**, Oxford, v. 57, p. 1397–1404, 2016.

KRIEGER-LISZKAY, A. Singlet oxygen production in photosynthesis. **Journal of Experimental Botany**, Oxford, v. 56, p. 337–346, 2005.

KROMDIJK, J. et al. Improving photosynthesis and crop productivity by accelerating recovery from photoprotection. **Science**, Washington, v. 354, p. 857–861, 2016.

KUDOH, H.; SONOIKE, K. Irreversible damage to photosystem I by chilling in the light: cause of the degradation of chlorophyll after returning to normal growth temperature. **Planta**, Berlin, v. 215, p. 541–548, 2002.

LAWSON, T.; BLATT, M. R. Stomatal size, speed, and responsiveness impact on photosynthesis and water use efficiency. **Plant Physiology**, Rockville, v. 164, p. 1556–1570, 2014.

LI, L.; ARO, E.-M.; MILLAR, A. H. Mechanisms of photodamage and protein turnover in photoinhibition. **Trends in Plant Science**, Amsterdam, v. 23, p. 667–676, 2018.

LI, X.-G. et al. Factors limiting photosynthetic recovery in sweet pepper leaves after

short-term chilling stress under low irradiance. **Photosynthetica**, Dodrecht, v. 42, p. 257–262, 2004.

LI, X.-P.; GILMORE, A. M.; NIYOGI, K. K. Molecular and global time-resolved analysis of a psbS gene dosage effect on pH- and xanthophyll cycle-dependent nonphotochemical quenching in photosystem II. **The Journal of Biological Chemistry**, Baltimore, v. 277, p. 33590–33597, 2002.

LOCATO, V.; CIMINI, S.; DE GARA, L. ROS and redox balance as multifaceted players of cross-tolerance: epigenetic and retrograde control of gene expression. **Journal of Experimental Botany**, Oxford, v. 69, p. 3373–3391, 2018.

LONG, S. P.; MARSHALL-COLON, A.; ZHU, X.-G. Meeting the global food femand of the future by engineering crop photosynthesis and yield potential. **Cell**, New York, v. 161, p. 56–66, 2015.

LÓPEZ, M. A. et al. Antagonistic role of 9-lipoxygenase-derived oxylipins and ethylene in the control of oxidative stress, lipid peroxidation and plant defence. **The Plant Journal**, Oxford, v. 67, p. 447–458, 2011.

LU, Y. Identification and roles of photosystem II assembly, stability, and repair factors in Arabidopsis. **Frontiers in Plant Science**, Lausanne, v. 7, p. 168, 2016.

MARCO, P. et al. Binding of ferredoxin to algal photosystem I involves a single binding site and is composed of two thermodynamically distinct events. **BBA - Bioenergetics**, Amsterdam, v. 1859, p. 234–243, 2018.

MARINHO, H. S. et al. Hydrogen peroxide sensing, signaling and regulation of transcription factors. **Redox Biology**, Amsterdam, v. 2, p. 535–562, 2014.

MAZOR, Y. et al. Structure of the plant photosystem I supercomplex at 2.6 Å resolution. **Nature Plants**, London, v. 3, p. 17014, 2017.

MEHLER, A. H. Studies on reactions of illuminated chloroplasts. I. Mechanism of the reduction of oxygen and other Hill reagents. **Archives of Biochemistry and Biophysics**, Amsterdam, v. 33, p. 65–77, 1951.

MHAMDI, A.; VAN BREUSEGEM, F. Reactive oxygen species in plant development. **Development**, Cambridge, v. 145, p. dev164376, 2018.

MITTLER, R. Oxidative stress, antioxidants and stress tolerance. **Trends in Plant Science**, Amsterdam, v. 7, p. 405–410, 2002.

MITTLER, R. et al. Reactive oxygen gene network of plants. **Trends in Plant Science**, Amsterdam, v. 9, p. 490–498, 2004.

MITTLER, R. ROS are good. **Trends in Plant Science**, Amsterdam, v. 22, p. 11–19, 2017.

MOSBLECH, A.; FEUSSNER, I.; HEILMANN, I. Oxylipins: structurally diverse metabolites from fatty acid oxidation. **Plant Physiology and Biochemistry**, Amsterdam, v. 47, p. 511–517, 2009.

MOSEBACH, L. et al. Association of ferredoxin:NADP+ oxidoreductase with the photosynthetic apparatus modulates electron transfer in Chlamydomonas reinhardtii. **Photosynthesis Research**, Dordrecht, v. 134, p. 291–306, 2017.

MUELLER, M. J. Archetype signals in plants: the phytoprostanes. **Current Opinion in Plant Biology**, Oxford, v. 7, p. 441–448, 2004.

MULLINEAUX, P. M. et al. ROS-dependent signalling pathways in plants and algae exposed to high light: Comparisons with other eukaryotes. **Free Radical Biology and Medicine**, New York, v. 122, p. 52–64, 2018.

MUNEKAGE, Y. et al. PGR5 is involved in cyclic electron flow around photosystem I and is essential for photoprotection in Arabidopsis. **Cell**, New York, v. 110, p. 361–371, 2002.

MUNEKAGE, Y. et al. Cyclic electron flow around photosystem I is essential for photosynthesis. **Nature**, London, v. 429, p. 579–582, 2004.

MUNEKAGE, Y. N.; GENTY, B.; PELTIER, G. Effect of PGR5 impairment on photosynthesis and growth in Arabidopsis thaliana. **Plant and Cell Physiology**, Oxford, v. 49, p. 1688–1698, 2008.

MUNNS, R. Genes and salt tolerance: bringing them together. **New Phytologist**, Cambridge, v. 167, p. 645–663, 2005.

NAKANO, Y.; ASADA, K. Hydrogen peroxide is scavenged by ascorbate-specific peroxidase in spinach chloroplasts. **Plant and Cell Physiology**, Oxford, v. 22, p. 867–880, 1981.

NANDHA, B. et al. The role of PGR5 in the redox poising of photosynthetic electron transport. **Biochimica et Biophysica Acta**, Amsterdam, v. 1767, p. 1252–1259, 2007.

NICKELSEN, J.; RENGSTL, B. Photosystem II assembly: from cyanobacteria to plants. **Annual Review of Plant Biology**, Palo Alto, v. 64, p. 609–635, 2013.

NIKKANEN, L.; TOIVOLA, J.; RINTAMÄKI, E. Crosstalk between chloroplast thioredoxin systems in regulation of photosynthesis. **Plant, Cell and Environment**, Oxford, v. 39, p. 1691–1705, 2016.

NISHIKAWA, Y. et al. PGR5-dependent cyclic electron transport around PSI contributes to the redox homeostasis in chloroplasts rather than CO2 fixation and biomass production in rice. **Plant and Cell Physiology**, Oxford, v. 53, p. 2117–2126, 2012.

NIXON, P. J. et al. Recent advances in understanding the assembly and repair of photosystem II. **Annals of Botany**, Oxford, v. 106, p. 1–16, 2010.

NOCTOR, G.; FOYER, C. H. Intracellular redox compartmentation and ROS-related communication in regulation and signaling. **Plant Physiology**, Rockville, v. 171, p. 1581–1592, 2016.

NOCTOR, G.; REICHHELD, J. P.; FOYER, C. H. ROS-related redox regulation and signaling in plants. **Seminars in Cell and Developmental Biology**, London, v. 80, p. 3–12, 2018.

O'LEARY, B. M. et al. Variation in leaf respiration rates at night correlates with carbohydrate and amino acid supply. **Plant Physiology**, Rockville, v. 174, p. 2261–2273, 2017.

O'LEARY, B. M.; PLAXTON, W. C. Plant respiration. In: **eLS**. Chichester: John Wiley & Sons, 2016.

OKEGAWA, Y. et al. A balanced PGR5 level is required for chloroplast development and optimum operation of cyclic electron transport around photosystem I. **Plant and Cell Physiology**, Oxford, v. 48, p. 1462–1471, 2007.

OZAWA, S.; ONISHI, T.; TAKAHASHI, Y. Identification and characterization of an assembly intermediate subcomplex of photosystem I in the green alga Chlamydomonas reinhardtii. **The Journal of Biological Chemistry**, Baltimore, v. 285, p. 20072–20079, 2010.

PADMASREE, K.; PADMAVATHI, L.; RAGHAVENDRA, A. S. Essentiality of mitochondrial oxidative metabolism for photosynthesis: optimization of carbon assimilation and protection against photoinhibition. **Critical Reviews in Biochemistry and Molecular Biology**, Philadelphia, v. 37, p. 71–119, 2002.

PAUL, M. J.; FOYER, C. H. Sink regulation of photosynthesis. **Journal of Experimental Botany**, Oxford, v. 52, p. 1383–1400, 2001.

PIERRE, S. et al. The ferredoxin docking site of photosystem I. **Biochimica et Biophysica Acta**, Amsterdam, v. 1555, p. 204–209, 2002.

PINTÓ-MARIJUAN, M.; MUNNÉ-BOSCH, S. Photo-oxidative stress markers as a measure of abiotic stress-induced leaf senescence: advantages and limitations. **Journal of Experimental Botany**, Oxford, v. 65, p. 3845–3857, 2014.

PLAXTON, W. C.; PODESTÁ, F. E. The functional organization and control of plant respiration. **Critical Reviews in Plant Sciences**, Philadelphia, v. 25, p. 159–198, 2006.

POWLES, S. B. Photoinhibition of Photosynthesis Induced by Visible Light. **Annual Review of Plant Physiology**, Palo Alto, v. 35, p. 15–44, 1984.

QIN, X. et al. Structural basis for energy transfer pathways in the plant PSI-LHCI supercomplex. **Science**, Washington, v. 348, p. 989–995, 2015.

RAGHAVENDRA, A. S.; PADMASREE, K. Beneficial interactions of mitochondrial metabolism with photosynthetic carbon assimilation. **Trends in Plant Science**, Amsterdam, v. 8, p. 546–553, 2003.

RAINES, C. A. The Calvin cycle revisited. **Photosynthesis Research**, Dordrecht, v. 75, p. 1–10, 2003.

RAINES, C. A. Increasing photosynthetic carbon assimilation in C3 plants to improve crop yield: current and future strategies. **Plant Physiology**, Rockville, v. 155, p. 36–42, 2011.

RAMEL, F. et al. Chemical quenching of singlet oxygen by carotenoids in plants. **Plant Physiology**, Rockville, v. 158, p. 1267–1278, 2012a.

RAMEL, F. et al. Carotenoid oxidation products are stress signals that mediate gene responses to singlet oxygen in plants. **Proceedings of the National Academy of Sciences of the United States of America**, Washington, v. 109, p. 5535–5540, 2012b.

RANTALA, S.; TIKKANEN, M. Phosphorylation-induced lateral rearrangements of thylakoid protein complexes upon light acclimation. **Plant Direct**, Oxford, v. 2, p. 1–12, 2018.

RAY, D. K. et al. Recent patterns of crop yield growth and stagnation. **Nature Communications**, London, v. 3, p. 1293–1297, 2012.

RUBAN, A. V. Evolution under the sun: optimizing light harvesting in photosynthesis. **Journal of Experimental Botany**, Oxford, v. 66, p. 7–23, 2015.

RUBAN, A. V et al. Identification of a mechanism of photoprotective energy dissipation in higher plants. **Nature**, London, v. 450, p. 575–579, 2007.

RUBAN, A. V. Nonphotochemical chlorophyll fluorescence quenching: mechanism and effectiveness in protecting plants from photodamage. **Plant Physiology**, Rockville, v. 170, p. 1903–1916, 2016.

RUBAN, A. V; JOHNSON, M. P.; DUFFY, C. D. P. The photoprotective molecular switch in the photosystem II antenna. **Biochimica et Biophysica Acta**, Amsterdam, v. 1817, p. 167–181, 2012.

SACHARZ, J. et al. The xanthophyll cycle affects reversible interactions between PsbS and light-harvesting complex II to control non-photochemical quenching. **Nature Plants**, London, v. 3, p. 16225, 2017.

SALESSE-SMITH, C. E. et al. Overexpression of Rubisco subunits with RAF1 increases Rubisco content in maize. **Nature Plants**, London, v. 4, p. 802–810, 2018.

SATOH, M. et al. Arabidopsis mutants affecting oxylipin signaling in photo-oxidative stress responses. **Plant Physiology and Biochemistry**, Amsterdam, v. 81, p. 90–95, 2014.

SAVCHENKO, T. et al. The hydroperoxide lyase branch of the oxylipin pathway protects against photoinhibition of photosynthesis. **Planta**, Berlin, v. 245, p. 1179–1192, 2017.

SCHEIBE, R. Malate valves to balance cellular energy supply. **Physiologia Plantarum**, Oxford, v. 120, p. 21–26, 2004.

SCHELLER, H. V.; HALDRUP, A. Photoinhibition of photosystem I. **Planta**, Berlin, v.

221, p. 5–8, 2005.

SCHREIBER, U. Redox changes of ferredoxin, P700, and plastocyanin measured simultaneously in intact leaves. **Photosynthesis Research**, Dordrecht, v. 134, p. 343–360, 2017.

SCHREIBER, U.; BILGER, W.; NEUBAUER, C. Chlorophyll fluorescence as a nonintrusive indicator for rapid assessment of in vivo photosynthesis. In: SCHULZE, E.-D.; CALDWELL, M. M. (Ed.). **Ecophysiology of Photosynthesis**. 1. ed. Berlin: Springer-Verlag, 1995. p. 49–70.

SCHREIBER, U.; KLUGHAMMER, C. Analysis of photosystem I donor and acceptor sides with a new type of online-deconvoluting kinetic LED-array spectrophotometer. **Plant and Cell Physiology**, Oxford, v. 57, p. 1454–1467, 2016.

SEJIMA, T. et al. Repetitive short-pulse light mainly inactivates photosystem I in sunflower leaves. **Plant and Cell Physiology**, Oxford, v. 55, p. 1184–1193, 2014.

SHARMA, P. et al. Reactive oxygen species, oxidative damage, and antioxidative defense mechanism in plants under stressful conditions. **Journal of Botany**, London, v. 2012, p. 1–26, 2012.

SHEN, J.-R. The structure of photosystem II and the mechanism of water oxidation in photosynthesis. **Annual Review of Plant Biology**, Palo Alto, v. 66, p. 4.1-4.26, 2015.

SHIKANAI, T. et al. Directed disruption of the tobacco ndhB gene impairs cyclic electron flow around photosystem I. **Proceedings of the National Academy of Sciences of the United States of America**, Washington, v. 95, p. 9705–9709, 1998.

SHIKANAI, T. Cyclic electron transport around photosystem I: genetic approaches. **Annual Review of Plant Biology**, Palo Alto, v. 58, p. 199–217, 2007.

SHIKANAI, T. Regulatory network of proton motive force: contribution of cyclic electron transport around photosystem I. **Photosynthesis Research**, Dordrecht, v. 129, p. 253–260, 2016.

SHUMBE, L.; BOTT, R.; HAVAUX, M. Dihydroactinidiolide, a high light-induced β-carotene derivative that can regulate gene expression and photoacclimation in Arabidopsis. **Molecular Plant**, Oxford, v. 7, p. 1248–1251, 2014.

SIMKIN, A. J. et al. Over-expression of the RieskeFeS protein increases electron transport rates and biomass yield. **Plant Physiology**, Rockville, v. 175, p. 134–145, 2017.

SLATTERY, R. A. et al. The impacts of fluctuating light on crop performance. **Plant Physiology**, Rockville, v. 176, p. 990–1003, 2018.

SMIRNOFF, N.; ARNAUD, D. Hydrogen peroxide metabolism and functions in plants. **New Phytologist**, Cambridge, v. 221, p. 1197–1214, 2019.

SOARES, C. et al. Plants facing oxidative challenges - a little help from the

antioxidant networks. **Environmental and Experimental Botany**, New York, v. 161, 4–25, 2018.

SONOIKE, K. et al. Destruction of photosystem I iron-sulfur centers in leaves of Cucumis sativus L. by weak illumination at chilling temperatures. **FEBS Letters**, Amsterdam, v. 362, p. 235–238, 1995.

SONOIKE, K. Photoinhibition of photosystem I: its physiological significance in the chilling sensitivity of plants. **Plant and Cell Physiology**, Oxford, v. 37, p. 239–247, 1996.

SONOIKE, K. et al. The mechanism of degradation of PsaB protein, a reaction center subunit of photosystem I, upon photoinhibition. **Plant Physiology**, Rockville, v. 53, p. 55–63, 1997.

SONOIKE, K. Photoinhibition of photosystem I. **Physiologia Plantarum**, Oxford, v. 142, p. 56–64, 2011.

SONOIKE, K.; TERASHIMA, I. Mechanism of photosystem-I photoinhibition in leaves of Cucumis sativus L. **Planta**, Berlin, v. 194, p. 287–293, 1994.

SOUZA, P. V. L. et al. Function and compensatory mechanisms among the components of the chloroplastic redox network. **Critical Reviews in Plant Sciences**, Philadelphia, 2018.

STIEHL, H. H.; WITT, H. T. Quantitative treatment of the function of plastoquinone in photosynthesis. **Zeitschrift für Naturforschung B**, Tübingen, v. 24, p. 1588–1598, 1969.

SU, X. et al. Structure and assembly mechanism of plant C2S2M2-type PSII-LHCLL supercomplex. **Science**, Washington, v. 357, p. 815–820, 2017.

SUGA, M. et al. Structure and energy transfer pathways of the plant photosystem I-LHCI supercomplex. **Current Opinion in Structural Biology**, Oxford, v. 39, p. 46–53, 2016.

SUN, J. et al. FACE-ing the global change: opportunities for improvement in photosynthetic radiation use efficiency and crop yield. **Plant Science**, New York, v. 177, p. 511–522, 2009.

SUORSA, M. et al. PROTON GRADIENT REGULATION5 is essential for proper acclimation of Arabidopsis photosystem I to naturally and artificially fluctuating light conditions. **The Plant Cell**, Rockville, v. 24, p. 2934–2948, 2012.

SUORSA, M. et al. PGR5 ensures photosynthetic control to safeguard photosystem I under fluctuating light conditions. **Plant Signaling & Behavior**, Austin, v. 8, p. e22714, 2013.

SUORSA, M. Cyclic electron flow provides acclimatory plasticity for the photosynthetic machinery under various environmental conditions and developmental stages. **Frontiers in Plant Science**, Lausanne, v. 6, p. 1–8, 2015.

SUORSA, M. et al. PGR5-PGRL1-dependent cyclic electron transport modulates linear electron transport rate in Arabidopsis thaliana. **Molecular Plant**, Oxford, v. 9, p. 271–288, 2016.

SUZUKI, N. et al. ROS and redox signalling in the response of plants to abiotic stress. **Plant, Cell and Environment**, Oxford, v. 35, p. 259–270, 2012.

TAKAGI, D. et al. Superoxide and singlet oxygen produced within the thylakoid membranes both cause photosystem I photoinhibition. **Plant Physiology**, Rockville, v. 171, p. 1626–1634, 2016a.

TAKAGI, D. et al. Photorespiration provides the chance of cyclic electron flow to operate for the redox-regulation of P700 in photosynthetic electron transport system of sunflower leaves. **Photosynthesis Research**, Dordrecht, v. 129, p. 279–290, 2016b.

TAKAGI, D.; MIYAKE, C. PROTON GRADIENT REGULATION 5 supports linear electron flow to oxidize photosystem I. **Physiologia Plantarum**, Oxford, v. 164, p. 337–348, 2018.

TAKAHASHI, M.; ASADA, K. Superoxide production in aprotic interior of chloroplast thylakoids. **Archives of Biochemistry and Biophysics**, Amsterdam, v. 267, p. 714–722, 1988.

TAKAHASHI, S.; BADGER, M. R. Photoprotection in plants: a new light on photosystem II damage. **Trends in Plant Science**, Amsterdam, v. 16, p. 53–60, 2011.

TAKAHASHI, S.; MURATA, N. How do environmental stresses accelerate photoinhibition? **Trends in Plant Science**, Amsterdam, v. 13, p. 178–182, 2008.

TERASHIMA, I.; FUNAYAMA, S.; SONOIKE, K. The site of photoinhibition in leaves of Cucumis sativus L. at low temperatures is photosystem I, not photosystem II. **Planta**, Berlin, v. 193, p. 300–306, 1994.

TIKHONOV, A. N. The cytochrome b6f complex at the crossroad of photosynthetic electron transport pathways. **Plant Physiology and Biochemistry**, Amsterdam, v. 81, p. 163–183, 2014.

TIKKANEN, M. et al. Thylakoid protein phosphorylation in higher plant chloroplasts optimizes electron transfer under fluctuating light. **Plant Physiology**, Rockville, v. 152, p. 723–735, 2010.

TIKKANEN, M. et al. Regulation of the photosynthetic apparatus under fluctuating growth light. **Philosophical Transactions of the Royal Society B: Biological Sciences**, London, v. 367, p. 3486–3493, 2012a.

TIKKANEN, M. et al. STN7 operates in retrograde signaling through controlling redox balance in the electron transfer chain. **Frontiers in Plant Science**, Lausanne, v. 3, p. 277, 2012b.

TIKKANEN, M. et al. Comparative analysis of mutant plants impaired in the main

regulatory mechanisms of photosynthetic light reactions - From biophysical measurements to molecular mechanisms. **Plant Physiology and Biochemistry**, Amsterdam, v. 112, p. 290–301, 2017.

TIKKANEN, M.; ARO, E.-M. Integrative regulatory network of plant thylakoid energy transduction. **Trends in Plant Science**, Amsterdam, v. 19, p. 10–17, 2014.

TIKKANEN, M.; GREBE, S. Switching off photoprotection of photosystem I – a novel tool for gradual PSI photoinhibition. **Physiologia Plantarum**, Oxford, v. 162, p. 156–161, 2018.

TIKKANEN, M.; RANTALA, S.; ARO, E.-M. Electron flow from PSII to PSI under high light is controlled by PGR5 but not by PSBS. **Frontiers in Plant Science**, Lausanne, v. 6, p. 521, 2015.

TIWARI, A. et al. Photodamage of iron-sulphur clusters in photosystem I induces non-photochemical energy dissipation. **Nature Plants**, London, v. 2, p. 16035, 2016.

TJUS, S. E.; MØLLER, B. L.; SCHELLER, H. V. Photosystem I is an early target of photoinhibition in barley illuminated at chilling temperatures. **Plant Physiology**, Rockville, v. 116, p. 755–764, 1998.

TYYSTJÄRVI, E.; ARO, E.-M. The rate constant of photoinhibition, measured in lincomycin-treated leaves, is directly proportional to light intensity. **Proceedings of the National Academy of Sciences of the United States of America**, Washington, v. 93, p. 2213–2218, 1996.

VINYARD, D. J.; ANANYEV, G. M.; CHARLES DISMUKES, G. Photosystem II: the reaction center of oxygenic photosynthesis. **Annual Review of Biochemistry**, Palo Alto, v. 82, p. 577–606, 2013.

VISHWAKARMA, A. et al. Importance of the alternative oxidase (AOX) pathway in regulating cellular redox and ROS homeostasis to optimize photosynthesis during restriction of the cytochrome oxidase pathway in Arabidopsis thaliana. **Annals of Botany**, Oxford, v. 116, p. 555–569, 2015.

von CAEMMERER, S.; FURBANK, R. T. Strategies for improving C4 photosynthesis. **Current Opinion in Plant Biology**, Oxford, v. 31, p. 125–134, 2016.

WADA, S. et al. Flavodiiron protein substitutes for cyclic electron flow without competing CO2 assimilation in rice. **Plant Physiology**, Rockville, v. 176, p. 1509–1518, 2018.

WANG, C.; TAKAHASHI, H.; SHIKANAI, T. PROTON GRADIENT REGULATION 5 contributes to ferredoxin-dependent cyclic phosphorylation in ruptured chloroplasts. **BBA - Bioenergetics**, Amsterdam, v. 1859, p. 1173–1179, 2018.

WANG, Y. et al. Overexpression of plasma membrane H+-ATPase in guard cells promotes light-induced stomatal opening and enhances plant growth. **Proceedings of the National Academy of Sciences of the United States of America**, Washington, v. 111, p. 533–538, 2014.

WASTERNACK, C.; HAUSE, B. Jasmonates: biosynthesis, perception, signal transduction and action in plant stress response, growth and development. An update to the 2007 review in Annals of Botany. **Annals of Botany**, Oxford, v. 111, p. 1021–1058, 2013.

WIENTJES, E.; VAN AMERONGEN, H.; CROCE, R. LHCII is an antenna of both photosystems after long-term acclimation. **Biochimica et Biophysica Acta**, Amsterdam, v. 1827, p. 420–426, 2013.

WINGLER, A. Transitioning to the next phase: the role of sugar signaling throughout the plant life cycle. **Plant Physiology**, Rockville, v. 176, p. 1075–1084, 2018.

WITTENBERG, G. et al. Identification and characterization of a stable intermediate in photosystem I assembly in tobacco. **The Plant Journal**, Oxford, v. 90, p. 478–490, 2017.

YADAV, D. K. et al. Singlet oxygen scavenging activity of plastoquinol in photosystem II of higher plants: electron paramagnetic resonance spin-trapping study. **Biochimica et Biophysica Acta**, Amsterdam, v. 1797, p. 1807–1811, 2010.

YAMAMOTO, H.; SHIKANAI, T. PGR5-dependent cyclic electron flow protects photosystem I under fluctuating light at donor and acceptor sides. **Plant Physiology**, Rockville, v. 179, p. 588–600, 2019.

YAMORI, W.; MAKINO, A.; SHIKANAI, T. A physiological role of cyclic electron transport around photosystem I in sustaining photosynthesis under fluctuating light in rice. **Scientific Reports**, London, v. 6, p. 20147, 2016.

YAMORI, W.; SHIKANAI, T. Physiological functions of cyclic electron transport around photosystem I in sustaining photosynthesis and plant growth. **Annual Review of Plant Biology**, Palo Alto, v. 67, p. 25.1-25.26, 2016.

YANG, Y.-J. et al. The effects of chilling-light stress on photosystems I and II in three Paphiopedilum species. **Botanical Studies**, Heidelberg, v. 58, p. 53, 2017.

ZAVAFER, A. et al. Mechanism of photodamage of the oxygen evolving Mn Cluster of Photosystem II by excessive light energy. **Scientific Reports**, London, v. 7, p. 7604, 2017.

ZHANG, S.; SCHELLER, H. V. Photoinhibition of photosystem I at chilling temperature and subsequent recovery in Arabidopsis thaliana. **Plant and Cell Physiology**, Oxford, v. 45, p. 1595–1602, 2004.

ZHANG, Z. et al. Characterization of PSI recovery after chilling-induced photoinhibition in cucumber (Cucumis sativus L.) leaves. **Planta**, Berlin, v. 234, p. 883–889, 2011.

ZIVCAK, M. et al. Repetitive light pulse-induced photoinhibition of photosystem I severely affects CO2 assimilation and photoprotection in wheat leaves. **Photosynthesis Research**, Dordrecht, v. 126, p. 449–463, 2015.

APPENDIX A – ABOUT THIS THESIS

This thesis is result of a partnership agreement (DOU section 3, n. 122, p. 65, 27 jun. 2018, ISSN 1677-7069) between the University of Turku (Finland) and the Universidade Federal do Ceará (Brazil) covering a program for the joint supervision and awarding of a single doctorate diploma to the PhD candidate. This thesis was also published by the University of Turku as follows:

Print:
LIMA-MELO, Y. **Consequences of photoinhibition of photosystem I on photosynthetic electron transport and carbon metabolism**. 2019. 138 p. Thesis (Doctor of Philosophy, Natural Sciences) – Faculty of Science and Engineering, University of Turku, Turku, Finland, 2019. ISBN 978-951-29-7714-7. ISSN 0082-7002.

Online:
LIMA-MELO, Y. **Consequences of photoinhibition of photosystem I on photosynthetic electron transport and carbon metabolism**. 2019. 75 p. Thesis (Doctor of Philosophy, Natural Sciences) – Faculty of Science and Engineering, University of Turku, Turku, Finland, 2019. ISBN 978-951-29-7715-4. ISSN 2343-3175.

The thesis publication and defence at the University of Turku occurred with the following additional information:

Place of PhD studies and research: University of Turku, Faculty of Science and Engineering, Department of Biochemistry, Laboratory of Molecular Plant Biology, Doctoral Programme in Molecular Life Sciences.

Supervisors: Prof. Eva-Mari Aro (University of Turku)
Dr. Peter Jared Gollan (University of Turku)

Reviewers: Prof. Luís Mauro G. Rosa (Universidade Federal do Rio Grande do Sul)
Dr. Peter Robert Kindgren (University of Copenhagen)

Opponent: Prof. Åsa Strand (Umeå University)

The originality of this thesis has been checked in accordance with the University of Turku quality assurance system using the Turnitin Originality Check service.

This thesis is composed of the following scientific articles, referred to in the text as Annexes A, B and C, and republished by kind permission of their respective original publishers:

ANNEX A – PUBLISHED ARTICLE I

GOLLAN, P. J.; LIMA-MELO, Y.; TIWARI, A.; TIKKANEN, M.; ARO, E.-M. Interaction between photosynthetic electron transport and chloroplast sinks triggers protection and signalling important for plant productivity. **Philosophical Transactions of the Royal Society B**, London, v. 372, p. 20160390, 2017.

ANNEX B – PUBLISHED ARTICLE II

LIMA-MELO, Y.; GOLLAN, P. J.; TIKKANEN, M.; SILVEIRA, J. A. G.; ARO, E.-M. Consequences of photosystem-I damage and repair on photosynthesis and carbon use in *Arabidopsis thaliana*. **The Plant Journal**, Oxford, v. 97, p. 1061–1072, 2019.

ANNEX C – PUBLISHED ARTICLE III

LIMA-MELO, Y.; ALENCAR, V. T. C. B.; LOBO, A. K. M.; SOUSA, R. H. V.; TIKKANEN, M.; ARO, E.-M.; SILVEIRA, J. A. G.; GOLLAN, P. J. Photoinhibition of photosystem I provides oxidative protection during imbalanced photosynthetic electron transport in *Arabidopsis thaliana*. **Frontiers in Plant Science**, Lausanne, v. 10, p. 916, 2019.

ANNEX A – PUBLISHED ARTICLE I

GOLLAN, P. J.; LIMA-MELO, Y.; TIWARI, A.; TIKKANEN, M.; ARO, E.-M. Interaction between photosynthetic electron transport and chloroplast sinks triggers protection and signalling important for plant productivity. **Philosophical Transactions of the Royal Society B**, London, v. 372, p. 20160390, 2017.

(Pages 78-90)

PHILOSOPHICAL TRANSACTIONS B

rstb.royalsocietypublishing.org

Research

Cite this article: Gollan PJ, Lima-Melo Y, Tiwari A, Tikkanen M, Aro E-M. 2017 Interaction between photosynthetic electron transport and chloroplast sinks triggers protection and signalling important for plant productivity. *Phil. Trans. R. Soc. B* **372**: 20160390.
http://dx.doi.org/10.1098/rstb.2016.0390

Accepted: 7 March 2017

One contribution of 16 to a discussion meeting issue 'Enhancing photosynthesis in crop plants: targets for improvement'.

Subject Areas:
plant science

Keywords:
photosynthesis regulation, PSI photoinhibition, chloroplast signalling, CO_2 fixation, oxylipins

Author for correspondence:
Eva-Mari Aro
e-mail: evaaro@utu.fi

†Primary address: Department of Biochemistry and Molecular Biology, Federal University of Ceará, CEP 60451-970, Fortaleza, Ceará, Brazil

Electronic supplementary material is available online at https://dx.doi.org/10.6084/m9.figshare.c.3820801.

THE ROYAL SOCIETY PUBLISHING

Interaction between photosynthetic electron transport and chloroplast sinks triggers protection and signalling important for plant productivity

Peter J. Gollan, Yugo Lima-Melo†, Arjun Tiwari, Mikko Tikkanen and Eva-Mari Aro

Molecular Plant Biology, Department of Biochemistry, University of Turku, 20014 Turku, Finland

E-MA, 0000-0002-2922-1435

The photosynthetic light reactions provide energy that is consumed and stored in electron sinks, the products of photosynthesis. A balance between light reactions and electron consumption in the chloroplast is vital for plants, and is protected by several photosynthetic regulation mechanisms. Photosystem I (PSI) is particularly susceptible to photoinhibition when these factors become unbalanced, which can occur in low temperatures or in high light. In this study we used the *pgr5 Arabidopsis* mutant that lacks ΔpH-dependent regulation of photosynthetic electron transport as a model to study the consequences of PSI photoinhibition under high light. We found that PSI damage severely inhibits carbon fixation and starch accumulation, and attenuates enzymatic oxylipin synthesis and chloroplast regulation of nuclear gene expression after high light stress. This work shows that modifications to regulation of photosynthetic light reactions, which may be designed to improve yield in crop plants, can negatively impact metabolism and signalling, and thereby threaten plant growth and stress tolerance.

This article is part of the themed issue 'Enhancing photosynthesis in crop plants: targets for improvement'.

1. Introduction

The pressing need to improve plant productivity has prompted a focus on increasing photosynthetic yield. One approach is to modify mechanisms that naturally downregulate photochemical efficiency [1–5], especially non-photochemical quenching (NPQ) of excitation from the major light-harvesting complex (LHCII), which protects photosystem II (PSII) during increases in light intensity [6,7]. Improving the rate of NPQ relaxation after a period of high light was recently shown to improve plant yield in fluctuating natural light by 15% [8]. Another avenue for improving photosynthetic yield is to increase the capacity for electron consumption in the chloroplast by strengthening transitory electron sinks in the chloroplast or permanent carbon sinks in specialized plant organs [1,2,8,9]. Strong sink demand not only improves growth and yield [10,11], but is important for tolerance to low temperature [12,13], where it is a factor in avoiding inhibition of photosystem I (PSI). Inhibition of electron consumption in the chloroplast, induced by low temperature, leads to accumulation of electrons in the photosynthetic electron transport chain, even in low light, causing formation of superoxide ($O_2^{\bullet -}$) that specifically damages iron-sulfur (FeS) clusters in PSI centres [14–16]. The same mechanism can also cause PSI photoinhibition under high irradiance in the absence of low temperature stress [17]. Recovery from PSI photoinhibition involves the

degradation and replacement of the entire PSI centre, which occurs over several days [18].

In this work, we addressed the role of proper regulation of photosynthetic electron transport reactions in the plant's response to a changing light environment. To this end we used an *Arabidopsis thaliana* mutant lacking the proton gradient regulation 5 (PGR5) protein, which is required for formation of a thylakoid membrane ΔpH under high light [19]. The molecular function of PGR5 has not been fully resolved, but the protein is commonly thought to be involved in the transport of electrons from PSI to plastoquinone (PQ) in one of two so-called 'cyclic electron transport' (CET) pathways (reviewed in [20]). The lack of lumen acidification means that during low-to-high light transitions the *pgr5* mutant can neither engage NPQ, nor control the transport of electrons from PQ to plastocyanin (PC) through the cytochrome b_6f complex [19,21]. This means that during high light phases, the flow of electrons through the linear electron transfer pathway is unregulated in *pgr5*, leaving PSI highly exposed to over-reduction and photoinhibition [17,19,22]. The *npq4* mutant was included here as a control where NPQ is also missing, but the control of cytochrome b_6f is retained [21,23]. Thus the difference between *pgr5* and *npq4* mainly concerns the regulation of electron flow via the cytochrome b_6f complex, which is fully operational in *npq4* but missing from *pgr5* in high light (reviewed in [20]). We confirm that imbalanced accumulation of electrons in the electron transport chain rapidly induces PSI damage in *pgr5* [17,22] and demonstrate the broad and severe effects on primary and secondary metabolism, as well as on chloroplast signalling and nuclear gene expression. Deeper understanding of these processes is required to avoid unexpected fitness penalties, and is a key step in developing sustainable strategies for more efficient utilization of photosynthesis in crop plants.

2. Material and methods

(a) Plants and growth conditions

Arabidopsis thaliana ecotypes Columbia-0 (Col-0) and Columbia *glabra 1* (*gl1*) were used as controls for *npq4* and *pgr5* mutants, respectively. Plants were grown for six weeks in a phytotron at 23°C, relative humidity 60%, 8 h photoperiod under constant white growth light (GL) of 120 µmol photons m^{-2} s^{-1}. High light (HL) treatments involved shifting plants from GL to 1000 µmol photons m^{-2} s^{-1} in a temperature-controlled growth chamber set at 23°C.

(b) Photochemistry and CO_2 assimilation measurements

Photosystems II and I photochemical parameters were simultaneously measured using a Dual-PAM-100 system (Walz, Germany) based on chlorophyll *a* fluorescence [24] and the P700 oxidation signal [25] methods, respectively. Measurements of photochemical parameters were taken with a photosynthetic photon flux density (PPFD) gradient of five increasing steps (23, 54, 127, 431 and 1029 µmol photons m^{-2} s^{-1}) measured in each leaf. Data were logged after 5 min from the start of each light intensity. CO_2 assimilation was measured in leaves in 400 ppm or 2000 ppm CO_2 at 23°C using the LI-6400XL Portable Infrared Gas Exchange System (LI-COR Biosciences, USA). Gas exchange parameters were taken with a PPFD gradient of eight increasing steps (0, 25, 50, 125, 300, 600, 1000 and 1600 µmol photons m^{-2} s^{-1}) measured in each leaf. Data were logged after infrared gas analyser (IRGA) parameters reached a steady-state value after the start of each light intensity (usually around 120 s).

(c) Starch quantification and electron microscopy

Starch content of leaves was measured using a total starch assay kit (Megazyme, Ireland) according to the accompanying protocol. From the same plants, the seventh leaf was harvested and fixed with glutaraldehyde for transmission electron microscopy (TEM) imaging at the Laboratory of Electron Microscopy at the University of Turku Medical Faculty, Turku, Finland.

(d) RNA isolation and transcriptome analysis

Whole rosettes were treated with GL and HL for the time periods described, during the middle of the photoperiod. Immediately following treatment, leaves were detached and frozen in liquid N. Leaf samples contained at least four leaves from separate individual plants. Frozen leaves were ground in liquid N and total RNA was isolated using TRIsure (Bioline, USA) according to the protocol supplied, with an additional final purification in 2.5 M LiCl overnight at −20°C. Total RNA was used in RNAseq library construction. Libraries were sequenced in 50 bp single end reads using Illumina Hiseq 2500 technology (BGI Tech Solutions, Hong Kong). Reads were aligned to the reference genome build *Arabidopsis thaliana* TAIR 10 with Ensembl genes and transcripts annotation, using Strand NGS 2.7 software (Agilent, USA). Aligned reads were normalized and quantified using the DESeq R package. Gene expression fold changes were calculated using a two-way ANOVA test on triplicate samples ($n = 3$) with Benjamini–Hochberg *p*-value correction to determine the false discovery rate (FDR) for each gene. Significantly enriched Gene Ontology for Biological Process (GO-BP) terms were identified within gene lists using the enrichment analysis tool of the Gene Ontology Consortium (http://geneontology.org/).

(e) 12-Oxo-phytodienoic acid measurements

Leaf tissues of plants were harvested and immediately frozen in liquid N. Ground samples were extracted in methanol, and metabolites were separated and detected by UPLC-MS. 12-Oxo-phytodienoic acid (OPDA) abundance was quantified relative to fresh weight in five samples ($n \geq 3$).

(f) Lipid peroxidation imaging and quantification

Lipid peroxidation was assessed by visualizing auto-luminescence *in planta* [26]. After light treatment, rosettes were incubated in darkness for 2 h, before the luminescence signal was collected for 20 min using an IVIS Lumina II system (Caliper Life Sciences, USA) containing an electrically cooled CCD camera.

(g) Singlet oxygen quantification with electron paramagnetic resonance

Singlet oxygen trapping was performed in isolated thylakoids from GL- and HL-treated WT and *pgr5* plants as described in [27] using a Miniscope (MS5000) electron paramagnetic resonance (EPR)-spectrometer equipped with a variable temperature controller (TC-HO4) and Hamamatsu light source (LC8). The isolated thylakoids equivalent to 150 µg ml^{-1} chlorophyll were illuminated under actinic light (2000 µmol photons m^{-2} s^{-1}) for 180 s in the presence of vacuum distilled 2,2,6,6-tetramethylpiperidine (TEMP) (50 mM). Subsequently, the samples were centrifuged at 6500*g* for 3 min and the supernatant was used for EPR measurements. The measurements were conducted at frequency 9.41 GHz, centre field 3363 G, field sweep 150 G, microwave power 3 mW and modulation frequency 100 kHz with modulation width of 2 G. The final spectra were obtained by three accumulations of each sample.

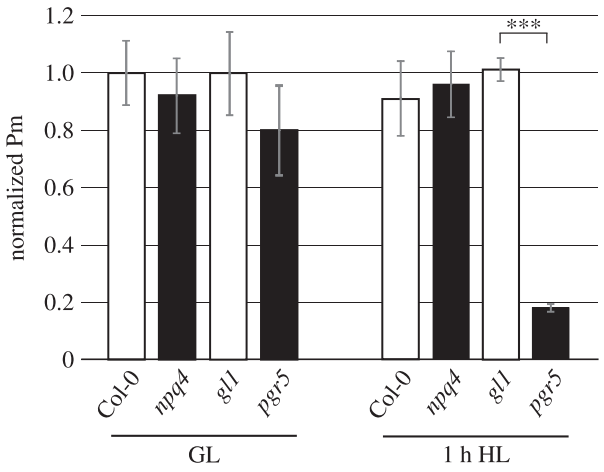

Figure 1. Functional PSI content in Col-0, *gl1*, *pgr5* and *npq4* plants previously treated with growth light (GL) or high light (HL). The maximum amount of oxidizable P700 (Pm) was determined using 5 s far-red irradiation followed by a saturating pulse of actinic light. Pm values are shown normalized to the respective WT GL sample. Error bars show standard deviation among replicates ($n = 4$). Asterisks represent significant differences between *pgr5* and *gl1* within the same light treatment (Student's *T* test, $p < 0.001$).

3. Results

(a) High light treatments induce different malfunctions in photosynthetic light reactions in *pgr5* and *npq4*

In order to separate the effects of cytochrome b_6f regulation from NPQ, we compared the *Arabidopsis pgr5* and *npq4* mutants, and their respective WTs *gl1* and Col-0. PSI function was determined using the maximum oxidation capacity of P700 at the PSI reaction centre (Pm), measured in parallel in plants that were previously treated for 1 h with either 120 µmol photons m^{-2} s^{-1} (GL) or 1000 µmol photons m^{-2} s^{-1} (HL). The Pm value in *pgr5* plants from GL was lower than in the other genotypes, although this difference was not statistically significant (figure 1). In *npq4* and both WTs the Pm was not affected by the 1 h HL treatment (figure 1). However HL treatment led to a severe decrease of Pm in *pgr5*, to around 25% of its GL level, as previously reported [17,19,22]. PSI donor side limitation was rapidly induced in *npq4* and both WTs in measurements where light intensities were higher than GL, irrespective of the previous light treatments, which corresponded with an equivalent decline in acceptor side limitation (figure 2*a*,*b*). Induction of PSI donor side limitation was completely missing from the *pgr5* mutant, whereas strong acceptor side limitation occurred in *pgr5* plants in light intensities above GL, which demonstrated excess electron transport in relation to stromal electron acceptors [21,28]. The *pgr5* mutants treated with HL for 1 h showed lower acceptor side limitation at higher light intensities, which is likely due to HL-induced PSI damage that decreased electron transport to the stromal acceptors.

The operational state of PSII was assessed using the fluorescence parameters F′, which is the fluorescence of chlorophyll *a* under actinic light, and Fm, which is the maximum chlorophyll *a* fluorescence. The F′/Fm calculation was used in preference to routine Fv/Fm calculations to avoid the confounding effect of PSI damage that is a critical factor in *pgr5* analysis [22,29]. In both GL- and HL-treated WT leaves, low F′/Fm values over increasing light intensity showed that PSII remained open (figure 2*c*). On the contrary, increases in F′/Fm occurred in GL-treated *pgr5*, and in both GL- and HL-treated *npq4* leaves, demonstrating an increase in the number of closed PSII reaction centres in the mutants at light intensities above GL (120 µmol photons m^{-2} s^{-1}). This can be attributed to the lack of NPQ under high light, which is shown in figure 2*d* to increase sharply at higher light intensities in WT, but not in the two mutants under the above-mentioned conditions. HL-treated *pgr5* plants behaved differently, demonstrating high F′/Fm at low light intensities. This may be due to PSI damage incurred during the 1 h HL treatment that limited PSI activity and caused over-reduction of the electron transport chain [17,30], leading to PSII closure in low light. The small decrease in F′/Fm in HL-treated *pgr5* leaves at high irradiance suggests that PSI damage may limit electron transfer in low light more than in high light.

(b) Photosystem I damage has direct consequences for stromal metabolism

In order to further assess the effects of the observed PSI damage on primary stromal metabolism in different light intensities, we first monitored the light curves of CO_2 fixation in WT, *pgr5* and *npq4* plants treated beforehand with GL and HL, as described in §3a above, under ambient CO_2 concentration (400 ppm). Light limitation of photosynthesis, as determined by the steepest part of each light curve of CO_2 fixation, occurred until a PPFD of approximately 120 µmol m^{-2} s^{-1} in all GL-treated plants and in HL-treated WT and *npq4* plants (figure 3*a*). Light saturation of CO_2 fixation above PPFD of 120 µmol m^{-2} s^{-1} demonstrated a shift to CO_2 as the limiting factor for photosynthesis. HL treatment caused a small decrease in the maximum level of CO_2 fixation under high PPFD in WT and *npq4* that was approximately the same as the level in GL-treated *pgr5*. In sharp contrast to the other plants, HL-treated *pgr5* showed much lower CO_2 fixation under low light intensities, with the maximum CO_2 fixation rate reduced to approximately 60% of GL levels. The shift from light limitation to CO_2 limitation in HL-treated *pgr5* occurred at a PPFD of around 400 µmol photons m^{-2} s^{-1}.

The light response curves of CO_2 fixation were repeated under high CO_2 concentration (2000 ppm) for the *pgr5* and WT plants that had been GL- and HL-treated exactly as before. Here, CO_2 fixation at high PPFD in both GL- and HL-treated *pgr5* was 2–2.5 fold higher compared to ambient CO_2. The level of CO_2 fixation in GL-treated *pgr5* was slightly elevated in comparison to GL- and HL-treated WT, while HL-treatment of *pgr5* reduced CO_2 fixation at high PPFD to around 70% of that measured for GL-treated plants (figure 3*b*). The light response curve of HL-treated *pgr5* at high CO_2 did not achieve a steady rate of CO_2 fixation within the PPFD range used, which shows that photosynthesis was not limited by CO_2 availability.

To determine the effect of PSI damage at the chloroplast metabolic level, starch content was investigated in WT and *pgr5* mutants that were subjected to the GL and HL treatments described above and then shifted to regular growth conditions until the end of the following day to allow diurnal starch accumulation. The starch contents of *pgr5* leaves treated with GL or HL were 50% and 25%, respectively, of WT levels under the same conditions. HL treatment approximately halved the starch content in *pgr5* compared to GL treatment (figure 4*a*). Another set of plants were HL-treated for 1 h and then, instead of transferring to GL, were

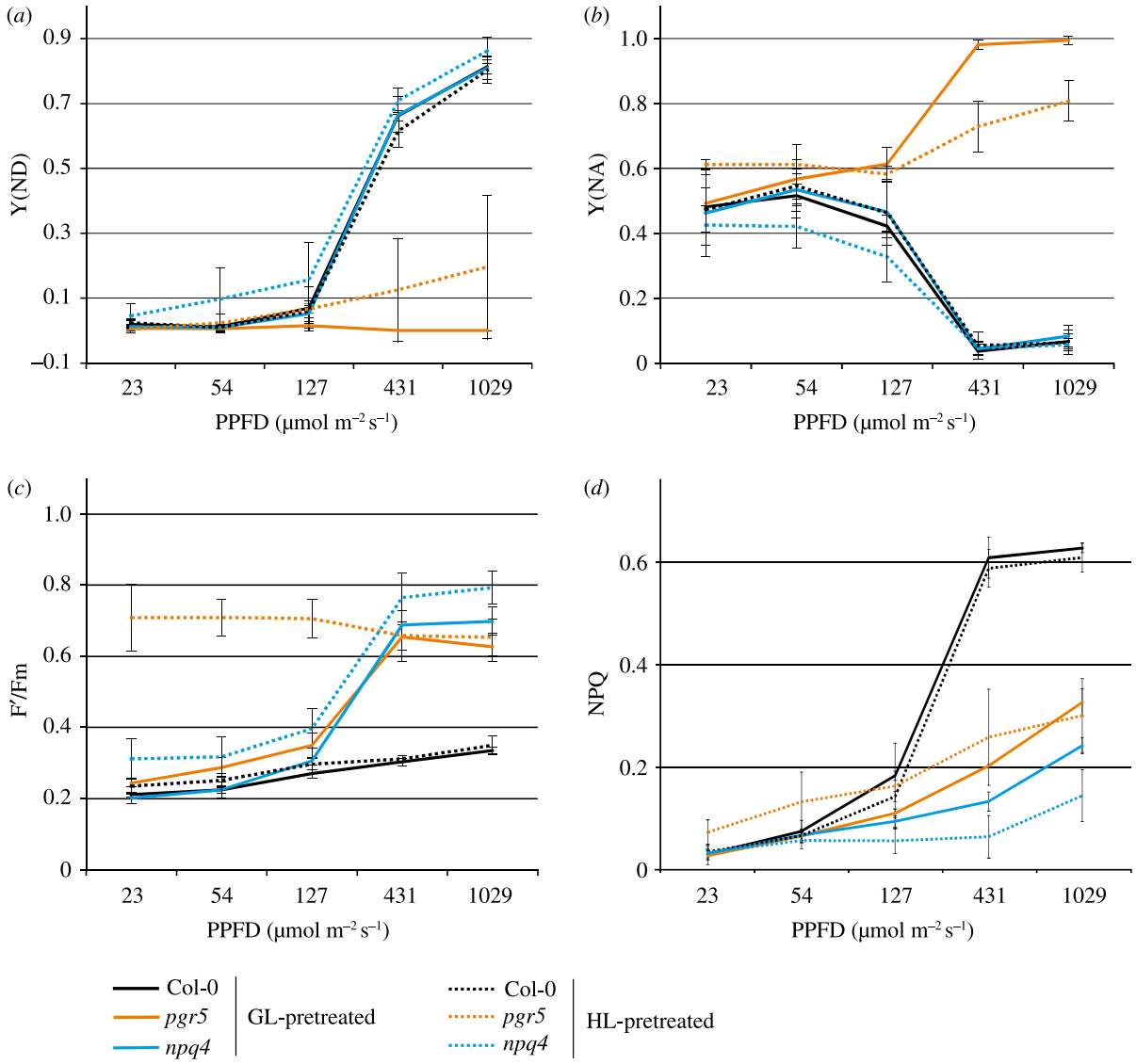

Figure 2. Analysis of PSI and PSII function under increasing light intensities by chlorophyll *a* fluorescence and P700 oxidation, in Col-0, *pgr5* and *npq4* plants pretreated with growth light (GL) or high light (HL). (*a*) Limitation of electron transfer to the donor (lumenal) side of PSI; (*b*) limitation of electron transfer from the acceptor (stromal) side of PSI; (*c*) the operational state of PSII reaction centres, which are open (active) at low F′/Fm values and closed (inactive) at high F′/Fm values; (*d*) non-photochemical quenching (1 − (Fm′/Fm)). Error bars show standard deviation among replicates ($n = 4$).

exposed to the same intensity of HL throughout the following day. These plants showed increases in starch content of around 100% for WT, and 350% for *pgr5*, in comparison to HL-treated plants that were shifted to GL (figure 4*a*). These increases in starch accumulation after 8 h in HL occurred alongside no change to Pm in WT plants, but a 50% reduction in Pm in *pgr5* plants, in comparison to 8 h in GL (figure 4*b*). Chloroplast ultrastructure (transmission electron micrographs) clearly showed the smaller size and lower abundance of accumulated starch granules in *pgr5* that had been treated with HL on the previous day, in comparison to WT leaves (figure 4*c*,*d*). The lower starch content in GL-treated *pgr5* compared to WT, as measured in the assay (figure 4*a*), was not evident from transmission electron micrographs (not shown).

(c) The transcription profiles of *pgr5* and *npq4* mutants are altered during light stress and recovery

The transcriptomes of *pgr5* mutants from GL, after 1 h of HL, and after 1 h of recovery in GL following HL treatment, were analysed to investigate the impact of thylakoid ΔpH on nuclear gene expression under changes in light intensity. Transcriptomes of the *npq4* mutant were analysed in parallel to identify transcriptional changes that in *pgr5* may be attributed to missing NPQ. Global effects of the *pgr5* mutation on gene expression were identified as enriched Gene Ontology (GO) terms within lists of significantly differentially-regulated genes. Of the six groups that were analysed (up- and down-regulated genes from each condition), only the downregulated genes in 1 h HL and 1 h GL recovery contained statistically significantly enriched GO terms (table 1). In both cases, the term 'jasmonic acid metabolic process' (GO:0009694) was the most highly enriched at around 12-fold, while other jasmonate-related signalling processes were also significantly enriched. Responses to HL (GO:0009644), hydrogen peroxide (H_2O_2; GL:0042542), salicylic acid (GO:0009751) and ethylene (GO:0009723) were also found to be enriched in downregulated genes in *pgr5* after HL stress and/or after 1 h recovery in GL (table 1).

The expression of individual genes undergoing significant fold change (FC) were investigated in further detail. The genes encoding enzymes involved in biosynthesis of OPDA, the chloroplast precursor for the hormone jasmonic

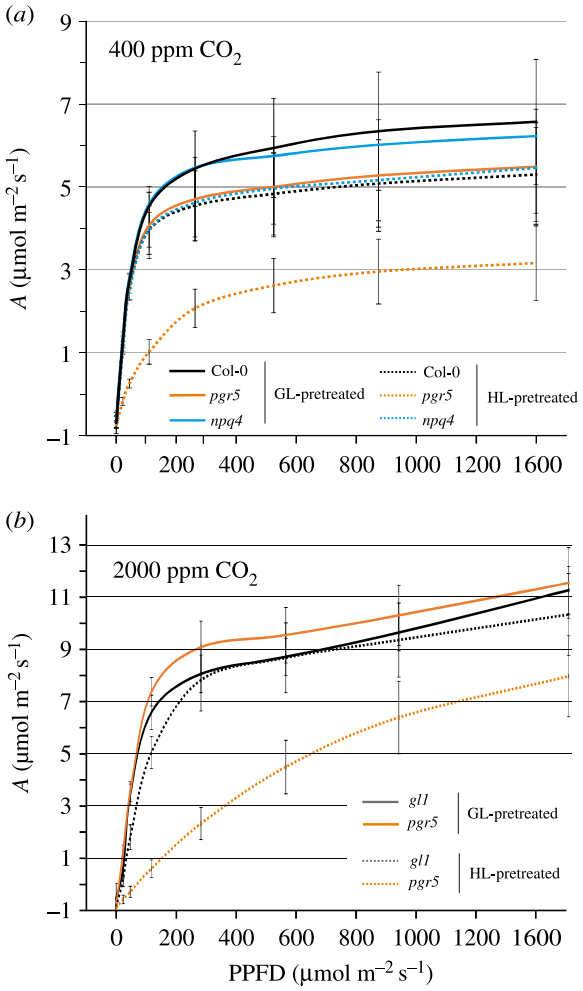

Figure 3. (*a*) Light curves of CO_2 fixation in Col-0, *pgr5* and *npq4* leaves pretreated with growth (GL), or high light (HL) at 400 ppm CO_2; (*b*) light curves of CO_2 fixation in *gl1* and *pgr5* leaves pretreated with growth (GL), or high light (HL) at 2000 ppm CO_2.

acid (JA), were strikingly downregulated in *pgr5* plants compared to WT under HL stress and during recovery. This included chloroplast lipid peroxidases, allene oxide synthase and cyclases, as well as the chloroplast lipase DAD1, OPDA reductase and numerous JA signalling regulation (JAZ) intermediates (table 2). In WT, oxylipin synthesis enzymes were significantly upregulated by HL and, in general, further upregulated during recovery (see electronic supplementary material, file S1); however, this did not occur in *pgr5*, which is seen as significant downregulation in HL and recovery compared to WT in most cases (table 2).

Based on the observed under-expression of genes involved in OPDA and oxylipin synthesis pathways in *pgr5*, relative to WT, the effect of light-induced OPDA signalling on nuclear gene expression was investigated in *pgr5* and *npq4* mutants. The expression of about 400 genes that were previously shown to be upregulated in response to OPDA treatment [31] was analysed in the current transcriptomics data. In all genotypes, these genes were expressed at relatively low levels in the original GL and were upregulated by HL treatment. In *npq4* and both WT plants, a large proportion of OPDA-induced genes was further upregulated during the recovery period (figure 5*a*). In contrast, most of these genes were under-expressed in *pgr5* in comparison to its WT (*gl1*) after 1 h HL, and after recovery for 1 h at GL (see electronic supplementary material, file S2 for transcription details).

The expression profiles of the 130 most strongly attenuated genes in *pgr5* were analysed in publicly-available expression data using the Genevestigator database [32]. Strong upregulation of this gene set was identified in HL and drought stresses and treatments with OPDA and methyl jasmonate, and also by infection with many biotic stresses including bacterial, fungal and herbivorous pathogens (electronic supplementary material, figure S1). The same gene set was considerably, but not entirely, downregulated in darkness, in iron deficiency, and in mutant plants with interrupted PSI function (*psad1-1* and *psae1-3*), and in mutants lacking the JA signalling intermediate coronatine insensitive 1 (*coi1*).

High light stress is well known to upregulate the so-called 'heat shock protein' (HSP) chaperones involved in abiotic stress response [33,34]. HSP gene transcription in *pgr5* was highly upregulated in HL (15–1000 FC) and subsequently downregulated during recovery, in a trend similar to WT (see electronic supplementary material, file S1). However, many HSPs and other heat shock factors were significantly less upregulated in *pgr5* in HL compared to WT (table 2), suggesting under-production of an abiotic stress signal in *pgr5* during HL. Expression of many abiotic stress-responsive genes is linked to H_2O_2 signalling [35,36], and so the expression of genes included in the GO term 'response to H_2O_2' (GO:0042542) was assessed in our RNAseq data. Strong upregulation of these genes under HL was evident in all genotypes, but was clearly lower in *pgr5* than in *npq4* and the WT plants (figure 5*b*). To investigate whether this may be due to increase in reactive oxygen species (ROS) scavenging in *pgr5*, the expression of almost 100 enzymes responsible for dealing with oxidative stress was assessed, including many superoxide dismutases, catalases and peroxidases. Among these genes, only the cytosolic ascorbate peroxidase (APX2) was significantly differentially-expressed in *pgr5* (table 2). Although strongly upregulated under HL in both *pgr5* (30 FC from GL) and WT (200 FC from GL), APX2 was markedly under-expressed in *pgr5* compared to WT.

Genes involved in iron metabolism, including several chloroplast ferritin (Fer) iron chaperones and ferric iron reductase (FRO) enzymes, were significantly upregulated in *pgr5* during and/or following HL stress, in comparison to its WT (table 2). In fact, Fer1 and Fer3 genes were both upregulated in all genotypes by HL stress in comparison to GL; however, the FC in *pgr5* (24 FC and 15 FC, respectively) was much greater than in WT (1.7 FC and 3.7 FC, respectively). FRO genes were downregulated by HL in all genotypes, but were strongly upregulated in *pgr5* during recovery.

(d) Light stress induces synthesis of chloroplast oxylipins in WT, *pgr5* and *npq4*

We next analysed and compared the abundance of OPDA in *pgr5*, *npq4* and the WT plants treated with the same high light stress and recovery regimes described in §3c. This analysis demonstrated an increase in OPDA abundance after 1 h recovery in GL in all genotypes (figure 6). OPDA levels in *pgr5* were significantly lower than the WT in original GL conditions and after 1 h HL ($p < 0.05$), as well as after 1 h recovery ($p < 0.001$).

The synthesis and signalling of oxylipins in *Arabidopsis* has been linked to the generation of singlet oxygen ($^1O_2$) in PSII reaction centres [37,38]. Considering lower OPDA abundance and downregulation of OPDA-regulated genes in *pgr5*,

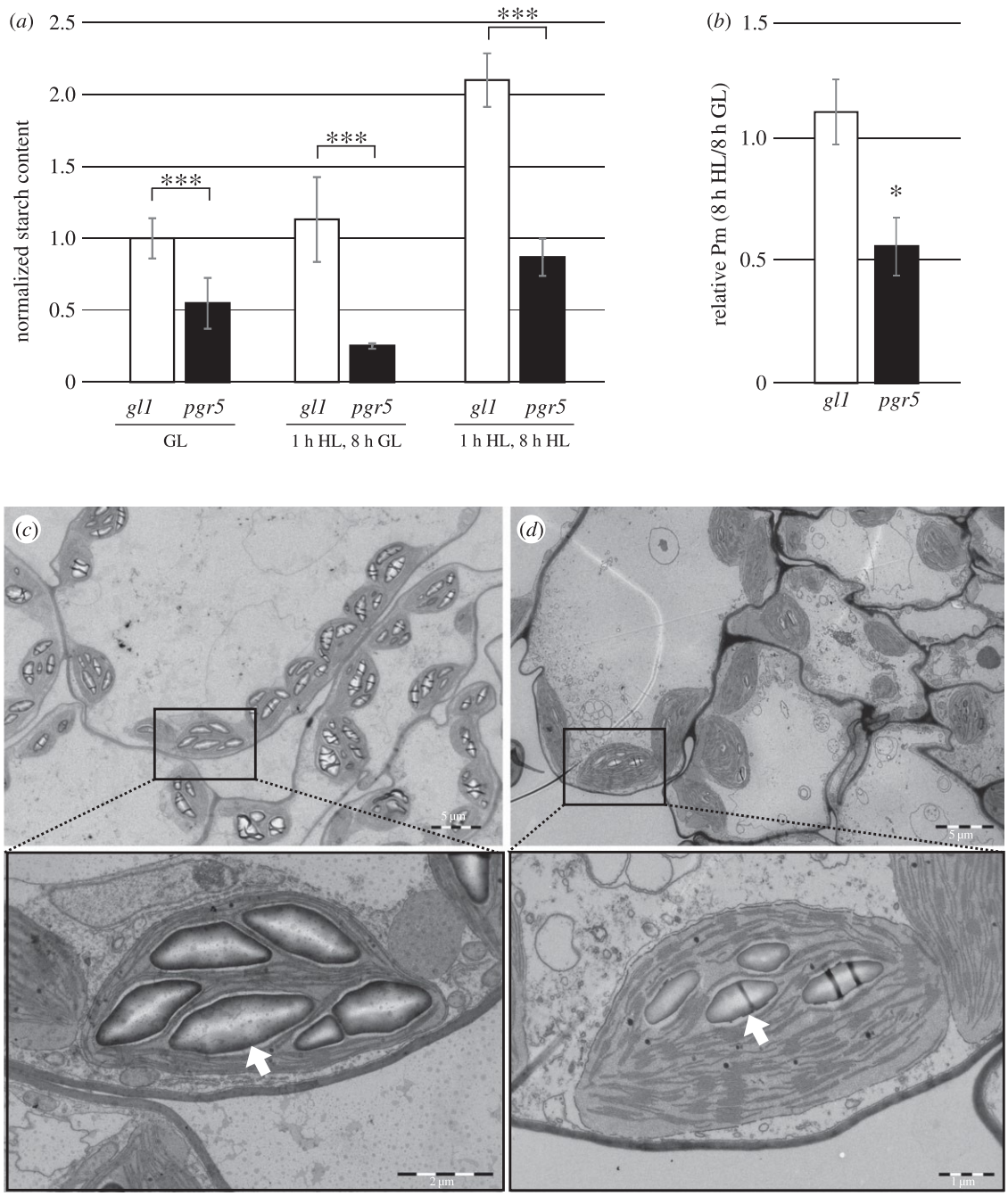

Figure 4. Starch accumulation in WT and *pgr5* plants treated with growth light (GL) or with high light (HL). (*a*) Plants were taken from GL, or treated with 1 h HL and then exposed to either regular growth conditions (8 h GL) or HL (8 h HL) during the following day. Samples were harvested at the end of the following day. Starch abundances were calculated as percentages of fresh weight and are shown normalized to the *gl1* GL sample. Error bars show standard deviation among replicates ($n = 3$). (*b*) Pm in *pgr5* and WT treated with 1 h HL and then 8 h HL, relative to Pm after 8 h GL in the same genotype; asterisks represent significant differences between *gl1* and *pgr5* (*Student's *t* test $p < 0.05$; ***Student's *t* test $p < 0.001$); (*c*,*d*) Transmission electron micrographs demonstrating the sizes and abundance of starch granules in leaf 7 of 1 h HL, 8 h GL treated WT (*c*) and *pgr5* (*d*) chloroplasts. Lower panels show high resolution views of selected areas of upper panels. White arrows indicate representative starch granules. Scale bars show size.

we investigated the production of $^1O_2$ in thylakoids with EPR, using an $^1O_2$-specific spin probe. Thylakoids isolated from HL-treated plants produced higher amounts of $^1O_2$ under saturating light than those isolated from GL-treated plants; however, the intensity of the $^1O_2$ signal was indistinguishable between *pgr5* and WT thylakoids, indicating equivalent production of $^1O_2$ in both genotypes (figure 7). HL-induced lipid peroxidation was qualitatively assessed *in planta* using a super-cooled CCD camera to image the native luminescence emitted by lipid peroxides [26]. This assay could not distinguish any differences in the level of lipid peroxidation between *pgr5* and WT after 1 h HL treatment (electronic supplementary material, figure S2).

4. Discussion

(a) Direct interaction between photosynthetic electron transport and stromal metabolism

Sudden increases in light intensity generate increased electron current through the photosynthetic system, which is

Table 1. Significantly enriched Gene Ontology Biological Process (GO-BP) terms in lists of genes differentially expressed in *pgr5* mutants.

GO term	description	included genes (total genes)[a]	fold enrichment	*p*-value (Bonferroni corrected)
enriched terms in downregulated genes; *pgr5* 1 h HL/*gl1* 1 h HL				
GO:0009694	jasmonic acid metabolic process	10 (27)	12.95	2.14×10^{-5}
GO:0009611	response to wounding	38 (184)	7.22	3.18×10^{-17}
GO:0009867	jasmonic acid-mediated signalling	12 (61)	6.88	6.84×10^{-4}
GO:0042542	response to hydrogen peroxide	10 (53)	6.60	9.38×10^{-3}
GO:0009644	response to high light intensity	11 (60)	6.41	4.13×10^{-3}
GO:0009751	response to salicylic acid	20 (171)	4.09	4.64×10^{-4}
GO:0009723	response to ethylene	27 (235)	4.02	5.33×10^{-6}
enriched terms in downregulated genes; *pgr5* 1 h GL recovery/*gl1* 1 h GL recovery				
GO:0009694	jasmonic acid metabolic process	12 (27)	11.77	2.14×10^{-6}
GO:0006568	tryptophan metabolic process	8 (24)	8.83	1.08×10^{-2}
GO:0009753	response to jasmonic acid	38 (178)	5.65	1.06×10^{-13}
GO:0009611	response to wounding	34 (184)	4.89	2.63×10^{-10}
GO:0009751	response to salicylic acid	27 (171)	4.18	2.49×10^{-6}

[a]Number of genes under each GO-BP term that were present in the *pgr5* differentially-expressed gene list, and total number of genes in the GO-BP term are shown in parentheses.

suppressed by activation of NPQ and downregulation of electron flow through the cytochrome b_6f complex (reviewed in [39]). Both mechanisms depend on acidification of the thylakoid lumen, and both are affected in the *pgr5* mutant under HL [19]. Subsequently, increases in light intensity create in *pgr5* an over-supply of electrons from the light reactions, relative to the electron-accepting capacity of the stroma, leading to acceptor-side limitation at PSI. Electrons then move to the alternative electron acceptor oxygen, creating ROS that damage the PSI FeS clusters and inactivate PSI [14,17]. HL treatment of *pgr5* plants for 1 h drastically decreased the concentration of operational PSI centres (figure 1). This is in agreement with previous studies that have also showed PSI inactivation to be induced in *pgr5* by increases in light intensity [17,19,22,40]. In this work we exploited HL-inducible PSI photoinhibition in *pgr5* to study the ensuing effects of PSI damage on metabolic processes in the chloroplast (figure 8).

In the current work, CO_2 fixation and starch accumulation were shown to be lower in *pgr5* compared to the WT, independent of light stress, while 1 h HL treatment of *pgr5* led to severe decreases in both traits (figures 3 and 4). A simple explanation for diminished primary and secondary metabolism in *pgr5* is the affected PSI electron transport, which is decreased in *pgr5* under GL [17] and severely inhibited by HL treatment (figure 1; [17,40]). Downregulated PSI activity would be expected to cause an under-supply of reducing power to the stroma, limiting metabolic reactions in *pgr5* chloroplasts, particularly after the HL exposure. Considering the role proposed for the PGR5 protein in CET, it may be argued that the observed decrease in stromal metabolism was due to limited ATP production in the *pgr5* mutant, and that PSI damage occurred through acceptor-side limitation caused by a low ATP : NADPH ratio [20,41]. However, we found that CO_2 fixation in GL-treated *pgr5* plants under 2000 ppm CO_2 was equivalent to the WT, and approximately double that measured at 400 ppm CO_2 (figure 3*b*), which rules out the possibility of ATP limitation of the Calvin–Benson–Bassham (CBB) cycle in *pgr5*. This result is in agreement with the CO_2 fixation rates in *PGR5*-knockdown rice lines that were similar to WT at both ambient CO_2 and high CO_2 [42]. A clear contradiction, however, appears between our results and a previous demonstration of inhibited CO_2 fixation in the *Arabidopsis pgr5* mutant at high CO_2 that was attributed to ATP deficiency [40]. This discrepancy may be partly due to the experimental set-up of the latter study, where plants were subjected to a six fold increase in light intensity for several minutes during the gas exchange analysis. This would have caused a degree of PSI photoinhibition in *pgr5*, which occurs very quickly during sudden increases in light intensities, as the authors pointed out [40]. Our light response curves of CO_2 fixation were designed to minimize PSI damage by exposing plants to only 2–3 min at each PPFD, and by applying an ascending order of light intensities.

HL-induced damage to PSI in *pgr5* was especially deleterious to CO_2 fixation under subsequent low light intensities, but this effect could be partially overcome by increasing the PPFD (figure 3). The high level of PSII closure in HL-treated plants under low PPFD (figure 2*c*) indicates that inhibited PSI activity causes over-reduction of electron carriers in the photosystem under low light phases (figure 8). Meanwhile high light intensities appear to more effectively excite the remaining functional PSI centres to improve CO_2 fixation (figure 3), causing a small decrease in PSII closure (figure 2*c*). Higher *per capita* PSI activity under HL would also explain the marked improvement in starch accumulation in HL-treated *pgr5* plants that were subsequently exposed to 8 h at 1000 µmol photons $m^{-2}\,s^{-1}$, despite 50% lower PSI activity, compared to those returned to GL for 8 h (figure 4). Such a scenario shows the importance of PSI protection under fluctuating light in order to maintain stromal metabolism, as highlighted in the devastating effect of fluctuating light on plants lacking PGR5 function [22,43].

Table 2. Distinctive differentially expressed genes in *pgr5* and *npq4 Arabidopsis* before and after high light stress (GL and 1 h HL, respectively) and during recovery (1 h GL). Numbers show log2-fold change in expression in *pgr5* and *npq4* mutants in comparison to the respective WT samples under identical treatments. Yellow indicates genes with ≥log2 (1) expression (significantly upregulated) and blue indicates genes with ≤log2 (−1) expression (significantly downregulated).

gene	description	*pgr5*/ *gl1* GL	*npq4*/ Col-0 GL	*pgr5*/ *gl1* 1 h HL	*npq4*/ Col-0 1 h HL	*pgr5*/ *gl1* 1 h GL	*npq4*/ Col-0 1 h GL	FDR[a]
oxylipin biosynthesis and signalling								
LOX2	lipoxygenases; chloroplast lipid	0.28	−0.08	−0.70	0.37	−1.15	−0.37	<0.01
LOX3	peroxidation	−0.31	−0.05	−1.58	0.31	−2.34	−1.39	<0.01
LOX4		−0.65	−0.36	−1.69	0.44	−2.10	−1.37	<0.01
AOS	allene oxide synthase	0.12	−0.19	−0.76	0.27	−1.48	−0.40	<0.01
AOC1	allene oxide cyclases	−0.27	−0.34	−1.32	−0.20	−1.97	−0.60	<0.01
AOC2		0.00	−0.29	−0.86	0.07	−1.15	−0.36	<0.01
AOC3		−1.17	0.06	−2.39	1.14	−1.47	−1.20	<0.01
DAD1	chloroplast lipase	−0.88	1.32	−2.94	0.53	−1.31	−1.20	<0.01
OPR3	OPDA reductase	−0.33	−0.30	−1.50	0.10	−1.71	−0.69	<0.01
JAZ1	jasmonic acid signalling regulation	−0.06	0.21	−1.85	0.57	−1.21	−0.72	<0.01
JAZ5	factors	−0.85	0.29	−1.61	0.63	−0.62	−0.52	<0.01
JAZ8		−0.70	−0.55	−1.80	−0.24	0.01	−1.00	<0.01
JAZ10		−0.90	−0.51	−2.33	1.67	−2.38	−0.93	<0.01
abiotic stress response								
HSP101	heat shock protein chaperones	0.043	0.21	−1.89	0.58	0.26	0.88	<0.01
HSP70b		0.16	−0.16	−2.10	1.66	−0.22	0.05	<0.01
HSP90-1		−0.39	−0.30	−1.58	0.07	−0.16	−0.36	<0.01
HSP70T-2		−0.83	−0.09	−2.00	0.34	0.26	0.34	<0.01
HSP22.0		0.06	0.05	−1.95	0.29	0.57	1.89	<0.01
HSP17.6A		−0.09	0.47	−1.40	0.05	−0.83	0.98	<0.01
AT1G07400		0.00	0.54	−1.55	0.22		−0.06	<0.01
ATHSFA2	stress-responsive transcription factor	1.32	−0.05	−1.61	−0.14	0.65	0.10	<0.01
APX2	ascorbate peroxidase, cytosolic	0.45	0.54	−2.30	−0.36	−0.38	0.34	<0.01
iron metabolism								
Fer1	ferritin, iron chaperones, ferric iron-	−0.02	−0.31	3.82	−0.31	1.95	0.79	<0.01
Fer2	binding in chloroplast	0.54	1.38	−0.48	−0.23	1.18	0.48	<0.01
Fer3		0.56	0.00	2.64	0.59	1.42	0.79	<0.01
Fer4		0.48	−0.07	1.04	0.24	1.56	0.67	<0.01
FRO1	ferric iron reductases involved in	0.02	−0.68	1.00	0.62	1.65	0.37	0.01
FRO6	membrane iron transport	0.03	0.07	0.74	−0.25	2.58	0.95	<0.01
FRO7		−0.09	0.02	0.92	0.01	1.72	0.63	<0.01
IRT3	iron transporter	−0.43	−0.32	1.04	−1.18	0.61	0.31	<0.01

[a]False discovery rate calculated using the Benjamini–Hochberg procedure.

(b) Photosystem I damage attenuates chloroplast signalling

Redox imbalance within the photosynthetic electron transport chain impacts the cell through retrograde signalling that modifies nuclear gene expression (reviewed in [44]). In this work we sought to understand how PSI damage affects gene expression and chloroplast signalling. We found oxylipin signalling to be the most severely affected pathway of expression regulation in the *pgr5* mutant. In the WT, HL led to strong upregulation of hundreds of transcripts known to respond to the oxylipin hormone OPDA [31], which duplicates the light-sensitivity of OPDA synthesis and signalling that has been reported previously [45–48]. These transcripts were also upregulated by HL in *pgr5* in comparison to the GL levels (figure 5*a*), but were dramatically under-expressed in the mutant after HL stress and after 1 h recovery in GL, compared to WT (table 2 and figure 5*a*). This transcription phenomenon is in line with

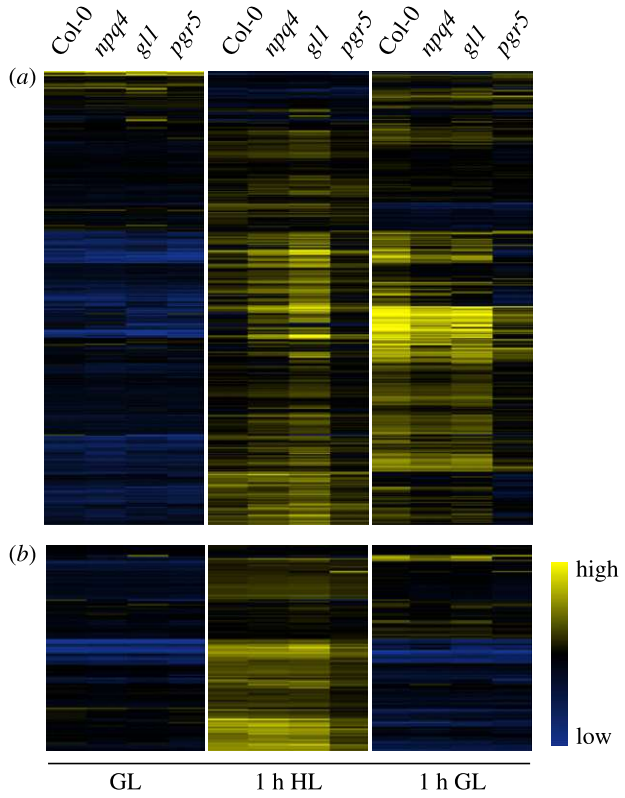

Figure 5. Clustered heatmap of high light-responsive genes in Col-0, *npq4*, *gl1*, and *pgr5* leaves before (GL) and after (1 h HL) high light treatments, or during recovery (1 h GL): (*a*) approximately 400 genes induced by 12-oxophytodienoic acid (OPDA) were downregulated in *pgr5* compared to *gl1* in 1 h HL and 1 h GL treatments (see text for details); (*b*) H_2O_2-responsive genes (GO:00423542) were upregulated by 1 h HL treatment, but were underexpressed in *pgr5* compared to the other genotypes. Clustered heatmap shows the absolute expression of each gene in Col-0, *gl1*, *npq4* and *pgr5* under each light treatment. Legend shows colours that represent high, intermediate and low expression.

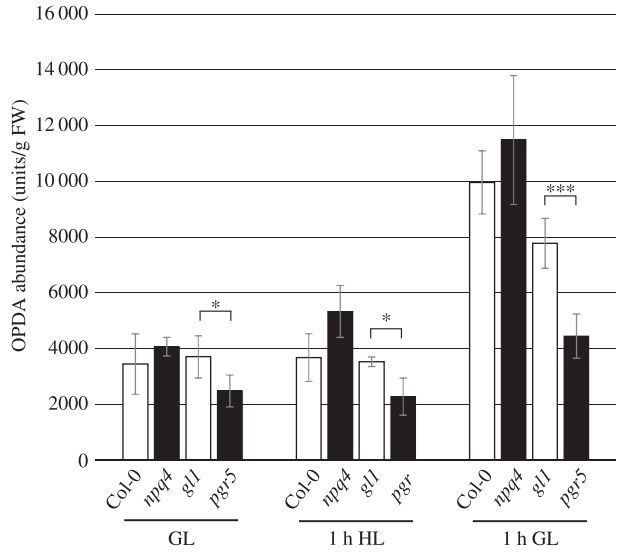

Figure 6. Abundance of OPDA in Col-0, *npq4*, *gl1* and *pgr5* leaves before (GL) and after 1 h HL treatments, and during recovery (1 h GL). Concentrations are expressed as peak area from mass spectrometry chromatograms/fresh weight. Error bars indicate standard deviation among replicate samples ($n \geq 3$). Asterisks represent significant differences between *gl1* and *pgr5* in GL and 1 h HL (*Student's *t* test $p < 0.05$) and 1 h GL (***Student's *t* test $p < 0.001$).

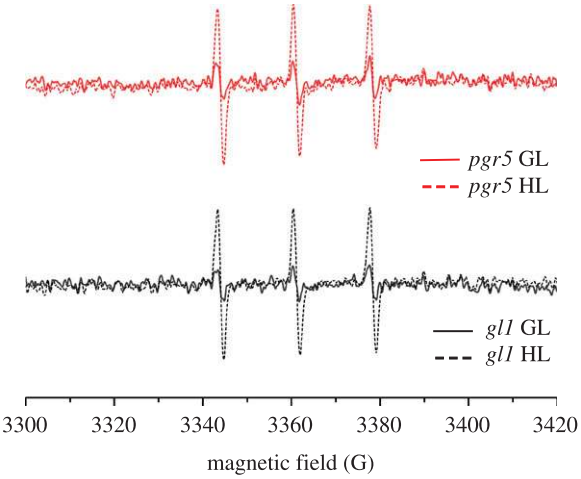

Figure 7. Singlet oxygen production in *gl1* and *pgr5* thylakoids pretreated with growth light (GL) or high light (HL). Traces show electron paramagnetic resonance (EPR) spectra with peaks indicating oxidized TEMP spin trap in the presence of purified thylakoids isolated from plants pretreated with 1 h GL (solid traces) or HL (dashed traces).

the production of only 55–70% of WT levels of OPDA in the *pgr5* under the conditions tested here (figure 6), and with the downregulated expression (relative to WT) of enzymes required for synthesis of OPDA (table 2). The opposite trend was evident in the *npq4* mutant, wherein OPDA (figure 6) and OPDA-sensitive transcripts (table 2 and figure 5*a*) were more abundant than in WT after the HL treatment, as expected [49,50]. Notably, upregulation of OPDA-sensitive genes was apparent after 1 h HL stress in all genotypes, whereas significant increases in OPDA abundance from GL levels were only apparent after 1 h recovery in GL. This may demonstrate the potency of OPDA as a transcription regulator, with undetected increases having a strong effect on expression induction.

Transcription of the genes encoding oxylipin enzymes is induced by OPDA [29], meaning that OPDA synthesis is auto-upregulated. This phenomenon can account for the large increases in OPDA concentration in all genotypes after 1 h recovery, i.e. the latest time-point (figure 6). The *pgr5* mutant had significantly lower OPDA concentrations than WT under all conditions analysed, prompting us to investigate factors upstream of OPDA biosynthesis in an attempt to delineate the cause and effect of low OPDA hormone and attenuated OPDA signalling in *pgr5*. Singlet oxygen ($^1O_2$), produced in the PSII reaction centre, is associated with upregulated expression of genes encoding oxylipin enzymes in *Arabidopsis* [38,51,52]. Accordingly, increased $^1O_2$ production in the *npq4* mutant [53] corroborates the upregulation of enzymatic oxylipin production in *npq4* observed here and elsewhere [45,49,50]. Furthermore, a minor increase in $^1O_2$ previously shown in chloroplasts treated with nigericin was attributed to the abolition of NPQ [53]. Since nigericin mimics the *pgr5* lesion by demolishing thylakoid ΔpH, we expected enhanced $^1O_2$ production in *pgr5* mutants in HL; however, we found no difference between *pgr5* and WT in $^1O_2$ production. The fact that our EPR measurements were performed on isolated thylakoids wherein NPQ could not be engaged might explain why *pgr5* did not produce more $^1O_2$ than WT, but this result also indicates that OPDA downregulation in *pgr5* is not due to any *under-production* of $^1O_2$ from PSII in HL, nor to a deficiency in lipid peroxidation (electronic supplementary material, figure S2) that provides the material for oxylipin production

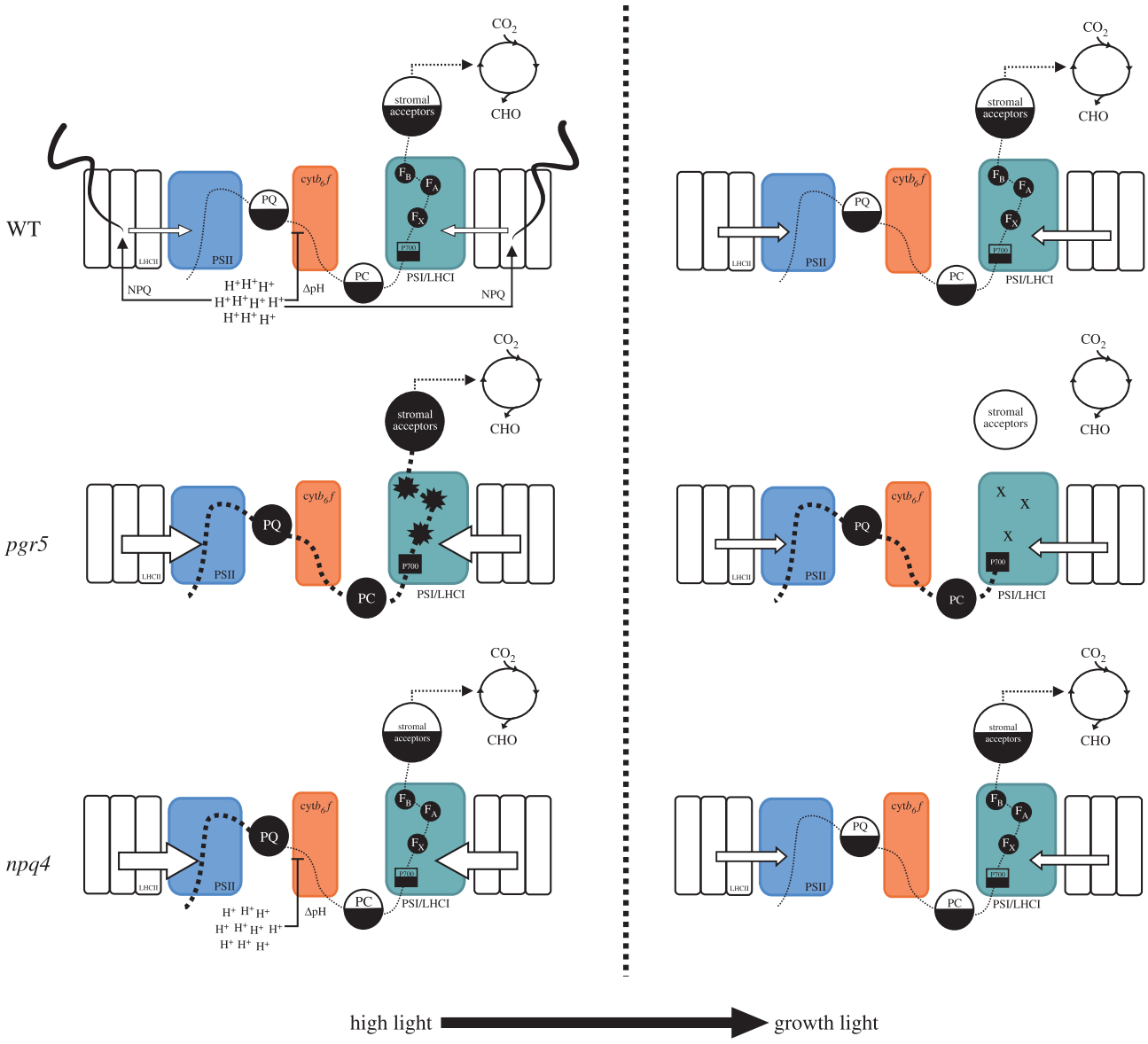

Figure 8. The consequences of distinct high light (HL) responses in WT, *pgr5* and *npq4* plants. In WT, HL causes lumen protonation that induces NPQ, which dissipates light-harvesting complex II (LHCII) excitation and maintains the plastoquinone (PQ) pool in a partially oxidized form. Lumen protonation also forms a thylakoid membrane proton gradient that slows electron transport through cytochrome b_6f, which maintains partially oxidized forms of the plastocyanin (PC) pool, P700 and the stromal electron acceptors. After a HL phase, lumen protonation, NPQ and cytochrome b_6f control are relaxed. The *pgr5* mutant lacks lumen protonation in HL, and therefore both NPQ and cytochrome b_6f control are impeded. PQ, PC, P700 and stromal electron acceptors become saturated and excess electrons move to O_2, forming ROS that inactivate F_A, F_B and F_X iron-sulphur clusters in PSI. After the HL phase, photoinhibited PSI is unable to transport electrons from P700, causing reduction of electron carriers of photosynthetic light reactions and oxidation of electron acceptors in the chloroplast stroma. This downregulates CO_2 reduction, which may contribute to decreases in starch accumulation and enzymatic oxylipin production. The *npq4* mutant lacks the PsbS protein, and therefore NPQ is absent under HL. The PQ pool can become over-reduced in HL; however, the partially oxidized states of PC, P700 and stromal acceptors are still maintained by lumen protonation and cytochrome b_6f control in *npq4*. After a HL phase, lumen protonation and cytochrome b_6f control are relaxed and the electron transport chain operates normally.

in the chloroplast [54,55]. The most likely explanation is down-regulation of chloroplast metabolism as a result of decreased PSI activity in *pgr5*. In support of this, the expression of OPDA-responsive genes is also downregulated in *Arabidopsis* mutants with inhibited PSI function (*psad1-1*, *psae1-3*; electronic supplementary material, figure S1), and in the *stn7* mutant which has decreased excitation of PSI [48].

PSI photoinhibition in HL-treated *pgr5* (figure 8) is also a likely justification for the strong upregulation of several ferritin chaperones and iron reductase enzymes (table 2). Ferritin expression is upregulated in response to excess iron, to mitigate oxidative stress through iron chelation [56]. In HL, especially in the *pgr5* mutant, sequestration and mobilization of iron may be particularly important for efficient turnover of damaged PSI and to avoid Fenton's reaction with H_2O_2 that produces destructive $^{\bullet}OH$ radicals [57]. These results highlight the specific role of iron metabolism in PSI damage and recovery.

The classical transcription response to abiotic stress, normally strongly induced by HL and involving upregulation of heat shock factors, protein chaperones and cytosolic ascorbate peroxidase (APX2), was significantly under-expressed in *pgr5* (table 2; figure 5*b*). Considering the damaging effect of HL on PSI in *pgr5*, this demonstrates that the classical 'HL

signalling' cannot be fully induced when PSI activity is inhibited. In comparison, abiotic stress-responsive gene expression in *npq4* was generally slightly (but not significantly) upregulated from WT levels (table 2). Abiotic stress signalling under HL stress is associated with photosynthetic production of H_2O_2 [35,36], which derives from superoxide anions ($O_2^{\bullet -}$) formed at the PSI acceptor side, within the PSI complex and/or in the PQ pool [58–60]. Downregulation of H_2O_2 signalling in HL-treated *pgr5* plants reiterates the signalling role of PSI and stromal factor(s) independently of the PQ redox state [48,61], which is similarly over-reduced in both *pgr5* and *npq4* mutants in HL (figure 2*c*; [21]). Under-production of H_2O_2 and the altered reduction state of the chloroplast likely impair many redox-regulated signalling pathways that operate through reduction of signalling intermediates, such as TGA transcription factors that regulate detoxification networks [31,62] or nonexpressor of pathogenesis-related 1 (NPR1) required for pathogenesis response (reviewed in [63]).

A large majority of the genes that were downregulated in HL-stressed *pgr5* compared to WT were found to be strongly induced by necrotrophic and herbivorous predators (electronic supplementary material, figure S1), underscoring the importance of both JA and its precursor OPDA, in instigating the response to fungal and insect attacks [64,65]. The transcript profiles of the HL-treated *pgr5* mutant indicate that PSI damage may severely compromise a plant's capacity to deal with stresses of both abiotic and biotic origins. This is likely to have contributed to the high mortality of *pgr5* mutants grown under field conditions [22]. Furthermore, these results reiterate the central role of light-harvesting and photosynthetic electron transport regulation in chloroplast signalling [44,48,49,66], which must be considered in assessments of the fitness and yield of plants with engineered photosynthesis.

Data accessibility. Additional data are provided as electronic supplementary material.

Authors' contributions. P.J.G., M.T. and E.-M.A. devised the research; P.J.G., Y.L.-M. and M.T. carried out the experiments and data analysis; A.T. performed EPR experiments; P.J.G., Y.L.-M., M.T. and E.-M.A. wrote the manuscript.

Competing interests. We declare we have no competing interests.

Funding. The authors acknowledge financial support from Academy of Finland projects 26080341 (P.J.G.), 307335 and 303757 (E.-M.A.), from CAPES foundation project BEX10758/14-3 (Y.L.-M.) and from CIMO project TM-16-10130 (E.-M.A.)

Acknowledgements. Transmission electron microscopy was carried out at the Electron Microscopy core facility of the University of Turku Medical Faculty, Turku, Finland. Metabolite analysis was done at the Viiki Metabolomics Unit, University of Helsinki, Viiki, Finland.

References

1. Zhu X, Long SP, Ort DR. 2010 Improving photosynthetic efficiency for greater yield. *Annu. Rev. Plant Biol.* **61**, 235–261. (doi:10.1146/annurev-arplant-042809-112206)
2. Parry MA, Reynolds M, Salvucci ME, Raines C, Andralojc PJ, Zhu XG, Price GD, Condon AG, Furbank RT. 2011 Raising yield potential of wheat. II. Increasing photosynthetic capacity and efficiency. *J. Exp. Bot.* **62**, 453–467. (doi:10.1093/jxb/erq304)
3. Murchie EH, Niyogi KK. 2011 Manipulation of photoprotection to improve plant photosynthesis. *Plant Physiol.* **155**, 86–92. (doi:10.1104/pp.110.168831)
4. Yamori W, Takahashi S, Makino A, Price GD, Badger MR, von Caemmerer S. 2011 The roles of ATP synthase and the cytochrome b6/f complexes in limiting chloroplast electron transport and determining photosynthetic capacity. *Plant Physiol.* **155**, 956–962. (doi:10.1104/pp.110.168435)
5. Niyogi KK, Grossman AR, Bjorkman O. 1998 *Arabidopsis* mutants define a central role for the xanthophyll cycle in the regulation of photosynthetic energy conversion. *Plant Cell* **10**, 1121–1134. (doi:10.1105/tpc.10.7.1121)
6. Jahns P, Holzwarth AR. 2012 The role of the xanthophyll cycle and of lutein in photoprotection of photosystem II. *Biochim. Biophys. Acta* **1817**, 182–193. (doi:10.1016/j.bbabio.2011.04.012)
7. Kromdijk J, Głowacka K, Leonelli L, Gabilly ST, Iwai M, Niyogi KK, Long SP. 2016 Improving photosynthesis and crop productivity by accelerating recovery from photoprotection. *Science* **354**, 857–861. (doi:10.1126/science.aai8878)
8. Ainsworth EA, Bush DR. 2011 Carbohydrate export from the leaf: a highly regulated process and target to enhance photosynthesis and productivity. *Plant Physiol.* **155**, 64–69. (doi:10.1104/pp.110.167684)
9. Adams III WW, Muller O, Cohu CM, Demmig-Adams B. 2013 May photoinhibition be a consequence, rather than a cause, of limited plant productivity? *Photosynth. Res.* **117**, 31–44. (doi:10.1007/s11120-013-9849-7)
10. Paul MJ, Foyer CH. 2001 Sink regulation of photosynthesis. *J. Exp. Bot.* **52**, 1383–1400. (doi:10.1093/jexbot/52.360.1383)
11. Leakey AD, Ainsworth EA, Bernacchi CJ, Rogers A, Long SP, Ort DR. 2009 Elevated CO_2 effects on plant carbon, nitrogen, and water relations: six important lessons from FACE. *J. Exp. Bot.* **60**, 2859–2876. (doi:10.1093/jxb/erp096)
12. Leonardos ED, Savitch LV, Huner N, Öquist G, Grodzinski B. 2003 Daily photosynthetic and C-export patterns in winter wheat leaves during cold stress and acclimation. *Physiol. Plant.* **117**, 521–531. (doi:10.1034/j.1399-3054.2003.00057.x)
13. Strand Å, Foyer C, Gustafsson P, Gardeström P, Hurry V. 2003 Altering flux through the sucrose biosynthesis pathway in transgenic *Arabidopsis thaliana* modifies photosynthetic acclimation at low temperatures and the development of freezing tolerance. *Plant Cell Environ.* **26**, 523–535. (doi:10.1046/j.1365-3040.2003.00983.x)
14. Inoue K, Sakurai H, Hiyama T. 1986 Photoinactivation sites of photosystem I in isolated chloroplasts. *Plant Cell Physiol.* **27**, 961–968.
15. Sonoike K, Terashima I. 1994 Mechanism of photosystem-I photoinhibition in leaves of *Cucumis sativus* L. *Planta* **194**, 287–293. (doi:10.1007/BF01101690)
16. Tjus SE, Moller BL, Scheller HV. 1998 Photosystem I is an early target of photoinhibition in barley illuminated at chilling temperatures. *Plant Physiol.* **116**, 755–764. (doi:10.1104/pp.116.2.755)
17. Tiwari A, Mamedov F, Grieco M, Suorsa M, Jajoo A, Styring S, Tikkanen M, Aro EM. 2016 Photodamage of iron–sulphur clusters in photosystem I induces non-photochemical energy dissipation. *Nat. Plants.* **2**, 16035. (doi:10.1038/nplants.2016.35)
18. Scheller HV, Haldrup A. 2005 Photoinhibition of photosystem I. *Planta* **221**, 5–8. (doi:10.1007/s00425-005-1507-7)
19. Munekage Y, Hojo M, Meurer J, Endo T, Tasaka M, Shikanai T. 2002 PGR5 is involved in cyclic electron flow around photosystem I and is essential for photoprotection in *Arabidopsis*. *Cell* **110**, 361–371. (doi:10.1016/S0092-8674(02)00867-X)
20. Yamori W, Shikanai T. 2016 Physiological functions of cyclic electron transport around photosystem I in sustaining photosynthesis and plant growth. *Annu. Rev. Plant Biol.* **67**, 81–106.
21. Tikkanen M, Rantala S, Aro EM. 2015 Electron flow from PSII to PSI under high light is controlled by PGR5 but not by PSBS. *Front. Plant Sci.* **6**, 521. (doi:10.3389/fpls.2015.00521)
22. Suorsa M *et al.* 2012 Proton Gradient Regulation5 is essential for proper acclimation of Arabidopsis photosystem I to naturally and artificially fluctuating

light conditions. *Plant Cell* **24**, 2934–2948. (doi:10.1105/tpc.112.097162)

23. Li X, Björkman O, Shih C, Grossman AR, Rosenquist M, Jansson S, Niyogi KK. 2000 A pigment-binding protein essential for regulation of photosynthetic light harvesting. *Nature* **403**, 391–395. (doi:10.1038/35000131)
24. Schreiber U, Bilger W, Neubauer C. 1995 Chlorophyll fluorescence as a nonintrusive indicator for rapid assessment of *in vivo* photosynthesis. In *Ecophysiology of photosynthesis* (eds E-D Schulze, MM Caldwell), pp. 49–70. Berlin, Germany: Springer.
25. Klughammer C, Schreiber U. 1998 Measuring P700 absorbance changes in the near infrared spectral region with a dual wavelength pulse modulation system. In *Photosynthesis: mechanisms and effects* (ed. G Garab), pp. 4357–4360. Dordrecht, The Netherlands: Kluwer Academic.
26. Birtic S, Ksas B, Genty B, Mueller MJ, Triantaphylidès C, Havaux M. 2011 Using spontaneous photon emission to image lipid oxidation patterns in plant tissues. *Plant J.* **67**, 1103–1115. (doi:10.1111/j.1365-313X.2011.04646.x)
27. Yadav DK, Kruk J, Sinha RK, Pospíšil P. 2010 Singlet oxygen scavenging activity of plastoquinol in photosystem II of higher plants: electron paramagnetic resonance spin-trapping study. *Biochim. Biophys. Acta* **1797**, 1807–1811. (doi:10.1016/j.bbabio.2010.07.003)
28. Tikkanen M, Mekala NR, Aro EM. 2014 Photosystem II photoinhibition-repair cycle protects photosystem I from irreversible damage. *Biochim. Biophys. Acta* **1837**, 210–215. (doi:10.1016/j.bbabio.2013.10.001)
29. Tikkanen M, Rantala S, Grieco M, Aro EM. 2017 Comparative analysis of mutant plants impaired in the main regulatory mechanisms of photosynthetic light reactions—from biophysical measurements to molecular mechanisms. *Plant Physiol. Biochem.* **112**, 290–301. (doi:10.1016/j.plaphy.2017.01.014)
30. Mekala NR, Suorsa M, Rantala M, Aro EM, Tikkanen M. 2015 Plants actively avoid state transitions upon changes in light intensity: role of light-harvesting complex II protein dephosphorylation in high light. *Plant Physiol.* **168**, 721–734. (doi:10.1104/pp.15.00488)
31. Mueller S, Hilbert B, Dueckershoff K, Roitsch T, Krischke M, Mueller MJ, Berger S. 2008 General detoxification and stress responses are mediated by oxidized lipids through TGA transcription factors in *Arabidopsis*. *Plant Cell* **20**, 768–785. (doi:10.1105/tpc.107.054809)
32. Hruz T, Laule O, Szabo G, Wessendorp F, Bleuler S, Oertle L, Widmayer P, Gruissem W, Zimmermann P. 2008 Genevestigator v3: a reference expression database for the meta-analysis of transcriptomes. *Adv. Bioinformatics.* **2008**, 420747.
33. Rossel JB, Wilson IW, Pogson BJ. 2002 Global changes in gene expression in response to high light in *Arabidopsis*. *Plant Physiol.* **130**, 1109–1120. (doi:10.1104/pp.005595)
34. Timperio AM, Egidi MG, Zolla L. 2008 Proteomics applied on plant abiotic stresses: role of heat shock proteins (HSP). *J. Proteomics.* **71**, 391–411. (doi:10.1016/j.jprot.2008.07.005)
35. Karpinski S, Reynolds H, Karpinska B, Wingsle G, Creissen G, Mullineaux P. 1999 Systemic signaling and acclimation in response to excess excitation energy in *Arabidopsis*. *Science* **284**, 654–657. (doi:10.1126/science.284.5414.654)
36. Jung HS, Crisp PA, Estavillo GM, Cole B, Hong F, Mockler TC, Pogson BJ, Chory J. 2013 Subset of heat-shock transcription factors required for the early response of *Arabidopsis* to excess light. *Proc. Natl Acad. Sci. USA* **110**, 14 474–14 479. (doi:10.1073/pnas.1311632110)
37. op den Camp RG *et al.* 2003 Rapid induction of distinct stress responses after the release of singlet oxygen in *Arabidopsis*. *Plant Cell* **15**, 2320–2332. (doi:10.1105/tpc.014662)
38. Ramel F, Birtic S, Ginies C, Soubigou-Taconnat L, Triantaphylides C, Havaux M. 2012 Carotenoid oxidation products are stress signals that mediate gene responses to singlet oxygen in plants. *Proc. Natl Acad. Sci. USA* **109**, 5535–5540. (doi:10.1073/pnas.1115982109)
39. Tikkanen M, Aro EM. 2014 Integrative regulatory network of plant thylakoid energy transduction. *Trends Plant Sci.* **19**, 10–17. (doi:10.1016/j.tplants.2013.09.003)
40. Munekage YN, Genty B, Peltier G. 2008 Effect of PGR5 impairment on photosynthesis and growth in *Arabidopsis thaliana*. *Plant Cell Physiol.* **49**, 1688–1698. (doi:10.1093/pcp/pcn140)
41. Leister D, Shikanai T. 2013 Complexities and protein complexes in the antimycin A-sensitive pathway of cyclic electron flow in plants. *Front. Plant Sci.* **4**, 161. (doi:10.3389/fpls.2013.00161)
42. Nishikawa Y, Yamamoto H, Okegawa Y, Wada S, Sato N, Taira Y, Sugimoto K, Makino A, Shikanai T. 2012 PGR5-dependent cyclic electron transport around PSI contributes to the redox homeostasis in chloroplasts rather than CO_2 fixation and biomass production in rice. *Plant Cell Physiol.* **53**, 2117–2126. (doi:10.1093/pcp/pcs153)
43. Yamori W, Makino A, Shikanai T. 2016 A physiological role of cyclic electron transport around photosystem I in sustaining photosynthesis under fluctuating light in rice. *Sci. Rep.* **6**, 20147. (doi:10.1038/srep20147)
44. Gollan PJ, Tikkanen M, Aro EM. 2015 Photosynthetic light reactions: integral to chloroplast retrograde signalling. *Curr. Opin. Plant Biol.* **27**, 180–191. (doi:10.1016/j.pbi.2015.07.006)
45. Demmig-Adams B, Cohu CM, Amiard V, Zadelhoff G, Veldink GA, Muller O, Adams WW. 2013 Emerging trade-offs—impact of photoprotectants (PsbS, xanthophylls, and vitamin E) on oxylipins as regulators of development and defense. *New Phytol.* **197**, 720–729. (doi:10.1111/nph.12100)
46. Satoh M, Tokaji Y, Nagano AJ, Hara-Nishimura I, Hayashi M, Nishimura M, Ohta H, Masuda S. 2014 *Arabidopsis* mutants affecting oxylipin signaling in photo-oxidative stress responses. *Plant Physiol. Biochem.* **81**, 90–95. (doi:10.1016/j.plaphy.2013.11.023)
47. Alsharafa K, Vogel MO, Oelze ML, Moore M, Stingl N, Konig K, Friedman H, Mueller MJ, Dietz KJ. 2014 Kinetics of retrograde signalling initiation in the high light response of *Arabidopsis thaliana*. *Phil. Trans. R. Soc. B* **369**, 20130424. (doi:10.1098/rstb.2013.0424)
48. Tikkanen M, Gollan PJ, Mekala NR, Isojarvi J, Aro EM. 2014 Light-harvesting mutants show differential gene expression upon shift to high light as a consequence of photosynthetic redox and reactive oxygen species metabolism. *Phil. Trans. R. Soc. B* **369**, 20130229. (doi:10.1098/rstb.2013.0229)
49. Frenkel M *et al.* 2009 Improper excess light energy dissipation in Arabidopsis results in a metabolic reprogramming. *BMC Plant Biol.* **9**, 1. (doi:10.1186/1471-2229-9-12)
50. Ramel F, Birtic S, Cuine S, Triantaphylides C, Ravanat JL, Havaux M. 2012 Chemical quenching of singlet oxygen by carotenoids in plants. *Plant Physiol.* **158**, 1267–1278. (doi:10.1104/pp.111.182394)
51. Shao N, Duan GY, Bock R. 2013 A mediator of singlet oxygen responses in *Chlamydomonas reinhardtii* and *Arabidopsis* identified by a luciferase-based genetic screen in algal cells. *Plant Cell* **25**, 4209–4226. (doi:10.1105/tpc.113.117390)
52. Ramel F *et al.* 2013 Light-induced acclimation of the *Arabidopsis* chlorina1 mutant to singlet oxygen. *Plant Cell* **25**, 1445–1462. (doi:10.1105/tpc.113.109827)
53. Roach T, Krieger-Liszkay A. 2012 The role of the PsbS protein in the protection of photosystems I and II against high light in *Arabidopsis thaliana*. *Biochim. Biophys. Acta* **1817**, 2158–2165. (doi:10.1016/j.bbabio.2012.09.011)
54. Mueller MJ. 2004 Archetype signals in plants: the phytoprostanes. *Curr. Opin Plant Biol.* **7**, 441–448. (doi:10.1016/j.pbi.2004.04.001)
55. Mosblech A, Feussner I, Heilmann I. 2009 Oxylipins: structurally diverse metabolites from fatty acid oxidation. *Plant Physiol. Biochem.* **47**, 511–517. (doi:10.1016/j.plaphy.2008.12.011)
56. Briat J, Duc C, Ravet K, Gaymard F. 2010 Ferritins and iron storage in plants. *Biochim. Biophys. Acta* **1800**, 806–814. (doi:10.1016/j.bbagen.2009.12.003)
57. Halliwell B, Gutteridge JM. 2015 *Free radicals in biology and medicine*. Oxford, UK: Oxford University Press.
58. Asada K. 2000 The water–water cycle as alternative photon and electron sinks. *Phil. Trans. R. Soc. Lond. B* **355**, 1419–1431. (doi:10.1098/rstb.2000.0703)
59. Mubarakshina MM, Ivanov BN. 2010 The production and scavenging of reactive oxygen species in the plastoquinone pool of chloroplast thylakoid membranes. *Physiol. Plant.* **140**, 103–110. (doi:10.1111/j.1399-3054.2010.01391.x)

60. Baniulis D, Hasan SS, Stofleth JT, Cramer WA. 2013 Mechanism of enhanced superoxide production in the cytochrome b_6f complex of oxygenic photosynthesis. *Biochemistry* **52**, 8975–8983. (doi:10.1021/bi4013534)
61. Piippo M, Allahverdiyeva Y, Paakkarinen V, Suoranta UM, Battchikova N, Aro EM. 2006 Chloroplast-mediated regulation of nuclear genes in *Arabidopsis thaliana* in the absence of light stress. *Physiol. Genomics* **25**, 142–152. (doi:10.1152/physiolgenomics.00256.2005)
62. Muench M, Hsin C, Ferber E, Berger S, Mueller MJ. 2016 Reactive electrophilic oxylipins trigger a heat stress-like response through HSFA1 transcription factors. *J. Exp. Bot.* **67**, 6139–6148. (doi:10.1093/jxb/erw376)
63. Noctor G, Foyer CH. 2016 Intracellular redox compartmentation and ROS-related communication in regulation and signaling. *Plant Physiol.* **171**, 1581–1592. (doi:10.1104/pp.16.00346)
64. Stintzi A, Weber H, Reymond P, Farmer EE. 2001 Plant defense in the absence of jasmonic acid: the role of cyclopentenones. *Proc. Natl Acad. Sci. USA* **98**, 12 837–12 842. (doi:10.1073/pnas.211311098)
65. Farmer EE, Alméras E, Krishnamurthy V. 2003 Jasmonates and related oxylipins in plant responses to pathogenesis and herbivory. *Curr. Opin. Plant Biol.* **6**, 372–378. (doi:10.1016/S1369-5266(03)00045-1)
66. Demmig-Adams B, Stewart JJ, Adams WW. 2014 Multiple feedbacks between chloroplast and whole plant in the context of plant adaptation and acclimation to the environment. *Phil. Trans. R. Soc. B* **369**, 20130244. (doi:10.1098/rstb.2013.0244)

ANNEX B – PUBLISHED ARTICLE II

LIMA-MELO, Y.; GOLLAN, P. J.; TIKKANEN, M.; SILVEIRA, J. A. G.; ARO, E.-M. Consequences of photosystem-I damage and repair on photosynthesis and carbon use in *Arabidopsis thaliana*. **The Plant Journal**, Oxford, v. 97, p. 1061–1072, 2019.

(Pages 92-103)

the plant journal

SEB Society for Experimental Biology

The Plant Journal (2019) **97,** 1061–1072 doi: 10.1111/tpj.14177

Consequences of photosystem-I damage and repair on photosynthesis and carbon use in *Arabidopsis thaliana*

Yugo Lima-Melo[1,2], Peter J. Gollan[1,*], Mikko Tikkanen[1], Joaquim A. G. Silveira[2] and Eva-Mari Aro[1,*]

[1]*Molecular Plant Biology, Department of Biochemistry, University of Turku, FI-20014 Turku, Finland, and*

[2]*Department of Biochemistry and Molecular Biology, Federal University of Ceará, CEP 60440-900, Fortaleza, CE, Brazil*

Received 1 August 2018; revised 19 November 2018; accepted 21 November 2018; published online 29 November 2018.

*For correspondence (e-mails petgol@utu.fi; evaaro@utu.fi).

SUMMARY

Natural growth environments commonly include fluctuating conditions that can disrupt the photosynthetic energy balance and induce photoinhibition through inactivation of the photosynthetic apparatus. Photosystem II (PSII) photoinhibition is efficiently reversed by the PSII repair cycle, whereas photoinhibited photosystem I (PSI) recovers much more slowly. In the current study, treatment of the *Arabidopsis thaliana* mutant *proton gradient regulation 5* (*pgr5*) with excess light was used to compromise PSI functionality in order to investigate the impact of photoinhibition and subsequent recovery on photosynthesis and carbon metabolism. The negative impact of PSI photoinhibition on CO_2 fixation was especially deleterious under low irradiance. Impaired starch accumulation after PSI photoinhibition was reflected in reduced respiration in the dark, but this was not attributed to impaired sugar synthesis. Normal chloroplast and mitochondrial metabolisms were shown to recover despite the persistence of substantial PSI photoinhibition for several days. The results of this study indicate that the recovery of PSI function involves the reorganization of the light-harvesting antennae, and suggest a pool of surplus PSI that can be recruited to support photosynthesis under demanding conditions.

Keywords: photosynthesis, PSI photoinhibition, PGR5, PSI recovery, CO_2 assimilation, starch, carbohydrates, mitochondrial metabolism.

INTRODUCTION

During photosynthesis, plants convert light energy into chemical energy for fixing atmospheric CO_2 in order to build complex carbon-based molecules that eventually comprise plant yield. As sessile organisms, plants are subjected to various environmental changes that modulate their photosynthetic activity. Among these, light intensity is especially important because it is directly related to the incidence of photons on the leaves. High light intensities and particularly the fluctuating light conditions that are normal under natural environments induce damage to the photosynthetic apparatus, leading to a condition of reduced photosynthetic capacity called photoinhibition (for reviews, see Powles, 1984; Aro *et al.*, 1993; Gururani *et al.*, 2015). Photosystem II (PSII) is especially susceptible to damage under high light conditions and the mechanisms of PSII photoinhibition have been studied extensively (Aro *et al.*, 1993; Gururani *et al.*, 2015), whereas photosystem I (PSI) photoinhibition has received less attention. Under optimal conditions, electrons discharged from the PSI reaction centre P700 are ejected to the PSI electron transfer chain, comprising the A_0, A_1 and the FeS centres, F_X, F_A and F_B (Amunts *et al.*, 2007; Kozuleva and Ivanov, 2016), and finally to ferredoxin (Fdx), whereas the electron hole $P700^+$ in the reaction centre is filled by the donation of an electron from plastocyanin (PC). PSI photoinhibition occurs when the capacity of stromal electron acceptors is saturated, but the flow of electrons from PC to $P700^+$ remains functional. It has been postulated that in PSI photoinhibition conditions, molecular oxygen functions as an electron acceptor from PSI, leading to the generation of reactive oxygen species (ROS), which can react with FeS centres at PSI and lead to the inhibition of electron transport activity (reviewed in Sonoike, 2011). PSI photoinhibition can occur at low temperatures (Havaux and Davaud, 1994; Terashima *et al.*, 1994; Tjus *et al.*, 1998), but can also occur under fluctuating light conditions (Suorsa *et al.*, 2012; Kono *et al.*, 2014; Tikkanen and Grebe, 2018) as well as under high light conditions (Tiwari *et al.*, 2016; Gollan *et al.*, 2017).

Recent studies have shown that PSI photoinhibition severely affects net carbon assimilation, photoprotection, starch accumulation, plant growth and retrograde signalling (Brestic *et al.*, 2015; Zivcak *et al.*, 2015; Yamori and Shikanai, 2016; Gollan *et al.*, 2017). In comparison with PSII, PSI is more resistant to photoinhibition (Barth *et al.*, 2001; Huang *et al.*, 2010), and the recovery of inhibited PSI, which is thought to involve the degradation of the protein complex and the replacement of damaged redox cofactors, is much slower (Li *et al.*, 2004; Zhang and Scheller, 2004; Sonoike, 2011; Zhang *et al.*, 2011; Tikkanen and Grebe, 2018). For this reason, PSI photoinhibition is believed to have more severe consequences on plant metabolism than PSII photoinhibition under environmental stress (Takagi *et al.*, 2016a).

Photosystem I (PSI) photoinhibition is mitigated by both upstream and downstream regulation mechanisms: the downstream mechanisms include an increase in chloroplast electron sink strength (Sonoike, 1995; Takagi *et al.*, 2016b), water–water cycle activity (Driever and Baker, 2011; Cai *et al.*, 2017) and antioxidant capacity (Takagi *et al.*, 2016a), and the upstream mechanisms involve regulating the flow of electrons from PSII to PSI (reviewed in Tikkanen and Aro, 2014; Yamamoto and Shikanai, 2019). Among the photosynthetic regulation mechanisms, the accumulation of protons in the thylakoid lumen and subsequent down-regulation of electron transport by the cytochrome b_6f complex is especially important for PSI protection. The proton gradient regulation 5 (PGR5) protein is necessary for lumen acidification, and has been shown to be a key player in protecting PSI functionality (Munekage *et al.*, 2002; Tiwari *et al.*, 2016). As a result of the absence of pH-dependent protection of PSI in *pgr5* mutant plants (Munekage *et al.*, 2002; Suorsa *et al.*, 2012; Kono *et al.*, 2014; Kono and Terashima, 2016; Tiwari *et al.*, 2016; Yamori *et al.*, 2016), exposure of *pgr5* plants to increased light intensity is a convenient system for the induction of PSI photoinhibition (Tiwari *et al.*, 2016; Gollan *et al.*, 2017). Using this system, we recently found that PSI damage severely inhibits carbon fixation and starch accumulation, and affects the chloroplast regulation of nuclear gene expression (Gollan *et al.*, 2017). The cumulative impact of this condition over the course of slow PSI recovery has not yet been clarified, however. In the current study, Arabidopsis *pgr5* mutants were used to investigate the consequences of PSI inhibition, and the subsequent recovery of PSI function over several days, on gas exchange and carbon assimilation processes. These results reveal important details about the depletion and restoration of photosynthesis and primary metabolism after severe PSI photoinhibition, and indicate that a substantial proportion of PSI may be surplus to the metabolic requirements of the plant under normal growth conditions, as has been proposed previously (Zhang and Scheller, 2004).

RESULTS

High light induces photosystem-II photoinhibition in both the wild type and the *pgr5* mutant

Both wild type (WT) and *pgr5* mutant Arabidopsis plants were treated with high light (HL) for 4 h, followed by 5 days of recovery in growth light (GL) conditions. The control sets of WT and *pgr5* mutant plants were treated similarly, but were exposed to GL alone without the 4 h of treatment under HL. Maximum chlorophyll *a* fluorescence (F_m) was used to assess PSII function in preference to the calculated F_v/F_m parameter, in order to avoid the confounding effect of PSI photoinhibition on fluorescence, especially on F_0 values (Tikkanen *et al.*, 2017; see Figure S1b). F_m measurements revealed that 4 h of HL treatment induced PSII photoinhibition in both the WT and the *pgr5* mutants (with decreases of 35 and 55%, respectively), compared with the GL levels (Figure 1a). After 24 h of recovery in GL, F_m values in WT plants were equivalent to pre-treatment levels, whereas F_m values in *pgr5* plants at 24 h after HL treatment were slightly lower than in GL-treated plants, and were fully restored to pre-treatment levels on recovery day 2 (Figure 1a).

High light inhibits P700 oxidation and ferredoxin reduction

In order to evaluate PSI photoinhibition and recovery, the maximum oxidation capacity of P700 at the PSI reaction centre (P_m) was monitored as an indicator of PSI functionality (Figure 1b). The results showed that *pgr5* mutants have lower levels of oxidizable PSI in normal GL conditions, in comparison with WT plants, as has been observed previously (Tiwari *et al.*, 2016; Gollan *et al.*, 2017). HL treatment induced an 80% decrease in the P_m value in *pgr5* plants compared with the P_m value of GL-treated control plants. The recovery of P_m in HL-treated *pgr5* plants occurred over a period of 4 days, after which time the P_m value of *pgr5* plants was restored to a similar level to that of untreated plants. A minor decrease in the P_m value was observed in the WT after 4 h of HL treatment, although there were no significant differences in P_m between GL- and HL-treated WT plants.

To further characterize the consequences of PSI photoinhibition on the photosynthetic electron transport chain, the redox state of the electron donor (PC) and acceptor (Fdx) pools of PSI were assessed (Figure 1c,d). HL-treated WT plants showed a slight decrease in the maximum reduced state of the ferredoxin pool (Fd_m), in comparison with GL-treated WT plants (Figure 1c), whereas HL-treated *pgr5* mutants showed a 60% decrease in Fd_m in comparison with GL-treated *pgr5* mutants. The Fd_m level in HL-treated *pgr5* was restored to control levels on recovery day 3. The maximum oxidized state of the plastocyanin pool (PC_m) in HL-treated *pgr5* plants was marginally, although significantly, higher in *pgr5* plants directly after treatment than in GL-treated *pgr5*

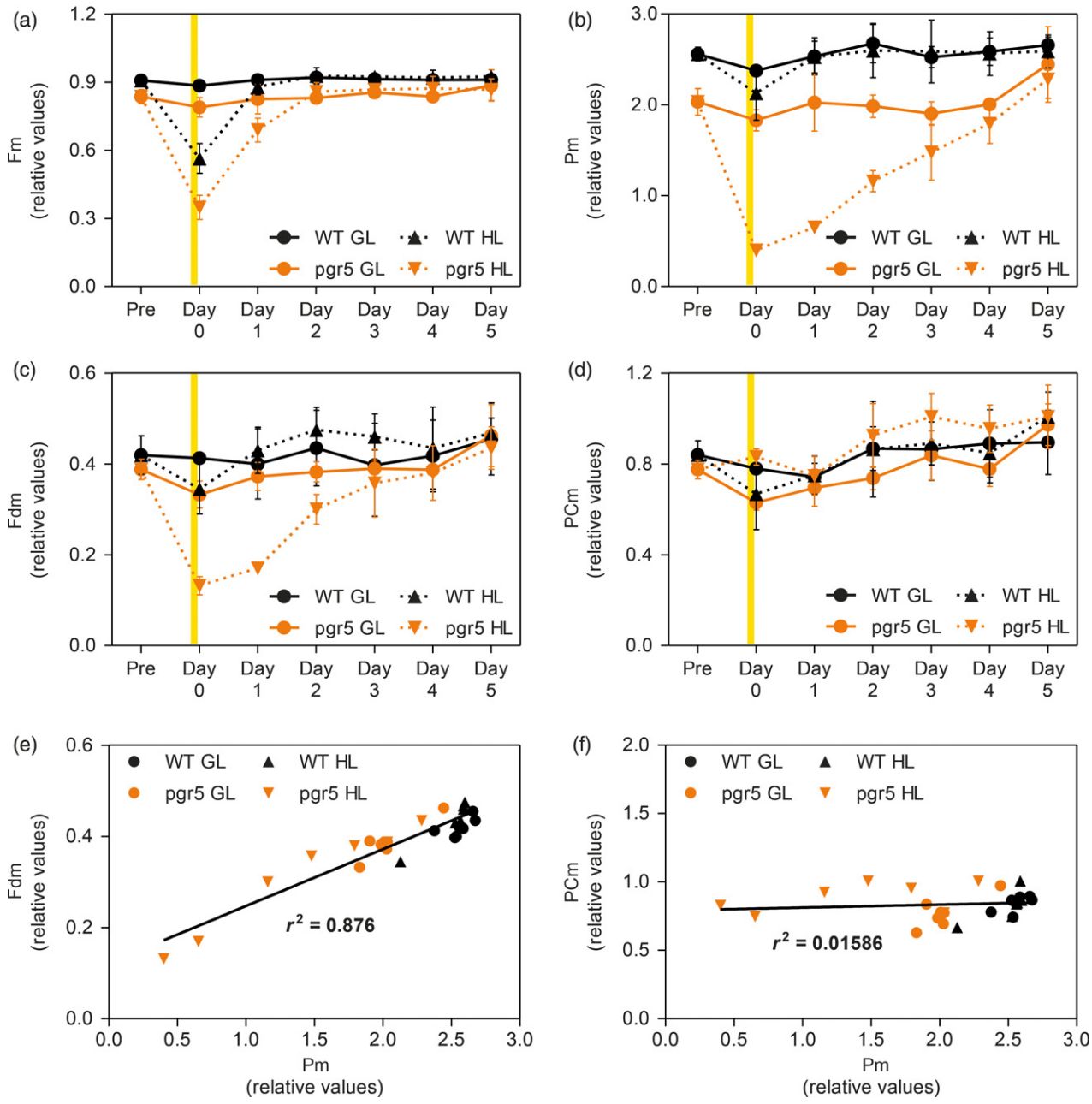

Figure 1. Parameters associated with the integrity of photosystem I (PSI) and photosystem II (PSII) in wild-type (WT) and *pgr5* plants with and without 4 h of treatment with high light (HL), and during a subsequent recovery phase of 5 days.
(a) Maximum chlorophyll *a* fluorescence (F_m); (b) maximum oxidizable P700 (P_m); (c) maximal reduction state of ferredoxin (Fdx_m); (d) maximum oxidation state of plastocyanin (PC_m), measured with a Dual/KLAS-NIR spectrophotometer in detached leaves of WT and *pgr5* plants exposed to growth light (GL, 125 μmol m^{-2} s^{-1}) or to 4 h of high light (HL, 1000 μmol m^{-2} s^{-1}) on day 0, and subsequently returned to GL conditions for recovery (days 1–5). Correlations between Fdx_m and P_m (e), and between PC_m and P_m (f), were plotted using the data shown in plots (a), (c) and (d). Error bars show the standard deviation among replicates ($n = 4$). Significant differences between treatments and between genotypes are indicated by non-overlapping error bars (Student's *t*-test, $P < 0.05$). The vertical yellow bar represents the application of 4 h of HL treatment.

plants, whereas PC_m also remained slightly higher in HL-treated *pgr5* during the recovery phase (Figure 1d). No differences in PC_m values between GL- and HL-treated WT plants were observed. A strong and positive correlation was observed between P_m and Fd_m (Figure 1e), but not between P_m and PC_m (Figure 1f).

PSI photoinhibition correlates with the depletion of the PsaB subunit

The abundance of PSI core subunit PsaB and the extrinsic stromal subunits PsaC and PsaD were assessed by immunoblots of thylakoid membranes isolated from WT and

pgr5 plants treated with GL, and during the course of PSI photoinhibition and recovery (Figure 2a–c). Total thylakoids were loaded on sodium dodecyl sulfate polyacrylamide gel electrophoresis (SDS-PAGE) according to chlorophyll equivalence, which corresponded with protein equivalence between samples, as shown by Coomassie Brilliant Blue-stained membranes (Figure 2e) and protein/chlorophyll ratio calculations (not shown). No differences in PSI subunits were apparent in thylakoids isolated from WT plants, between GL and HL treatments, whereas the abundance of PsaB was noticeably lower in *pgr5* thylakoids isolated from leaves immediately after HL treatment, in comparison with pre-treatment controls. Cross reactions between anti-PsaB antibody and the product of approximately 18 kDa were observed in *pgr5* thylakoids isolated from HL-treated plants directly after HL treatment (Figure S2), but other known PsaB degradation fragments (Sonoike, 1996; Sonoike *et al.*, 1997; Kudoh and Sonoike, 2002) were not detected. After 4 days of recovery in GL, PsaB protein in *pgr5* thylakoids remained less abundant than in untreated controls (Figures 2 and S2). PsaC and PsaD protein levels were not noticeably different in *pgr5* thylakoids isolated from HL-treated leaves, in comparison with GL and WT controls (Figure 2b,c).

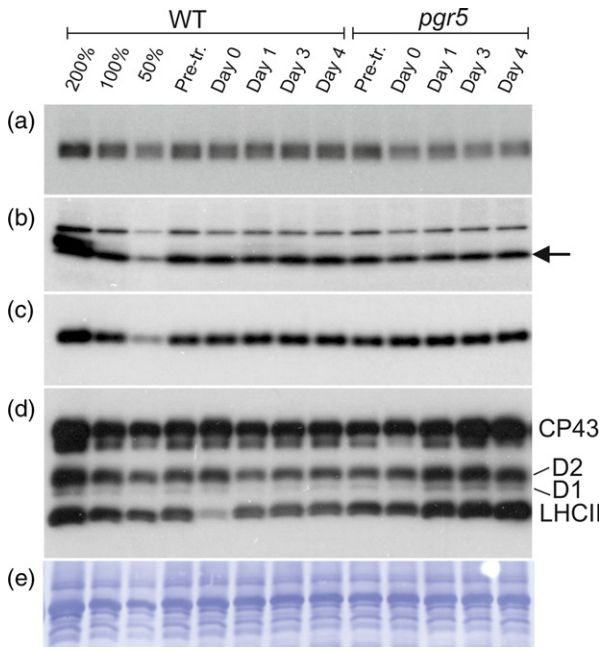

Figure 2. The impact of photosystem I (PSI) photoinhibition on the abundance of PSI protein subunits and thylakoid protein phosphorylation.
Immunoblots against PsaB (a), PsaC (b), PsaD (c) and phosphorylated threonine residues (d) performed on thylakoid membranes isolated from wild-type (WT) and *pgr5* plants before treatment (Pre-tr.), directly after 4 h of treatment with 1000 μmol m^{-2} s^{-1} (day 0) and during the following 4 days of recovery in 125 μmol m^{-2} s^{-1} (recovery day 2 omitted because of spatial constraints). Dilution series (200–50%) of the WT Pre-tr. sample were included for each antibody. All lanes (except the dilution series) contain 0.5 μg of chlorophyll; Coomassie brilliant blue staining of a representative polyvinylidene difluoride (PVDF) membrane (e) is included to show the protein equivalence between lanes. Arrow in (b) indicates the specific PsaC cross reaction. Phosphorylated photosynthetic proteins are indicated in (d).

Changes in thylakoid protein phosphorylation were detected by Western blotting with an anti-phosphothreonine antibody. The results showed a strong decrease in phosphorylated LHCII and a slight increase in phosphorylated PSII core proteins CP43, D1 and D2 directly after 4 h of HL treatment (day 0) of WT leaves, in comparison with samples harvested prior to treatment (Figure 2d). Moderate phosphorylation of both LHCII and PSII core proteins was observed in WT samples during recovery days 1–4. In contrast with the WT, the LHCII phosphorylation state was not diminished by the HL treatment of *pgr5* plants, whereas the phosphorylation of LHCII and PSII core proteins was substantially greater in the *pgr5* mutant during recovery, compared with untreated plants.

Capacity for CO_2 assimilation after HL treatment is light intensity dependent in both genotypes

To better understand the consequences of PSI photoinhibition and the subsequent slow recovery of PSI function on primary metabolism, the CO_2 assimilation rates of WT and *pgr5* mutants were measured under light intensities of 50, 125 and 1000 μmol m^{-2} s^{-1} during the pre-treatment (pre) of our experimental protocol, after HL treatment (day 0) and during the subsequent recovery period (days 1–5). In each case, *pgr5* leaves showed a distinct inhibition of CO_2 assimilation rates (*A*) immediately after the HL treatment; however, the magnitude of the decrease depended on the intensity of the light used for the measurement (Figure 3). When measured under low light conditions, *pgr5* showed almost no CO_2 assimilation immediately after HL treatment, whereas HL-treated WT plants showed only around a 50% reduction in *A* (Figure 3a). CO_2 assimilation under low light was restored to the pre-treatment level in HL-treated *pgr5* after 3 days of recovery, whereas for WT plants a full recovery was already observed after 24 h.

When *A* was measured under 125 μmol m^{-2} s^{-1} (GL), HL-treated *pgr5* mutants displayed an 80% decrease in CO_2 assimilation, but after 24 h of recovery in GL (day 1) there was no significant difference between HL- and GL-treated *pgr5*. Small increases in *A* were observed in HL-treated WT plants on days 2 and 3 of recovery, compared with the GL-treated WT (Figure 3b). Under a measuring light of 1000 μmol m^{-2} s^{-1}, CO_2 assimilation in HL-treated *pgr5* immediately after treatment was 45% lower than in untreated *pgr5* leaves, whereas inversely the WT showed a 45% increase compared with untreated leaves (Figure 3c). In both genotypes, CO_2 assimilation measured under 1000 μmol m^{-2} s^{-1} was slightly higher in the HL-treated plants during the recovery phase (i.e. days 1–3) in comparison with their respective GL-treated control plants.

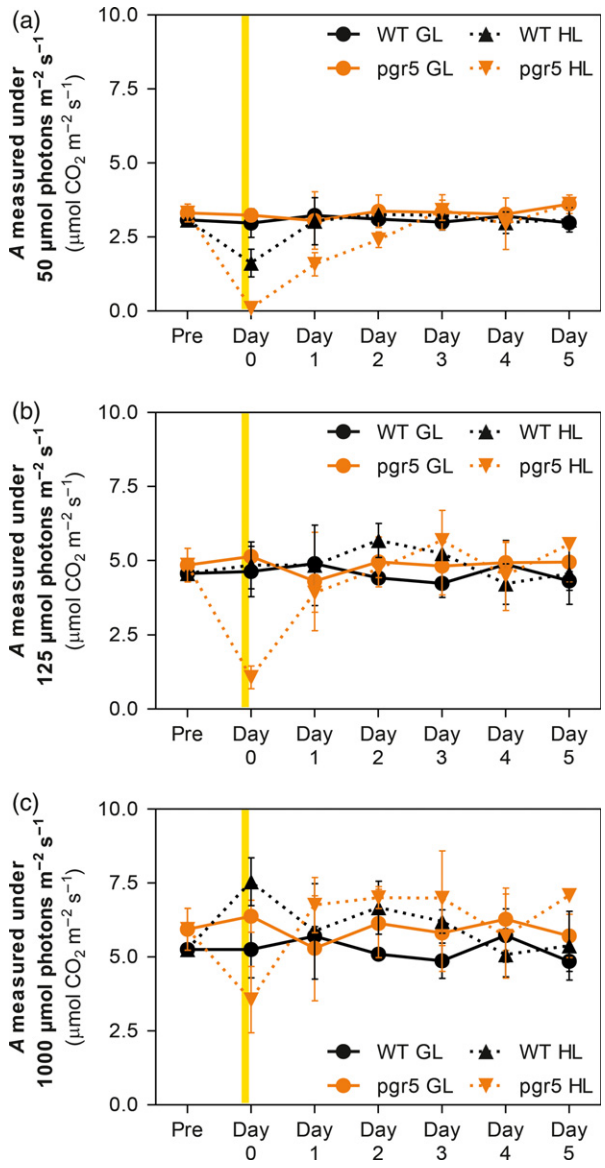

Figure 3. The impact of photosystem I (PSI) photoinhibition on CO_2 assimilation under different light intensities.
Changes in net CO_2 assimilation (*A*) in leaves of WT and *pgr5* plants before treatment (Pre), after exposure to either growth light (GL, 125 µmol m^{-2} s^{-1}) or to 4 h of high light (HL, 1000 µmol m^{-2} s^{-1}) (day 0) and during the subsequent 5 days of recovery under growth light (days 1–5). Gas exchange measurements were performed under (a) 50 µmol photons m^{-2} s^{-1}, (b) 125 µmol photons m^{-2} s^{-1} and (c) 1000 photons µmol m^{-2} s^{-1}. Error bars show standard deviations among replicates ($n = 4$). Significant differences between treatments and genotypes are indicated by non-overlapping error bars (Student's *t*-test, $P < 0.05$). The vertical yellow bar represents the application of the HL treatment.

Plotting these data as light response curves for each recovery day clearly illustrated a depression of the initial part of the curve in HL-treated *pgr5* leaves on day 0, indicating the increased light limitation of photosynthesis, which was not seen after 24 h of recovery (days 1–5; Figure S3).

High light stress altered carbohydrate metabolism

To further characterize the effects of PSI photoinhibition and recovery on plant primary metabolism, we evaluated the concentration of key molecules of carbohydrate metabolism in WT and *pgr5* leaves from plants exposed to HL treatment and recovery, as previously described. Starch content was 85% higher in WT directly after HL treatment in comparison with the concentration found in plants grown under GL, whereas there was no significant change in starch content in *pgr5* directly after HL treatment (Figure 4a). After 24 h of recovery, starch concentrations were substantially lower in both WT and *pgr5* leaves (50 and 65%, respectively), compared with leaves immediately after HL treatment. In *pgr5* plants, starch levels steadily increased during recovery days 2–4, reaching values similar to GL-treated *pgr5* plants by day 4. HL-treated WT leaves also contained less starch than GL-treated WT controls until day 4 (Figure 4a).

Glucose and fructose contents were evaluated as an index of sugar metabolism status. The HL treatment induced substantial increases in glucose and fructose concentrations in both WT and *pgr5* leaves, with an 85 and 70% increase in glucose, respectively, and a 210 and 85% increase in fructose, respectively, compared with the respective GL-treated controls (Figure 4b,c). During the initial 2 days of recovery in GL, glucose concentrations in WT and *pgr5* were slightly but significantly lower than in GL-treated controls. After 3 days of recovery, glucose concentrations in HL-treated leaves of both genotypes were equivalent to those found in GL-exposed leaves. Fructose concentrations measured in GL- and HL-treated WT and *pgr5* plants during the recovery phase were very similar (Figure 4c).

Wild-type and *pgr5* plants display distinct changes in mitochondrial respiration

Mitochondrial metabolism is directly related to photosynthetic energy production, and therefore mitochondrial respiration rates were evaluated in leaves of GL- and HL-treated WT and *pgr5* plants (Figure 5). Daytime respiration, measured by changes in CO_2 flux after 15 min of dark adaptation (Brooks and Farquhar, 1985), was around 50% higher in WT plants directly after HL treatment compared with GL levels, whereas a slight increase was also observed in HL-treated *pgr5* in comparison with the GL control (Figure 5a). There were no significant differences between GL- and HL-treated plants for both WT and *pgr5* plants during the recovery phase, however. The effect of PSI photoinhibition on dark respiration rates was evaluated by measuring O_2 uptake in WT and *pgr5* leaves throughout the 4 h of dark incubation directly following 4 h of HL or GL treatment (Figure 5b). In all cases, the rate of O_2 uptake showed a consistent and linear decline over a 4 h period in

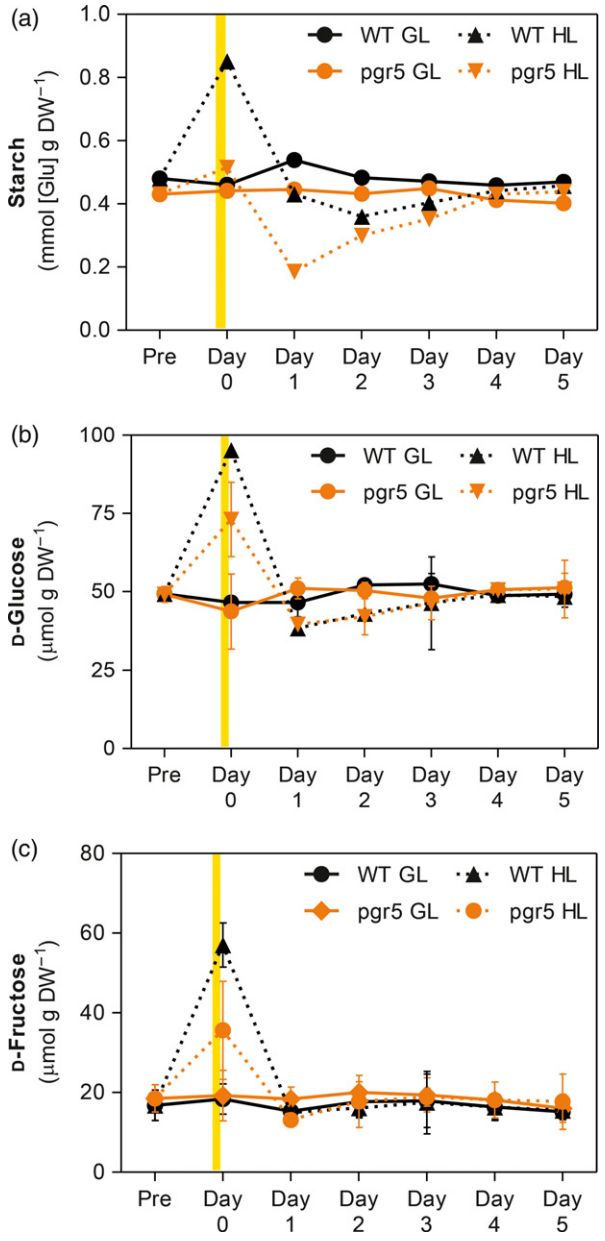

Figure 4. The effects of photosystem I (PSI) photoinhibition on the accumulation of carbohydrates.
Abundances of (a) starch; (b) D-glucose; (c) D-fructose in leaves of wild-type (WT) and *pgr5* plants before treatment (Pre), after exposure to either growth light (GL, 125 μmol m^{-2} s^{-1}) or to 4 h of high light (HL, 1000 μmol m^{-2} s^{-1}) (day 0) and during the subsequent 5 days under growth light (days 1–5). Error bars show the standard deviation among replicates (n = 4). Significant differences between treatments and genotypes are indicated by non-overlapping error bars (Student's t-test, $P < 0.05$). The vertical yellow bar represents the application of 4 h of HL treatment.

the dark (Figure 5b). The rates of decrease in the GL-treated genotypes and in HL-treated *pgr5* leaves were closely correlated, and were about three times faster than the rate of decrease in HL-treated WT leaves (Figure 5b). Analysis of O_2 uptake during night-time respiration (measured each night during the recovery period, 6 h after sunset) showed no significant effects of HL treatment in WT plants (Figure 5c), whereas in the *pgr5* mutants night-time respiration decreased significantly in the second night after HL treatment and recovered to the level of GL-treated plants by the following night (Figure 5d).

DISCUSSION

When photosynthetic electron transport exceeds the capacity of electron acceptors, both PSI and PSII are susceptible to photoinhibition through the activity of ROS, although the mechanisms of inhibition and repair differ vastly between the two photosystems. PSII photoinhibition is quickly reversed by the efficient PSII repair cycle (reviewed in Aro *et al.*, 1993), whereas the recovery of photoinhibited PSI takes place very slowly (Li *et al.*, 2004; Zhang and Scheller, 2004; Sonoike, 2011; Zhang *et al.*, 2011). Therefore, PSI is robustly protected from over-reduction, especially by regulation of electron transport through the cyt b_6f complex that is sensitive to lumenal pH (reviewed in Tikhonov, 2014). In the current study, we used HL treatment of Arabidopsis WT and *pgr5* mutant plants to study the interactions between PSII and PSI photoinhibition, and their effects on photosynthesis and sugar metabolism during light stress and recovery in normal growth conditions.

Recovery of PSI photoinhibition affects photosynthetic electron transport

The substantial decreases in F_m in both WT and *pgr5* plants after 4 h of HL exposure is attributed to PSII photoinhibition, including both light-harvesting complex II (LHCII) excitation quenching and PSII damage through an over-reduction of the electron transport chain and subsequent excitation back-pressure on PSII. F_m was fully restored within 24 h in HL-treated WT plants, but restoration took longer in *pgr5* (discussed below). In contrast, the maximum level of P700 oxidation (P_m) was severely diminished in the *pgr5* mutant after HL treatment and was slowly restored to the level of untreated controls over 4 days of recovery in GL, whereas only a minor decrease in P_m was apparent in HL-treated WT leaves. Although PSII photoinhibition may have made a small contribution to low P_m measured in *pgr5*, by decreasing linear electron transport (Baker *et al.*, 2007), the decrease of P_m in HL-treated WT was minor and not statistically significant, despite a substantially lower F_m in the same plants. Instead, the severe PSI photoinhibition in *pgr5* is attributed to the inactivation of FeS clusters F_A, F_B and F_X, inhibiting electron transport from reduced P700 (Inoue *et al.*, 1986; Sonoike and Terashima, 1994; Tiwari *et al.*, 2016). Despite the protective effect of PSII photoinhibition on PSI over-reduction (Tjus *et al.*, 1998; Tikkanen *et al.*, 2014), PSII inactivation in *pgr5* during the HL treatment did not effectively protect PSI. A larger decrease in F_m and a slower restoration of F_m

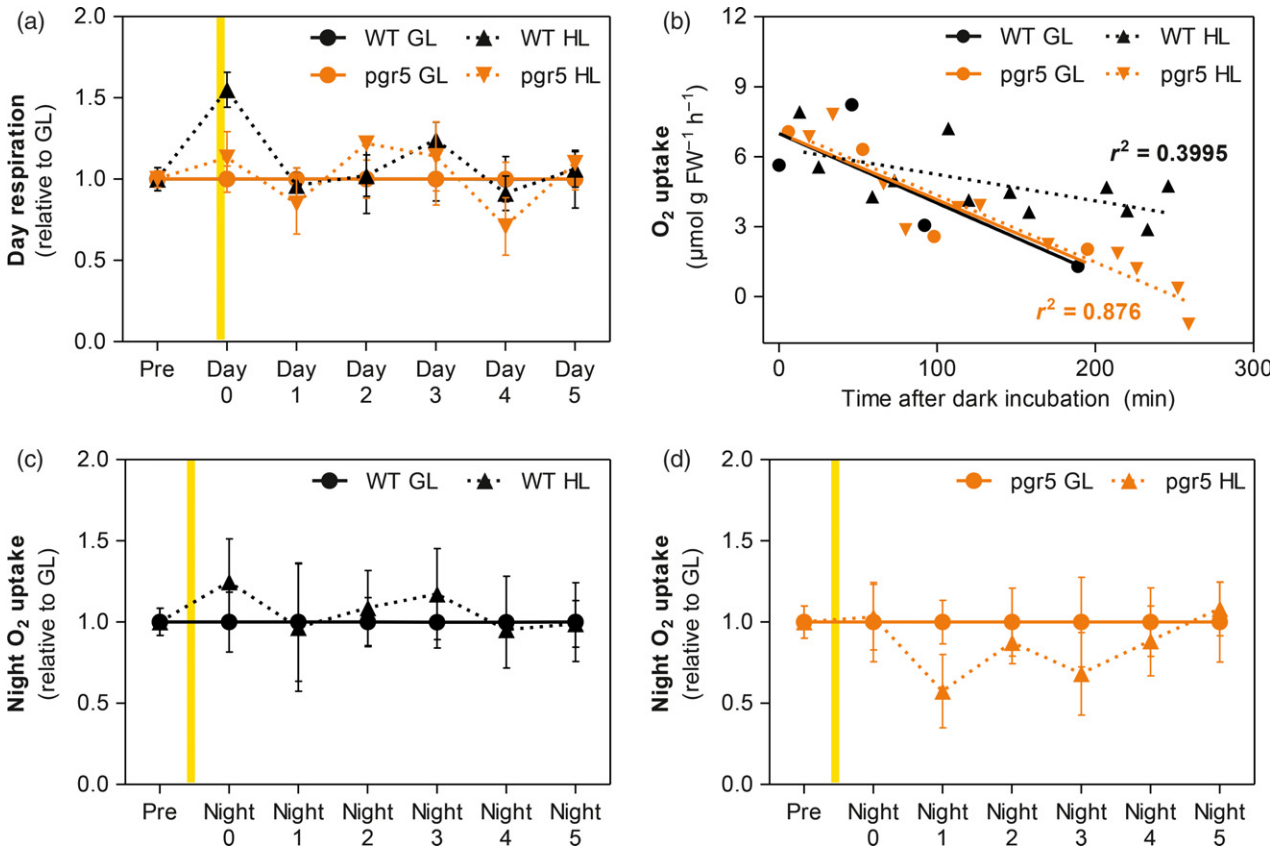

Figure 5. The effects of photosystem I (PSI) damage on mitochondrial respiration.
(a) Daytime respiration (measured after 15 min of incubation in darkness) after 4 h of high light (HL, 1000 μmol m^{-2} s^{-1}) treatment of wild-type (WT) and *pgr5* plants, and during the subsequent recovery over a period of 5 days, shown relative to controls treated with growth light (GL, 125 μmol m^{-2} s^{-1}) alone. (b) Decline in the rate of O_2 uptake in leaves of GL- and HL-treated WT and *pgr5* plants throughout the 4 h of dark incubation directly after treatment with HL or GL; r^2 values represent the correlation of trend lines that were fitted to data points from HL-treated samples (dotted lines). (c and d) Night-time O_2 uptake in leaves of WT (c) and *pgr5* (d) plants treated with 4 h of HL, measured 6 h after 'sunset'. HL data are shown relative to GL-treated controls. Error bars show the standard deviation among replicates ($n = 4$). Significant differences between treatments and genotypes are indicated by non-overlapping bars (Student's *t*-test, $P < 0.05$). The vertical yellow bar represents the application of 4 h of HL treatment.

levels in *pgr5* compared with WT after HL treatments (Figure 1) indicate strong excitation pressure on PSII, which is induced by PSI photoinhibition (Kudoh and Sonoike, 2002; Zhang and Scheller, 2004). Full recovery from PSII photoinhibition in HL-treated *pgr5*, as shown by the restoration of F_m (Figure 1) and F_v/F_m (Figure S1a), was achieved after 48 h in GL, however, despite the persistence of severe PSI photoinhibition and an abnormally high PSII excitation pressure at this time point (see Figure S1b,d). PSII recovery may be partly attributed to the increase in LHCII protein phosphorylation observed in HL-treated *pgr5* (Figure 2d), which would increase the channelling of excitation from phospho-LHCII towards PSI centres. In fact, damaged PSI is an efficient quencher of excited LHCII, with the effect of relaxing the excitation pressure within the electron transport chain (Tiwari *et al.*, 2016). Increased levels of both LHCII and PSII core protein phosphorylation in *pgr5* plants are similar to the effects induced by 'state-2 light', and are likely to facilitate the recovery of both PSI and PSII after PSI photoinhibition (Tikkanen *et al.*, 2008; Mekala *et al.*, 2015). High LHCII phosphorylation in *pgr5* directly after HL treatment showed an absence of STN7 kinase inactivation, reflecting the relatively oxidized state of the stromal redox system as a result of impaired electron transport through the partially inactivated PSI pool (Rintamäki *et al.*, 2000). This effect of stromal 'under-reduction' was also evident in the severely diminished Fdx_m during PSI photoinhibition and recovery, showing that Fdx was more oxidized in HL-treated *pgr5* plants (Figure 1) and that normal Fdx reduction recovered in strong correlation with P_m recovery. The decline in Fdx_m did not result from any changes in thylakoid-associated Fdx abundance (Figure S2), but instead reflects the inability of inhibited PSI to transport enough electrons to the stroma to fully reduce its primary electron acceptor Fdx.

The metabolic penalty of PSI photoinhibition varies according to light intensity

The assimilation of CO_2 and starch synthesis can be compromised by both PSI and PSII photoinhibition (Munekage

et al., 2008; Nishikawa *et al.*, 2012; Belgio *et al.*, 2015; Gollan *et al.*, 2017); however, PSI photoinhibition is likely to have more persistent consequences for plant fitness because of the relatively slow recovery compared with PSII. In the current work, the inactivation of PSI caused an almost complete loss of CO_2 assimilation when measured under low light (with a photosynthetic photon flux density, PPFD, of 50 μmol m^{-2} s^{-1}; Figure 3a), and the recovery of CO_2 assimilation capacity over 3 days in GL followed the trend of P_m and Fdx_m recovery that reflects the slow restoration of PSI activity. The contribution of PSII photoinhibition to low CO_2 assimilation in HL-treated *pgr5* cannot be excluded, as a decrease in CO_2 fixation was also detected in HL-treated WT leaves with intact PSI, under low light. This may be linked to a diminished yield from the partially damaged PSII pool, as well as increased consumption of NADPH and ATP for PSII repair at the expense of the Calvin–Benson–Bassham (CBB) cycle reactions (Murata and Nishiyama, 2018). Nonetheless, the effect of severe PSI photoinhibition on limiting the stromal content of NADPH and ATP is the primary reason for the decreased CO_2 fixation observed here. The diminished abundance of stromal reductants (discussed above) may lead to the relative oxidation of ferredoxin-thioredoxin reductase (FTR) and the stromal thioredoxin network, resulting in an impaired redox activation of the CBB cycle enzymes under non-saturating light conditions (Haldrup *et al.*, 2003; Buchanan, 2016; Nikkanen *et al.*, 2016).

Treatment of *pgr5* with HL has a smaller negative impact on CO_2 assimilation when measured under an irradiance of 125 μmol photons m^{-2} s^{-1}, compared with 50 μmol m^{-2} s^{-1}, and a smaller again under 1000 μmol m^{-2} s^{-1}. This result is in line with our previous study, which showed PSI photoinhibition to be especially deleterious to primary metabolism under low light intensities (Gollan *et al.*, 2017). These results clearly demonstrate that PSI photoinhibition does not necessarily limit primary metabolism, as higher light intensities require fewer functional PSI centres to transport the electrons required for primary metabolism. This can be explained in the context of PSI quantum yield (Φ_{PSI}), which is high under light limitation and decreases over increasing light intensities as the formation of $P700^+$ increases (Baker *et al.*, 2007). PSI photoinhibition would therefore intensify high Φ_{PSI}, especially under low light, whereas improved PSI efficiency in high irradiance would increase electron transport, thus enabling higher rates of metabolism. This light intensity-dependent effect on CO_2 fixation is similar to the observation that higher intensities of far-red light were required to oxidize P700 directly after chilling-induced PSI photoinhibition, compared with untreated plants (Kudoh and Sonoike, 2002; Zhang and Scheller, 2004). In addition to improved CO_2 fixation under high irradiance, the current results also show that CO_2 fixation under lower irradiances in HL-treated *pgr5* recovered to the level of GL-treated controls after 24 h of recovery (Figures 3b and S3b), despite PSI operating at only around 35% of its full capacity (according to P_m values) at that point. The capability of a partially inactivated PSI population to support normal CO_2 assimilation rates during recovery, even at low light intensity, shows an improvement in PSI efficiency after photoinhibition. This may be attributed to the increase in PSI antenna size under strong LHCII phosphorylation (Figure 2d), or may suggest the recruitment of a pool of photo-oxidisable PSI centres that is not involved in electron transport under normal conditions (Zhang and Scheller, 2004).

The natural outcome of CO_2 assimilation is the synthesis of triose phosphate, which can be exported from the chloroplast and converted to sucrose in the cytosol or can be retained in the chloroplast for starch synthesis to support metabolism in the dark (Stitt *et al.*, 2010). The concentrations of simple sugars such as glucose and fructose were found to be higher in both genotypes after HL treatment, compared with GL-treated controls, as a result of high photosynthetic activity during 4 h of HL exposure; however, the rapid onset of PSI photoinhibition in *pgr5* and subsequent limitation of CO_2 assimilation is likely to be responsible for approximately 50% less glucose and fructose concentration in *pgr5*, compared with WT, after HL treatment (day 0). Nonetheless, the levels of these sugars were equivalent in *pgr5* and WT plants throughout the recovery period (days 1–5), which show that normal sugar synthesis can be sustained in the presence of considerable PSI inhibition. In contrast, starch accumulation was substantially lower in *pgr5* than in WT, upon recovery, for several days after HL treatment. Even directly after the treatment, the starch content in *pgr5* leaves was only marginally higher than the pre-treatment levels, despite the 50–75% increase in sugars in those plants and a doubling of starch levels in the WT. These results suggest that the impairment of starch synthesis by PSI inhibition may be independent of CO_2 fixation and the accumulation of sugars. Instead, a shortfall of reducing power caused by the combined effect of PSI damage and low irradiance (growth light) may leave little energy available for starch synthesis, as limited reductants are used to support more immediate metabolic demands, including sugar synthesis. It is also possible that PSI damage and the subsequent under-reduction of stromal acceptors (discussed above) has a negative impact on redox activation of chloroplast stromal enzymes, such as the starch-branching ADP-Glc pyrophosphorylase (AGPase), which is redox regulated by NADPH-thioredoxin reductase C (NTRC; Michalska *et al.*, 2009). It should be noted that WT plants also had less starch on days 1–2 after HL treatment, compared with untreated controls, suggesting that the HL treatment affected starch accumulation independent of PSI photoinhibition; however, the starch deficiency in *pgr5* plants was much greater than in the WT.

The damage sustained by PSI in HL-treated *pgr5* mutants was shown to impair mitochondrial respiration, relative to that in the WT, during both day and night. The rates of day respiration increased in both genotypes directly after HL treatment, although to a smaller degree in *pgr5*, and were largely unaffected by PSI inhibition during the recovery phase (Figure 5a). These results correlated with the accumulation of simple sugars (Figure 4b,c), and therefore it is reasonable to assume that the reduced day respiration rate in *pgr5*, compared with the WT, after 4 h of HL treatment was a consequence of the low synthesis/accumulation of simple sugars. In comparison, night respiration (Figure 5c,d) followed the trend of starch accumulation (Figure 4a), which was negatively affected by PSI inhibition during recovery. This is in accordance with the role of starch in supporting night-time metabolism (Graf *et al.*, 2010), and suggests that growth and development processes occurring during the night may be particularly susceptible to PSI photoinhibition.

Assessing PSI photoinhibition through PSI damage, PSI function, and primary metabolism during recovery from PSI photoinhibition

PSI photoinhibition was accompanied by the rapid depletion of PsaB content from thylakoids of HL-treated *pgr5* plants, with around 50% of WT PsaB levels remaining after 4 h of HL treatment (Figure 2). This was in contrast to studies of light/chilling stress-induced PSI photoinhibition that showed PsaB degradation occurring only after several hours in recovery at normal temperature (Kudoh and Sonoike, 2002; Zhang and Scheller, 2004). This difference may be related to the inhibitory effect of chilling temperatures on proteolytic enzyme activity (Kudoh and Sonoike, 2002), which was not a factor in our experiment. The proteolytic removal and turnover of PSI complexes was not apparent at all in the current study, however, as there was no detectable decrease in the abundance of PsaC and PsaD subunits (Figure 2). Furthermore, most of the proteolytic PsaB fragments reported in chilling experiments (e.g. Sonoike *et al.*, 1997) were not detected and no significant changes were observed in chlorophyll abundance or in chlorophyll *a*/*b* ratio (not shown) in photoinhibited thylakoids. These disparities may indicate mechanistic differences in PSI photoinhibition between chilling stress and HL treatment of *pgr5*. In the former case, the downregulation of stromal metabolism in light leads to an over-reduction of PSI and ROS-induced photoinhibition (Sonoike, 2006), but at the same time the lower ATP consumption induces pH-dependent regulation of electron transport, which is likely to afford some protection to PSI (Kanazawa and Kramer, 2002). No such protection occurs in *pgr5* mutants (Munekage *et al.*, 2002; Suorsa *et al.*, 2012). Instead, the PSI reaction centre of HL-exposed *pgr5* is assaulted by a relentless current of reducing power, which quickly overwhelms stromal acceptors and results in the rapid ROS-induced destruction of PSI cofactors and core proteins (Tiwari *et al.*, 2016), perhaps similar to the effects reported in Inoue *et al.* (1989). PSI photoinhibition induced by chilling stress is likely to be less severe, especially in cold-tolerant Arabidopsis, instead triggering the controlled proteolytic degradation of PsaB and other PSI subunits to prevent further ROS formation (Tjus *et al.* 1998; Kudoh and Sonoike, 2002; Zhang and Scheller, 2004).

When the observations described above are considered together with the recovery of normal P700 oxidation within 4 days under GL, it appears that severely damaged PSI complexes may not be repaired within the time frame of the current study. Increased LCHII phosphorylation is likely to compensate, at least partially, for decreased PSI oxidation capacity at limiting light conditions (GL), whereas the restoration of PSI function may also take place by substituting damaged reaction centre proteins/cofactors and recycling other subunits. Indeed, the turnover of PSI core proteins PsaA and PsaB was recently found to be faster than the turnover of peripheral subunits (Li *et al.*, 2018), suggesting that further investigation into PSI damage and repair after different types of injury, using quantitative protein mass spectrometry, is warranted. The PSI assembly complex known as 'PSI*', lacking peripheral subunits and LHCI antennae (Ozawa *et al.*, 2010; Wittenberg *et al.*, 2017), may be a reserve of immature PSI that is visible in P_m measurements, although inactive in electron transport, which can be brought online to support electron transport and metabolism under demanding conditions such as low light intensity or after PSI photoinhibition.

EXPERIMENTAL PROCEDURES

Plant material and growth conditions

The *Arabidopsis thaliana* L. Heynh. *pgr5* mutant (Munekage *et al.*, 2002) and its reference ecotype Columbia *glabrous 1* wild type (WT) were used for all experiments. Plants were grown in a growth chamber at a constant temperature of 23 °C, with 60% relative humidity and under an 8-h photoperiod of white GL with a PPFD of 125 μmol photons m^{-2} s^{-1} for 6 weeks after sowing. Plants were either kept under GL for the reference treatment or shifted to a high light (HL) treatment of 1000 μmol photons m^{-2} s^{-1} in a controlled growth chamber set at 23 °C/60% relative humidity for 4 h. The shift to HL treatment occurred 1 h after the beginning of the photoperiod. After 4 h of treatment, HL-treated plants were used for the first measurements (day 0) and then returned to GL until the end of the experimental period (day 5). All *in vivo* measurements and plant harvesting were performed at the same time every day (i.e. 5 h after the beginning of the photoperiod), except for the O_2 uptake measurements, which were performed as described below. The experiments were repeated at least twice and at least three biological replicates were used in every experiment.

Photochemistry measurements

The photochemical parameters of PSI and PSII were simultaneously measured using a Dual-PAM-100 system (WALZ, https://

www.walz.com) based on chlorophyll *a* fluorescence (Schreiber *et al.*, 1995) and the P700 oxidation signal (Klughammer and Schreiber, 1998), respectively. F_0 and F_m measurements were taken from detached leaves after 30 min of dark acclimation. F' measurements were taken after 5 min exposure to actinic light intensities of 125 μmol photons m^{-2} s^{-1} for GL and 1000 μmol photons m^{-2} s^{-1} for HL. Maximal reduction values of ferredoxin (Fdx_m) and maximum oxidation values of P700 (P_m) and plastocyanin (PC_m) were measured with a Kinetic LED-Array Spectrophotometer (WALZ), through the deconvolution of their redox changes in intact leaves (Klughammer and Schreiber, 2016). Measurements were performed as previously described (Schreiber and Klughammer, 2016; Schreiber, 2017).

Gas exchange measurements

Leaf CO_2 exchange was measured at 400 ppm CO_2 and 23 °C using the LI-6400XL Portable Infrared Gas Analyzer system (LI-COR, https://www.licor.com). Leaves were acclimated in the dark for 15 min and the CO_2 assimilation values of each leaf were assessed with a PPFD gradient of 0, 50, 125 and 1000 μmol photons m^{-2} s^{-1}. Data were taken after the infrared gas analyser parameters reached a steady-state value following the onset of the respective PPFD (usually around 120 s). The results from 0 PPFD measurements were used to estimate day respiration, which is the rate of CO_2 evolution from processes other than photorespiration (Brooks and Farquhar, 1985). O_2 uptake was measured for 5 min in darkness at 23 °C using an 'OX-NP' oxygen microsensor (Unisense, https://www.unisense.com) from three detached leaves submerged in 50 mM sodium phosphate buffer (pH 7.2) in a gas-tight vial fitted with a rubber septum. Leaves were dark acclimated for at least 15 min prior to each O_2 consumption rate measurement.

Carbohydrates quantification

Leaves were collected, frozen until the last day of the experiment and oven dried at 60 °C for 72 h for the determination of starch, D-glucose and D-fructose contents. The total starch concentration was determined using the K-TSTA assay kit (Megazyme, https://www.megazyme.com). D-glucose and D-fructose concentrations were determined using the K-SUFRG assay kit (Megazyme) after ethanolic extraction (80% v/v) at 99 °C for 15 min. Assays were performed according to the manufacturer's protocols.

Immunoblotting

Thylakoids were isolated from mature leaves as previously described (Järvi *et al.*, 2011). Total thylakoid proteins equivalent to 0.5 μg chlorophyll were separated by SDS-PAGE, transferred to polyvinylidene difluoride (PVDF) membranes and blotted with polyclonal antibodies against PsaB (AS10 695; Agrisera, https://www.agrisera.com), PsaC (AS10 939; Agrisera) and PsaD (a kind gift from Prof. Poul Erik Jensen).

ACKNOWLEDGEMENTS

The authors acknowledge financial support from: Academy of Finland projects 26080341 (P.J.G.), and 307335 and 303757 (E.-M.A.); CAPES project BEX10758/14-3 (Y.L.-M.); CIMO project TM-16-10130 (E.-M.A.); and from CNPq (Y.L.-M. and J.A.G.S). The authors are grateful to Virpi Paakkarinen for technical assistance and Professor Jose T.A. Oliveira for his valuable comments.

CONFLICT OF INTEREST

The co-authors of this manuscript declare no conflicts of interest.

SUPPORTING INFORMATION

Additional Supporting Information may be found in the online version of this article.

Figure S1. The impact of PSI photoinhibition on chlorophyll *a* fluorescence parameters.

Figure S2. The impact of PSI photoinhibition on the PsaB subunit degradation of PSI and the abundance of thylakoid membrane-associated ferredoxin (Fdx).

Figure S3. The impact of PSI photoinhibition and recovery on CO_2 assimilation.

REFERENCES

Amunts, A., Drory, O. and Nelson, N. (2007) The structure of a plant photosystem I supercomplex at 3.4 Å resolution. *Nature*, **447**, 58–63.

Aro, E.-M., Virgin, I. and Andersson, B. (1993) Photoinhibition of photosystem II. Inactivation, protein damage and turnover. *Biochim. Biophys. Acta*, **1143**, 113–134.

Baker, N.R., Harbinson, J. and Kramer, D.M. (2007) Determining the limitations and regulation of photosynthetic energy transduction in leaves. *Plant, Cell Environ.* **30**, 1107–1125.

Barth, C., Krause, G.H. and Winter, K. (2001) Responses of photosystem I compared with photosystem II to high-light stress in tropical shade and sun leaves. *Plant, Cell Environ.* **24**, 163–176.

Belgio, E., Ungerer, P. and Ruban, A. (2015) Light-harvesting superstructures of green plant chloroplasts lacking photosystems. *Plant, Cell Environ.*, **38**, 2035–2047.

Brestic, M., Zivcak, M., Kunderlikova, K., Sytar, O., Shao, H. and Kalaji, H.M. (2015) Low PSI content limits the photoprotection of PSI and PSII in early growth stages of chlorophyll b-deficient wheat mutant lines. *Photosynth. Res.* **125**, 151–166.

Brooks, A. and Farquhar, G.D. (1985) Effect of temperature on the CO_2/O_2 specificity of ribulose-1,5-bisphosphate carboxylase/oxygenase and the rate of respiration in the light: estimates from gas-exchange measurements on spinach. *Planta*, **165,** 397–406.

Buchanan, B.B. (2016) The path to thioredoxin and redox regulation in chloroplasts. *Annu. Rev. Plant Biol.* **67**, 1–24.

Cai, Y.-F., Yang, Q.-Y., Li, S.-F., Wang, J.-H. and Huang, W. (2017) The water-water cycle is a major electron sink in Camellia species when CO_2 assimilation is restricted. *J. Photochem. Photobiol. B*, **168**, 59–66.

Driever, S.M. and Baker, N.R. (2011) The water-water cycle in leaves is not a major alternative electron sink for dissipation of excess excitation energy when CO_2 assimilation is restricted. *Plant, Cell Environ.* **34**, 837–846.

Gollan, P.J., Lima-Melo, Y., Tiwari, A., Tikkanen, M. and Aro, E.-M. (2017) Interaction between photosynthetic electron transport and chloroplast sinks triggers protection and signalling important for plant productivity. *Philos. Trans. R. Soc. Lond. B. Biol. Sci.* **372**, 20160390.

Graf, A., Schlereth, A., Stitt, M. and Smith, A.M. (2010) Circadian control of carbohydrate availability for growth in Arabidopsis plants at night. *Proc. Natl Acad. Sci. USA*, **107**, 9458–9463.

Gururani, M.A., Venkatesh, J. and Tran, L.-S.P. (2015) Regulation of photosynthesis during abiotic stress-induced photoinhibition. *Mol. Plant*, **8**, 1304–1320.

Haldrup, A., Lunde, C. and Scheller, H.V. (2003) Arabidopsis thaliana plants lacking the PSI-D subunit of photosystem I suffer severe photoinhibition, have unstable photosystem I complexes, and altered redox homeostasis in the chloroplast stroma. *J. Biol. Chem.* **278**, 33276–33283.

Havaux, M. and Davaud, A. (1994) Photoinhibition of photosynthesis in chilled potato leaves is not correlated with a loss of photosystem-II activity. *Photosynth. Res.* **40**(1), 75–92.

Huang, W., Zhang, S.B. and Cao, K.F. (2010) The different effects of chilling stress under moderate illumination on photosystem II compared with photosystem I and subsequent recovery in tropical tree species. *Photosynth. Res.* **103**, 175–182.

Inoue, K., Sakurai, H. and Hiyama, T. (1986) Photoinactivation sites of photosystem I in isolated chloroplasts. *Plant Cell Physiol.* **27**, 961–968.

Inoue, K., Fujii, T., Yokoyama, E., Matsuura, K., Hiyama, T. and Sakurai, H. (1989) The photoinhibition site of photosystem I in isolated

chloroplasts under extremely reducing conditions. *Plant Cell Physiol.* **30**(1), 65–71.

Järvi, S., Suorsa, M., Paakkarinen, V. and Aro, E.-M. (2011) Optimized native gel systems for separation of thylakoid protein complexes: novel super- and mega-complexes. *Biochem. J.* **439**, 207–214.

Kanazawa, A. and Kramer, D.M. (2002) In vivo modulation of nonphotochemical exciton quenching (NPQ) by regulation of the chloroplast ATP synthase. *Proc. Natl Acad. Sci. USA*, **99**(20), 12789–12794.

Klughammer, C. and Schreiber, U. (1998) Measuring P700 absorbance changes in the near infrared spectral region with a dual wavelength pulse modulation system. In *Photosynthesis: Mechanisms and Effects*, vol V (Garab, G., ed). Dordrecht: Kluwer Academic Publishers, pp. 4357–4360.

Klughammer, C. and Schreiber, U. (2016) Deconvolution of ferredoxin, plastocyanin, and P700 transmittance changes in intact leaves with a new type of kinetic LED array spectrophotometer. *Photosynth. Res.* **128**, 195–214.

Kono, M. and Terashima, I. (2016) Elucidation of photoprotective mechanisms of PSI against fluctuating light photoinhibition. *Plant Cell Physiol.* **57**, 1405–1414.

Kono, M., Noguchi, K. and Terashima, I. (2014) Roles of the cyclic electron flow around PSI (CEF-PSI) and O_2-dependent alternative pathways in regulation of the photosynthetic electron flow in short-term fluctuating light in Arabidopsis thaliana. *Plant Cell Physiol.* **55**, 990–1004.

Kozuleva, M.A. and Ivanov, B.R. (2016) The mechanisms of oxygen reduction in the terminal reducing segment of the chloroplast photosynthetic electron transport chain. *Plant Cell Physiol.* **57**, 1397–1404.

Kudoh, H. and Sonoike, K. (2002) Irreversible damage to photosystem I by chilling in the light: cause of the degradation of chlorophyll after returning to normal growth temperature. *Planta*, **215**(4), 541–548.

Li, X.-G., Wang, X.-M., Meng, Q.-W. and Zou, Q. (2004) Factors limiting photosynthetic recovery in sweet pepper leaves after short-term chilling stress under low irradiance. *Photosynthetica*, **42**, 257–262.

Li, L., Aro, E.-M. and Millar, H. (2018) Mechanisms of photodamage and protein turnover in photoinhibition. *Trends Plant Sci.* **23**, 667–676.

Mekala, N.R., Suorsa, M., Rantala, M., Aro, E.M. and Tikkanen, M. (2015) Plants actively avoid state-transitions upon changes in light intensity-role of light-harvesting complex II protein dephosphorylation in high light. *Plant Physiol.* **168**, 721–734 pp-00488.

Michalska, J., Zauber, H., Buchanan, B.B., Cejudo, F.J. and Geigenberger, P. (2009) NTRC links built-in thioredoxin to light and sucrose in regulating starch synthesis in chloroplasts and amyloplasts. *Proc. Natl Acad. Sci. USA*, **106**, 9908–9913.

Munekage, Y., Hojo, M., Meurer, J., Endo, T., Tasaka, M. and Shikanai, T. (2002) PGR5 is involved in cyclic electron flow around photosystem I and is essential for photoprotection in Arabidopsis. *Cell*, **110**, 361–371.

Munekage, Y.N., Genty, B. and Peltier, G. (2008) Effect of PGR5 impairment on photosynthesis and growth in Arabidopsis thaliana. *Plant Cell Physiol.* **49**, 1688–1698.

Murata, N. and Nishiyama, Y. (2018) ATP is a driving force in the repair of photosystem II during photoinhibition. *Plant, Cell Environ.* **41**, 285–299.

Nikkanen, L., Toivola, J. and Rintamäki, E. (2016) Crosstalk between chloroplast thioredoxin systems in regulation of photosynthesis. *Plant, Cell Environ.* **39**, 1691–1705.

Nishikawa, Y., Yamamoto, H., Okegawa, Y., Wada, S., Sato, N., Taira, Y., Sugimoto, K., Makino, A. and Shikanai, T. (2012) PGR5-dependent cyclic electron transport around PSI contributes to the redox homeostasis in chloroplasts rather than CO_2 fixation and biomass production in rice. *Plant Cell Physiol.* **53**, 2117–2126.

Ozawa, S.I., Onishi, T. and Takahashi, Y. (2010) Identification and characterization of an assembly intermediate subcomplex of photosystem I in the green alga Chlamydomonas reinhardtii. *J. Biol. Chem.* **285**(26), 20072–20079.

Powles, S.B. (1984) Photoinhibition of photosynthesis induced by visible light. *Ann. Rev. Plant Physiol.* **35**, 15–44.

Rintamäki, E., Martinsuo, P., Pursiheimo, S. and Aro, E.-M. (2000) Cooperative regulation of light-harvesting complex II phosphorylation via the plastoquinol and ferredoxin-thioredoxin system in chloroplasts. *Proc. Natl Acad. Sci. USA*, **97**, 11644–11649.

Schreiber, U. (2017) Redox changes of ferredoxin, P700, and plastocyanin measured simultaneously in intact leaves. *Photosynth. Res.* **134**, 343–360.

Schreiber, U. and Klughammer, C. (2016) Analysis of photosystem I donor and acceptor sides with a new type of online-deconvoluting kinetic LED-array spectrophotometer. *Plant Cell Physiol.* **57**, 1454–1467.

Schreiber, U., Bilger, W. and Neubauer, C. (1995) Chlorophyll fluorescence as a nonintrusive indicator for rapid assessment of in vivo photosynthesis. In *Ecophysiology of Photosynthesis* (Schulze, E. D. and Caldwell, M. M., eds). Berlin: Springer, pp. 49–70.

Sonoike, K. (1995) Selective photoinhibition of photosystem I in isolated thylakoid membranes from cucumber and spinach. *Plant Cell Physiol.* **36** (5), 825–830.

Sonoike, K. (1996) Degradation of psaB gene product, the reaction center subunit of photosystem I, is caused during photoinhibition of photosystem I: possible involvement of active oxygen species. *Plant Sci.* **115**, 157–164.

Sonoike, K. (2006) Photoinhibition and protection of photosystem I. In *Photosystem I*. Dordrecht: Springer, pp. 657–668.

Sonoike, K. (2011) Photoinhibition of photosystem I. *Physiol. Plant.* **142**, 56–64.

Sonoike, K. and Terashima, I. (1994) Mechanism of photosystem-I photoinhibition in leaves of Cucumis sativus L. *Planta*, **194**, 287–293.

Sonoike, K., Kamo, M., Hihara, Y., Hiyama, T. and Enami, I. (1997) The mechanism of the degradation of psaB gene product, one of the photosynthetic reaction center subunits of photosystem I, upon photoinhibition. *Photosynth. Res.* **53**, 55–63.

Stitt, M., Sulpice, R. and Keurentjes, J. (2010) Metabolic networks: how to identify key components in the regulation of metabolism and growth. *Plant Physiol.* **152**, 428–444.

Suorsa, M., Järvi, S., Grieco, M. *et al.* (2012) PROTON GRADIENT REGULATION5 is essential for proper acclimation of Arabidopsis photosystem I to naturally and artificially fluctuating light conditions. *Plant Cell*, **24**, 2934–2948.

Takagi, D., Takumi, S., Hashiguchi, M., Sejima, T. and Miyake, C. (2016a) Superoxide and singlet oxygen produced within the thylakoid membranes both cause photosystem I photoinhibition. *Plant Physiol.* **171**, 1626–1634.

Takagi, D., Hashiguchi, M., Sejima, T., Makino, A. and Miyake, C. (2016b) Photorespiration provides the chance of cyclic electron flow to operate for the redox-regulation of P700 in photosynthetic electron transport system of sunflower leaves. *Photosynth. Res.* **129**, 279–290.

Terashima, I., Funayama, S. and Sonoike, K. (1994) The site of photoinhibition in leaves of Cucumis sativus L. at low temperatures is photosystem I, not photosystem II. *Planta*, **193**, 300–306.

Tikhonov, A.N. (2014) The cytochrome b6f complex at the crossroad of photosynthetic electron transport pathways. *Plant Physiol. Biochem.* **81**, 163–183.

Tikkanen, M. and Grebe, S. (2018) Switching off photoprotection of photosystem I – a novel tool for gradual PSI photoinhibition. *Physiol. Plant.* **162**, 156–161.

Tikkanen, M., Nurmi, M., Kangasjärvi, S. and Aro, E. M. (2008). Core protein phosphorylation facilitates the repair of photodamaged photosystem II at high light. *Biochim. Biophys. Acta*, **1777**(11), 1432–1437.

Tikkanen, M. and Aro, E.-M. (2014) Integrative regulatory network of plant thylakoid energy transduction. *Trends Plant Sci.* **19**, 10–17.

Tikkanen, M., Mekala, N.R. and Aro, E.-M. (2014) Photosystem II photoinhibition-repair cycle protects Photosystem I from irreversible damage. *Biochem. Biophys. Acta*, **1837**, 210–215.

Tikkanen, M., Rantala, S., Grieco, M. and Aro, E.-M. (2017) Comparative analysis of mutant plants impaired in the main regulatory mechanisms of photosynthetic light reactions - From biophysical measurements to molecular mechanisms. *Plant Physiol. Biochem.* **112**, 290–301.

Tiwari, A., Mamedov, F., Grieco, M., Suorsa, M., Jajoo, A., Styring, S., Tikkanen, M. and Aro, E.-M. (2016) Photodamage of iron–sulphur clusters in photosystem I induces non-photochemical energy dissipation. *Nat. Plants*, **2**, 16035.

Tjus, S.E., Moller, B.L. and Scheller, H.V. (1998) Photosystem I is an early target of photoinhibition in barley illuminated at chilling temperatures. *Plant Physiol.* **116**, 755–764.

Wittenberg, G., Järvi, S., Hojka, M., Tóth, S.Z., Meyer, E.H., Aro, E.M., Schöttler, M.A. and Bock, R. (2017) Identification and characterization of a stable intermediate in photosystem I assembly in tobacco. *Plant J.* **90** (3), 478–490.

Yamamoto, H. and Shikanai, T. (2019) PGR5-dependent cyclic electron flow protects photosystem i under fluctuating light at donor and acceptor sides. *Plant Physiol.* [Epub ahead of print]. https://doi.org/10.1104/pp.18.01343

Yamori, W. and Shikanai, T. (2016) Physiological functions of cyclic electron transport around photosystem I in sustaining photosynthesis and plant growth. *Annu. Rev. Plant Biol.* **67**, 81–106.

Yamori, W., Makino, A. and Shikanai, T. (2016) A physiological role of cyclic electron transport around photosystem I in sustaining photosynthesis under fluctuating light in rice. *Sci. Rep.* **6**, 20147.

Zhang, S. and Scheller, H.V. (2004) Photoinhibition of photosystem I at chilling temperature and subsequent recovery in Arabidopsis thaliana. *Plant Cell Physiol.* **45**, 1595–1602.

Zhang, Z., Jia, Y., Gao, H., Zhang, L., Li, H. and Meng, Q. (2011) Characterization of PSI recovery after chilling-induced photoinhibition in cucumber (*Cucumis sativus* L.) leaves. *Planta*, **234**, 883–889.

Zivcak, M., Brestic, M., Kunderlikova, K., Sytar, O. and Allakhverdiev, S.I. (2015) Repetitive light pulse-induced photoinhibition of photosystem I severely affects CO_2 assimilation and photoprotection in wheat leaves. *Photosynth. Res.* **126**, 449–463.

ANNEX C – PUBLISHED ARTICLE III

LIMA-MELO, Y.; ALENCAR, V. T. C. B.; LOBO, A. K. M.; SOUSA, R. H. V.; TIKKANEN, M.; ARO, E.-M.; SILVEIRA, J. A. G.; GOLLAN, P. J. Photoinhibition of photosystem I provides oxidative protection during imbalanced photosynthetic electron transport in *Arabidopsis thaliana*. **Frontiers in Plant Science**, Lausanne, v. 10, p. 916, 2019.

(Pages 105-117)

frontiers in Plant Science

ORIGINAL RESEARCH
published: 12 July 2019
doi: 10.3389/fpls.2019.00916

Photoinhibition of Photosystem I Provides Oxidative Protection During Imbalanced Photosynthetic Electron Transport in *Arabidopsis thaliana*

Yugo Lima-Melo[1,2], Vicente T. C. B. Alencar[1], Ana K. M. Lobo[1], Rachel H. V. Sousa[1], Mikko Tikkanen[2], Eva-Mari Aro[2], Joaquim A. G. Silveira[1] and Peter J. Gollan[2]**

[1] Department of Biochemistry and Molecular Biology, Federal University of Ceará, Fortaleza, Brazil, [2] Molecular Plant Biology, Department of Biochemistry, University of Turku, Turku, Finland

OPEN ACCESS

Edited by:
Éva Hideg,
University of Pécs, Hungary

Reviewed by:
Jean-David Rochaix,
Université de Genève, Switzerland
Alexander G. Ivanov,
Bulgarian Academy of Sciences, Bulgaria

***Correspondence:**
Joaquim A. G. Silveira
silveira@ufc.br
Peter J. Gollan
petgol@utu.fi;
peter.gollan@utu.fi

Specialty section:
This article was submitted to Plant Abiotic Stress, a section of the journal Frontiers in Plant Science

Received: *08 March 2019*
Accepted: *28 June 2019*
Published: *12 July 2019*

Citation:
Lima-Melo Y, Alencar VTCB, Lobo AKM, Sousa RHV, Tikkanen M, Aro E-M, Silveira JAG and Gollan PJ (2019) Photoinhibition of Photosystem I Provides Oxidative Protection During Imbalanced Photosynthetic Electron Transport in Arabidopsis thaliana. Front. Plant Sci. 10:916. doi: 10.3389/fpls.2019.00916

Photosynthesis involves the conversion of sunlight energy into stored chemical energy, which is achieved through electron transport along a series of redox reactions. Excess photosynthetic electron transport might be dangerous due to the risk of molecular oxygen reduction, generating reactive oxygen species (ROS) over-accumulation. Avoiding excess ROS production requires the rate of electron transport to be coordinated with the capacity of electron acceptors in the chloroplast stroma. Imbalance between the donor and acceptor sides of photosystem I (PSI) can lead to inactivation, which is called PSI photoinhibition. We used a light-inducible PSI photoinhibition system in *Arabidopsis thaliana* to resolve the time dynamics of inhibition and to investigate its impact on ROS production and turnover. The oxidation state of the PSI reaction center and rates of CO_2 fixation both indicated strong and rapid PSI photoinhibition upon donor side/acceptor side imbalance, while the rate of inhibition eased during prolonged imbalance. PSI photoinhibition was not associated with any major changes in ROS accumulation or antioxidant activity; however, a lower level of lipid oxidation correlated with lower abundance of chloroplast lipoxygenase in PSI-inhibited leaves. The results of this study suggest that rapid activation of PSI photoinhibition under severe photosynthetic imbalance protects the chloroplast from over-reduction and excess ROS formation.

Keywords: photosystem I, photosynthesis, ROS, CO_2 fixation, photoinhibition, P700, redox

INTRODUCTION

Light is vital for photosynthesis, but when supplied in excess it can damage the photosynthetic apparatus and cause photo-oxidative stress. This condition occurs during states of photosynthetic imbalance, when the electron pressure in the photosynthetic electron transport chain exceeds the capacity of reducing power consumption by sink pathways, which is usually associated with stressful environmental conditions. As a result, transient or sustained production of reactive oxygen species (ROS) can occur. Excessive accumulation of ROS can impair metabolic homeostasis through oxidative damage to cells because of their high reactivity with lipids, proteins, and nucleic acids (McCord, 2000; Apel and Hirt, 2004; Munns, 2005; Sharma et al., 2012). On the other hand,

ROS play an important role in signaling pathways essential for acclimation to environmental conditions (for recent reviews, see Mittler, 2017; Czarnocka and Karpiński, 2018; Mullineaux et al., 2018). ROS can induce signaling responses directly, or indirectly by driving redox changes that modulate signaling networks (de Souza et al., 2017; Exposito-Rodriguez et al., 2017; Noctor et al., 2018; Souza et al., 2018). In addition, oxidation by-products, including oxidized lipids and pigments, transduce signals (Mueller et al., 2008; Mosblech et al., 2009; López et al., 2011; Ramel et al., 2012; Satoh et al., 2014). Because ROS are harmful at high concentrations, but at the same time are important for signaling and plant acclimation, the precise control of ROS concentrations is critical for metabolic homeostasis. Accordingly, plants control photosynthetic ROS production by regulating light-harvesting and electron transport (reviewed in Tikkanen and Aro, 2014), in particular through protonation of the thylakoid lumen that requires the proton gradient regulation 5 (PGR5) protein (Munekage et al., 2002; Suorsa et al., 2012). In the chloroplast stroma, ROS concentrations are regulated by antioxidant systems involving numerous redox enzymes, including the superoxide dismutases (SOD), which catalyze the dismutation of superoxide radical ($O_2^{\bullet-}$) to hydrogen peroxide (H_2O_2), that in turn can be subsequently reduced to water by ascorbate peroxidases (APX) and other peroxidases through the Foyer–Halliwell–Asada cycle, using ascorbate (ASC), glutathione (GSH) and thioredoxins as electron donors (Asada, 1999; Foyer and Shigeoka, 2011).

A central consequence of photo-oxidative stress is inactivation of the photosystems, a phenomenon known as "photoinhibition" (reviewed in Aro et al., 1993; Gururani et al., 2015). Photoinhibition decreases photosynthetic capacity and can therefore be deleterious to plant growth and yield (Takahashi and Murata, 2008; Kato et al., 2012; Simkin et al., 2017). Photosystem I (PSI) is particularly resistant to photoinhibition under oxidative stress conditions, due to the high efficacy of protective mechanisms that regulate the flow of electrons to the PSI donor side, including non-photochemical quenching (NPQ), lumen pH-dependent regulation of cytochrome *b6f* activity, and even PSII photoinhibition (reviewed in Tikkanen and Aro, 2014). Electron consumption at the PSI acceptor side through the Calvin-Benson cycle, photorespiration, cyclic and pseudo-cyclic electron flow are also protective factors that prevent PSI over-reduction (Yamori, 2016; Li et al., 2018).

Despite this, PSI photoinhibition occurs under specific conditions of excessive electron pressure from PSI electron donors on the lumenal side, or/and insufficient capacity of electron acceptors at the stromal side. Under these stress conditions, reduction of O_2 produces $O_2^{\bullet-}$ that can inactivate PSI iron-sulfur (FeS) clusters and cause PSI inhibition (Sonoike and Terashima, 1994; Sonoike, 1995; Takagi et al., 2016; Tiwari et al., 2016). In contrast to PSII, the recovery of inhibited PSI has been shown to occur very slowly, over several days (Barth et al., 2001; Kudoh and Sonoike, 2002; Huang et al., 2010; Lima-Melo et al., 2019). PSI photoinhibition in wild type plants has been observed under low irradiance at chilling temperatures, due to down-regulation of stromal electron sinks (Inoue et al., 1986; Terashima et al., 1994; Tjus et al., 1998; Zhang and Scheller, 2004) as well as under fluctuating light (Kono et al., 2014). On the other hand, resistance against PSI photoinhibition can be induced by acclimation to low temperature and high light conditions (Ivanov et al., 1998, 2012). Severe PSI photoinhibition can occur when pH-dependent control of electron transport is inactivated, such as in plants lacking the PGR5 protein (Munekage et al., 2002; Nandha et al., 2007; Suorsa et al., 2012; Tiwari et al., 2016). High light treatment of the *pgr5* mutant of *Arabidopsis thaliana* has provided an inducible model for PSI inhibition that has been used to study the mechanisms of PSI damage and the impacts of PSI photoinhibition on photosynthesis and metabolism of plants (Tiwari et al., 2016; Gollan et al., 2017; Lima-Melo et al., 2019). Exposure of *pgr5* to sudden increases in light intensity causes PSI FeS cluster damage (Tiwari et al., 2016) and degradation of PSI subunit proteins (Suorsa et al., 2012; Lima-Melo et al., 2019).

Although several studies have shown that PSI photoinhibition is triggered by ROS (Sonoike and Terashima, 1994; Sonoike, 1995; Sejima et al., 2014; Takagi et al., 2016), the correlation between PSI photoinhibition and ROS metabolism is not clear. In the current study, we investigated the dynamics of PSI photoinhibition in *pgr5* mutants under high light stress, and the relationship between PSI photoinhibition and ROS accumulation associated with occurrence of oxidative stress at the whole leaf level. Our data suggest that PSI photoinhibition is a mechanism to prevent excessive ROS production in order to minimize oxidative stress, at the expense of carbon assimilation and normal growth.

MATERIALS AND METHODS

Plants, Growth and Treatment Conditions

The *proton gradient regulation 5* (*pgr5*) mutant plants of *A. thaliana* L. Heynh. ecotype Columbia, which are in the *glabrous 1* genetic background (Munekage et al., 2002), were used alongside wild-type (WT) *glabrous 1* plants in all experiments. Plants were grown for 6 weeks in a growth chamber at 23°C, relative humidity 60%, 8/16 h of light/dark photoperiod under constant white light of 125 μmol photons m^{-2} s^{-1} (GL). For high light (HL) treatments, plants were shifted from GL to 1,000 μmol photons m^{-2} s^{-1} for 1 h, while control groups were kept under GL. Experiments were repeated at least twice and at least three independent replicates were used in every experiment.

Photochemical and Gas Exchange Measurements

Photosystem II and photosystem I photochemistry were measured simultaneously using a Dual-PAM-100 system (Walz, Germany) based on chlorophyll *a* fluorescence (Schreiber et al., 1995) and P700 absorbance (Klughammer and Schreiber, 1998). Detached leaves were analyzed after 30 min of dark acclimation. Gas exchange measurements (net CO_2 assimilation, *A*; transpiration, *E*; stomatal conductance, g_S; and internal CO_2 concentration, *Ci*) were performed in detached leaves after 15 min dark acclimation, using a LI-6400XT Portable Infrared Gas Analyzer (IRGA) equipped with an LED source (LI-COR Biosciences, United States). The environmental conditions inside

the IRGA chamber were: 400 ppm CO_2, 1.0 ± 0.2 kPa VPD and 25°C. For the net CO_2 assimilation (A) time-course assay, A was recorded every 15 s during changes of light intensity between GL and HL with the following protocol: 15 min of dark, 30 min of GL, 60 min of HL, 60 min of GL, 30 min of HL. For rapid light curves, a PPFD gradient of five increasing steps (0, 50, 125, 500, and 1,000 μmol photons m^{-2} s^{-1}) was used. Gas exchange data were logged after IRGA parameters reached steady-state values after the start of each light intensity (usually around 120 s). The water use efficiency (WUE) and the maximum carboxylation efficiency were calculated as A/E and A/Ci, respectively.

Leaf Membrane Damage and H_2O_2 Content

Leaf membrane damage (MD) was estimated through the electrolyte leakage method (Blum and Ebercon, 1981). Detached leaves (5 plants, 2 leaves from each plant) were placed in tubes containing deionized water and incubated in a shaking water bath at 25°C for 24 h. After measuring electric conductivity (L1), the solution was heated at 95°C for 1 h and then cooled to 25°C, after which the second electric conductivity (L2) was measured. Membrane damage was calculated as MD = (L1/L2) × 100. The H_2O_2 content was quantified using the Amplex Red Hydrogen Peroxide/Peroxidase Assay Kit (Life Technologies, Carlsbad, CA, United States) according to the manufacturer protocols. Fresh leaves were ground to a fine powder in liquid N_2 followed by the addition of potassium phosphate buffer (final concentration of 100 mM; pH 7.5). The absorbance at 560 nm was measured to quantify the H_2O_2 concentration (Zhou et al., 1997) and results were expressed as μmol H_2O_2 g^{-1} fresh weight (FW).

Histochemical Detection of Superoxide and Hydrogen Peroxide

Nitroblue tetrazolium (NBT) and diaminobenzidine (DAB) staining were performed for *in situ* detection of superoxide ($O_2^{\bullet-}$) and hydrogen peroxide (H_2O_2) accumulation, respectively, in leaves, as previously described (Ogawa et al., 1997; Thordal-Christensen et al., 1997). High light-treated leaves were detached and submerged in tubes containing DAB solution [4.67 mM DAB; 1% isopropanol (v/v) and 0.1% Triton (v/v)] or NBT solution [0.1% NBT (m/v) and 10 mM NaN_3 in 10 mM potassium phosphate buffer, pH 7.8], both protected from light, and incubated for 24 h. For NBT staining, leaves were moved to petri dishes containing water and treated with light (approximately 20 μmol m^{-2} s^{-1}) for 30 min prior to the end of the 24 h incubation. DAB- and NBT-stained leaves were then incubated in a bleaching solution [TCA 0.15% (m/v) diluted in ethanol:chloroform (4:1 v/v)] for 48 h. Stained leaves were then submerged in 80% ethanol and heated (70°C) in a water bath for 15 min, followed by several washes with 80% ethanol until complete removal of pigments. Leaves were then dried and photographed.

Lipid Peroxidation (TBARS Content and Autoluminescence Imaging)

Lipid peroxidation was estimated according to the formation of thiobarbituric acid-reactive substances (TBARS; Heath and Packer, 1968). Fresh leaves were ground to a fine powder in liquid N_2 followed by the addition of TCA [final concentration of 5% (w/v)]. After centrifugation at 12,000 × g for 15 min, 500 μl of the supernatants were immediately diluted in 2 ml of a solution containing 0.5% (w/v) of thiobarbituric acid (TBA) and 20% (w/v) of TCA and heated at 95°C in a water bath for 1 h. After cooling to 25°C, the solutions were centrifuged at 10,000 × g for 5 min and supernatants were collected for absorbance readings at 532 and 660 nm using a spectrophotometer. The absorption values at 660 nm obtained from blank samples without leaf tissue were subtracted. The concentration of TBARS was calculated using the absorption coefficient of the thiobarbituric acid-malondialdehyde complex (TBA-MDA), which is 155 mM^{-1} cm^{-1}, and the results were expressed as nmol TBA-MDA g^{-1} FW. Lipid peroxidation was also assessed by the autoluminescence of leaves and rosettes according to the method described in Birtic et al. (2011). Detached leaves or rosettes treated with GL (control), HL or physical wounding with forceps were incubated in darkness for 2 h before the luminescence signal was collected over 20 min on an electrically cooled charged-couple device (CCD) camera, using an IVIS Lumina II system (Caliper Life Sciences, United States).

Protein Extraction and Enzymatic Activity Assays

Fresh leaves were ground to a fine powder in liquid N_2 followed by the addition of potassium phosphate buffer (final concentration of 100 mM; pH 7.0) containing EDTA (final concentration of 1 mM). The homogenate was centrifuged at 15,000 × g at 4°C for 15 min, and the resulting supernatant was used for determination of all enzymatic activities. Total soluble protein content was measured according to Bradford (1976), and all the activities were expressed on the basis of protein. All enzymatic activities were determined spectrophotometrically. Superoxide dismutase (SOD; EC 1.15.1.1) activity was determined based on inhibition of nitro blue tetrazolium chloride (NBT) photoreduction (Giannopolitis and Reis, 1977). The reaction mixture contained 75 μM NBT, 20 μM riboflavin, and 100 μl of the protein extract, all diluted in 50 mM potassium phosphate buffer (pH 6.0) containing 1 mM EDTA in a final volume of 2 ml, which was incubated under illumination (30 μmol photons m^{-2} s^{-1}) at 25°C for 5 min. The absorbance was measured at 540 nm. One SOD activity unit (U) was defined as the amount of enzyme required to inhibit 50% of the NBT photoreduction, expressed as U mg^{-1} protein min^{-1}. Catalase (CAT; EC 1.11.1.6) activity was based on the reduction of H_2O_2 (Beers and Sizer, 1952; Havir and McHale, 1987). The reaction mixture contained 20 mM H_2O_2, and 25 μl of the protein extract, all diluted in 50 mM potassium phosphate buffer (pH 7.0) in a final volume of 1.5 ml. The reaction was started by adding the protein extract and the decrease in absorbance at 240 nm at 30°C was monitored for 300 s. CAT activity

was calculated using the molar extinction coefficient of H_2O_2 (40 mM^{-1} cm^{-1}) and expressed as μmol H_2O_2 mg^{-1} protein min^{-1}. APX (EC 1.11.1.11) activity was measured based on the oxidation of ascorbate (ASC) (Nakano and Asada, 1981) in a reaction mixture containing 0.45 mM ASC, 3 mM H_2O_2, and 50 μl of the protein extract, all diluted in 100 mM potassium phosphate buffer (pH 7.0) containing 1 mM EDTA in a final volume of 1.5 ml. The reaction was started by adding the H_2O_2 solution and the decrease in absorbance at 290 nm at 25°C was monitored for 300 s. APX activity was expressed as μmol ASC mg^{-1} protein min^{-1}. Monodehydroascorbate reductase (MDHAR; EC 1.6.5.4) activity was assayed based on the generation of monodehydroascorbate (MDHA) free radicals by ascorbate oxidase (AO; 1.10.3.3) and following oxidation of NADH (Hossain et al., 1984) in a reaction mixture containing 0.1 mM NADH, 2.5 ASC, 0.84 units/ml AO, and 75 μl of the protein extract. The reaction mixture was adjusted to 725 μl with 50 mM Tris-HCl buffer (pH 7.6). The reaction was started by adding the AO solution and the decrease in absorbance at 340 nm at 25°C was monitored for 300 s. MDHAR activity was calculated using the extinction coefficient of NADH (6.2 mM^{-1} cm^{-1}) and expressed as nmol NADH mg^{-1} protein min^{-1}. Dehydroascorbate reductase (DHAR; EC 1.8.5.1) activity was assayed based on the oxidation of GSH (Nakano and Asada, 1981) in a reaction mixture containing 2.5 mM GSH, 0.2 mM dehydroascorbate (DHA), and 50 μl of the protein extract, all diluted in 50 mM potassium phosphate (pH 7.0) in a final volume of 1.5 ml. The reaction was started by adding the DHA solution and the increase in absorbance at 265 nm at 25°C was monitored for 300 s. DHAR activity was expressed as nmol NADH mg^{-1} protein min^{-1}.

Gene Expression Analysis

Plants were treated with GL and HL, after which leaves were detached and frozen in liquid N_2. Leaf samples contained four leaves from individual plants. Frozen leaves were ground to a powder in liquid N_2 and total RNA was purified using TRIsure (Bioline, United States), according to the protocol supplied, with an additional final purification in 2.5 M LiCl overnight at −20°C. RNAseq libraries were constructed, and libraries were sequenced in 50 bp single-end reads using Illumina Hiseq 2500 technology (BGI Tech Solutions, Hong Kong). Reads were aligned to the reference genome (*A. thaliana* TAIR 10) using Strand NGS 2.7 software (Agilent, United States). Aligned reads were normalized and quantified using the DESeq R package. Gene expression fold changes were calculated using a two-way ANOVA test on triplicate samples (n = 3) with Benjamini–Hochberg p-value correction to determine the false discovery rate (FDR) for each gene.

Western Blotting

Leaf tissue was ground to a powder in liquid nitrogen and then incubated in 20 mM Tris buffer (pH 7.8) containing 2% SDS for 20 min at 37°C, followed by 5 min centrifugation at 15,000 × g. The supernatant containing total leaf protein was used for Western blotting. 10 μg of total protein were separated on SDS-PAGE gels containing 12% acrylamide, transferred to polyvinylidene difluoride (PVDF) membranes and blotted with polyclonal antibodies against LOX-C antiserum (AS07 258; Agrisera).

RESULTS

High Light Rapidly Induces PSI Photoinhibition in *pgr5* Mutants

Photosynthetic parameters were monitored in leaves of wild-type (WT) and *pgr5* mutant plants that were grown under 125 μmol photons m^{-2} s^{-1} (growth light; GL) and then exposed to 1,000 μmol photons m^{-2} s^{-1} (high light; HL). Chlorophyll *a* fluorescence and P700 absorbance were measured during 5 h HL treatments. The PSI photoinhibition levels were estimated through the evaluation of the maximum oxidation of P700 at the PSI reaction center (P_m). Before the HL treatment, the average P_m value of WT leaves (1.2) was almost 30% higher than that of *pgr5* leaves (0.85; see 0 h in **Figure 1A**). The P_m value of WT leaves remained virtually unchanged through the 5 h HL treatment, whereas the same parameter in *pgr5* decreased to 60% of the pre-treatment level after only 15 min under HL, with further decreases to 45 and 35% after 30 min and 1 h HL, respectively. P_m in HL-treated *pgr5* reached a steady-state value of around 0.15 (20% of pre-treatment P_m) after 3 h of HL treatment.

PSII photoinhibition was evaluated by monitoring the decrease of the maximum chlorophyll *a* fluorescence (F_m) during the same time-course experiment. The F_m values before the onset of the HL treatment were almost identical in WT and *pgr5* (**Figure 1B**). After 15 min, F_m values decreased to 0.75 and 0.65 in WT and *pgr5*, respectively, and then showed a steady decline over the course of the 5 h HL treatment in both genotypes. In contrast, the HL-induced decline in the calculated F_v/F_m (maximum quantum efficiency of PSII) parameter was substantially greater in the *pgr5* mutant (**Figure 1C**), which corresponded to significantly higher levels of minimum chlorophyll *a* fluorescence (F_o) after 30 min HL exposure, when compared to WT (**Figure 1D**).

Time-Resolved Diminution of CO_2 Assimilation During PSI Photoinhibition

In order to investigate the consequences of progressive HL-induced photoinhibition of PSI on net CO_2 assimilation rate (A) and respiration in WT and *pgr5* mutant plants, these processes were evaluated during cycles of GL and HL exposure (**Figure 2**). In both genotypes, similar rates of CO_2 assimilation and day-time respiration (measured by CO_2 evolution in the dark) were observed in GL-treated plants (**Figure 2A**). During the first minutes of the transition from GL to HL, A increased at a rate of approximately 1.6–1.7 μmol CO_2 m^{-2} s^{-1} *per* min in both WT and *pgr5* plants (**Figure 2B**). After approximately 10 min in HL, WT A decreased until the end of the first hour of HL treatment at a rate of approximately 0.03 μmol CO_2 m^{-2} s^{-1} *per* min, while A decline in *pgr5* during the HL treatment was far more rapid than in the WT, especially during the early phase of HL exposure (0.11 μmol CO_2 m^{-2} s^{-1} *per* min) compared to

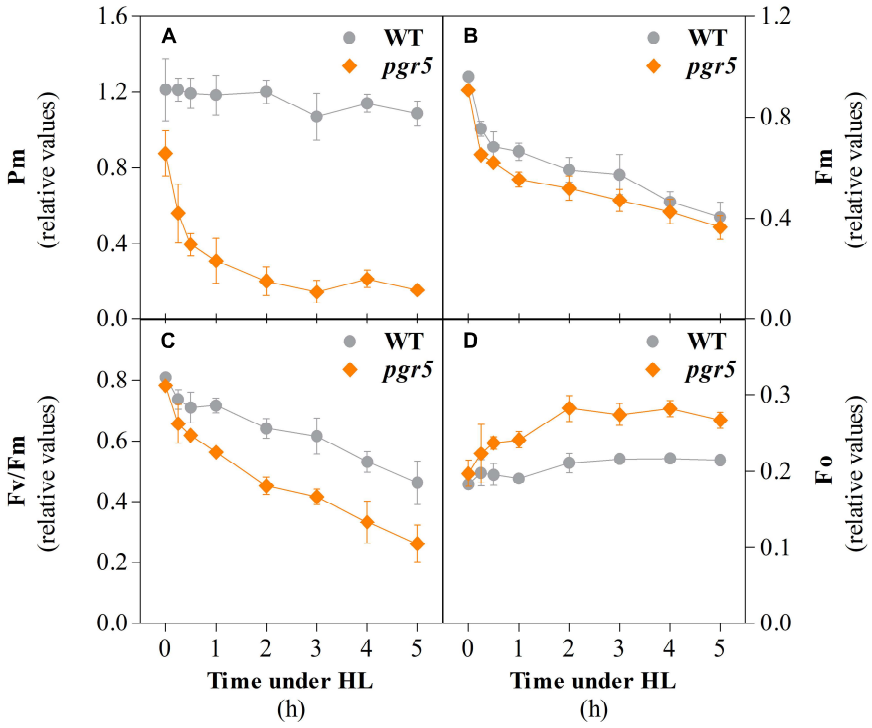

FIGURE 1 | Parameters associated with PSI and PSII integrity in wild type (WT) and *pgr5* mutants during treatment with high light (HL). Maximum oxidizable P700 (P_m, **A**); maximum chlorophyll *a* fluorescence (F_m, **B**); maximum efficiency of PSII (F_v/F_m, **C**); minimum chlorophyll *a* fluorescence (F_o, **D**) measured in detached leaves of WT and *pgr5* plants grown under a photosynthetic photon flux density of 125 μmol m^{-2} s^{-1} and treated with 1,000 μmol m^{-2} s^{-1} for 5 h. Error bars show standard deviation among replicates ($n = 4$). Significant differences between genotypes are indicated by non-overlapping error bars (Student's *t*-test, $p < 0.05$).

the latter phase (0.05 μmol CO_2 m^{-2} s^{-1} *per* min) of treatment (**Figure 2C**). At the end of the 1 h HL treatment, *A* was 40% lower in *pgr5* mutants than in WT (**Figures 2A,C**). Under a second phase of GL following the HL treatment, *A* in WT leaves was slightly lower than the level observed in the first GL phase prior to the HL treatment, while the rate in HL-treated *pgr5* mutants was approximately 0 μmol CO_2 m^{-2} s^{-1} (**Figure 2A**). A second HL treatment after 1 h GL induced another rapid increase in CO_2 fixation for both genotypes, and in each case the maximum initial rates under the second treatment were approximately equivalent to the rates observed before the end of the previous HL treatment (7.5 μmol CO_2 m^{-2} s^{-1} in WT and 5 μmol CO_2 m^{-2} s^{-1} in *pgr5*), corresponding to approximately 35% lower CO_2 fixation in *pgr5* than in WT during the second HL treatment (**Figure 2A**). Notably, the rate of increase in *A* during the second HL treatment was slower in both WT and *pgr5* (0.13 and 0.16 μmol CO_2 m^{-2} s^{-1} *per* min, respectively; **Figure 2D**) in comparison to the rates of increase during the first HL treatment (1.74 and 1.58 μmol CO_2 m^{-2} s^{-1} *per* min, respectively; **Figure 2B**). The rate of decline in *A* during the second HL treatment was similar between WT and *pgr5* (**Figure 2E**), and smaller than that observed during the first HL treatment (**Figure 2C**).

Analyses of gas exchange in WT and *pgr5* plants pre-treated with GL or HL for 1 h were conducted using light-response curves to investigate the effects of PSI photoinhibition under different irradiances. CO_2 assimilation rates over increasing light intensities were similar in both WT and *pgr5* plants treated with GL and were substantially decreased in both genotypes after 1 h HL treatment (**Figure 3A**). Significantly lower *A* values were observed in HL-treated *pgr5* compared to HL-treated WT, especially in the region of the curve measured under irradiances below 200 μmol photons m^{-2} s^{-1} (**Figure 3A**). Higher internal CO_2 concentration (C_i) was recorded in HL-treated *pgr5* at the lowest irradiances of the light curve when compared to all other plants, while there were no significant differences in *Ci* at high irradiances (**Figure 3B**). Stomatal conductance (g_s) values were higher in GL-treated *pgr5* when compared to GL-treated WT, and were substantially lower in both genotypes after the HL treatment, compared to GL-treated plants (**Figure 3C**). No differences in g_s values between the genotypes were observed after the HL treatment. The changes in transpiration rate (*E*) over the light curve were similar to that observed for g_s (**Figure 3D**). The trends observed in the maximum carboxylation efficiency (A/C_i)-PPFD curve were similar to those in the *A*-PPFD curve (**Figures 3A,E**, respectively), although the difference between the HL-treated *pgr5* and the other groups was more evident, as a consequence of the higher C_i values under low irradiances (**Figure 3B**). Water use efficiency (WUE) was strikingly lower in the HL-treated *pgr5* mutants when measured under low irradiances, compared to the other treatments (**Figure 3F**), reflecting the very low *A* measured in those leaves (**Figure 3A**).

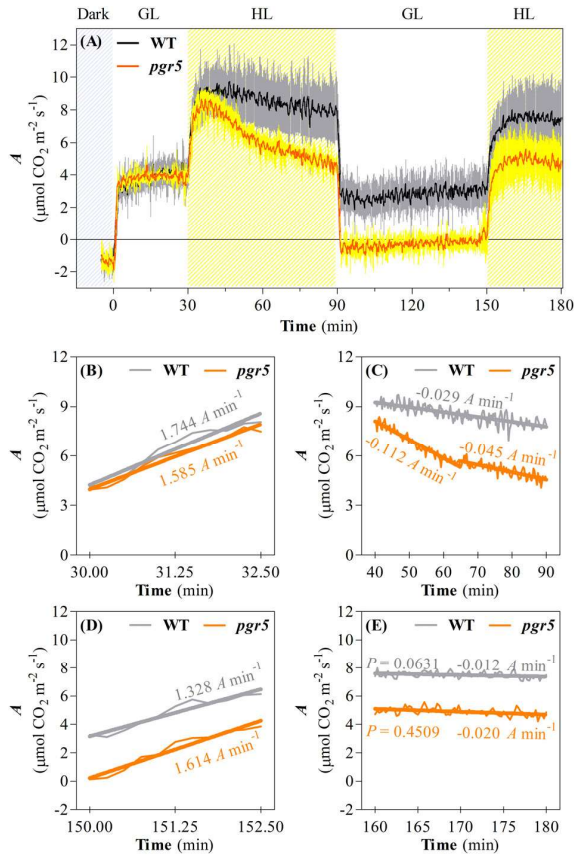

FIGURE 2 | Changes in net CO_2 assimilation during a time-course PSI photoinhibition. **(A)** CO_2 assimilation (*A*) in leaves of WT and *pgr5* mutants during changes of light intensity between growth light (GL; 125 µmol m^{-2} s^{-1}) and high light (HL; 1,000 µmol m^{-2} s^{-1}). Hatched gray and hatched yellow sections indicate dark and HL treatments, respectively. Error margins are shown in gray (WT) and yellow (*pgr5*) and indicate standard deviation among replicates ($n = 6$). Significant differences between treatments and genotypes are indicated by non-overlapping error bars (Student's *t*-test, $p < 0.05$). Linear regression lines of changes in *A* drawn in key steps of the time-course like the onset of the first HL treatment **(B)**, during the first HL treatment **(C)**, the onset of the second HL treatment **(D)**, and during the second HL treatment **(E)**. *P*-values were calculated to estimate if the slopes are significantly different from zero. All *P*-values were lower than 0.0001, except where shown in **(E)**.

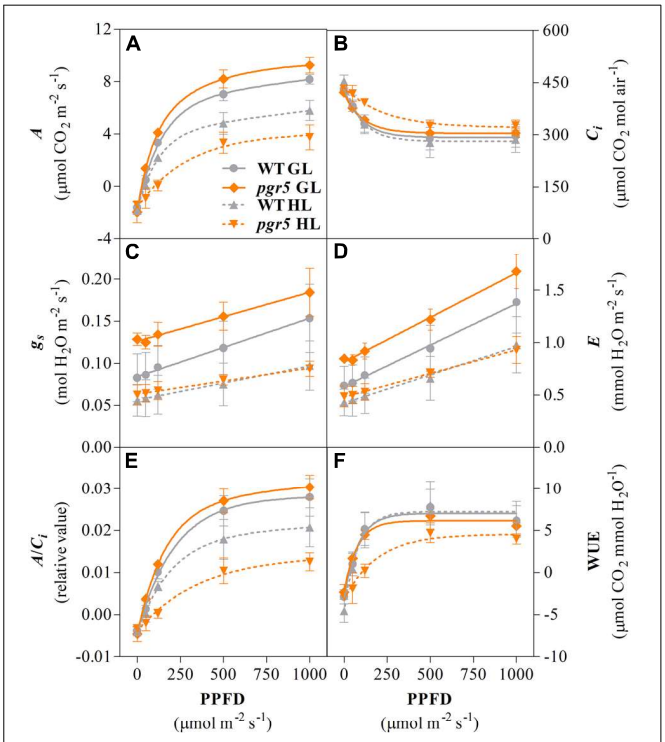

FIGURE 3 | Gas exchange response to increasing light intensity. Net CO_2 assimilation rate (*A*, **A**); internal CO_2 concentration (C_i, **B**); stomatal conductance rate (g_s, **C**); transpiration rate (*E*, **D**); maximum carboxylation efficiency (A/C_i, **E**); water use efficiency (WUE, **F**) measured in leaves of WT and *pgr5* plants previously treated with growth light (GL; 125 µmol m^{-2} s^{-1}) or high light (HL; 1,000 µmol m^{-2} s^{-1}) for 1 h. Error bars show standard deviation among replicates ($n = 4$). Significant differences between treatments and genotypes are indicated by non-overlapping error bars (Student's *t*-test, $p < 0.05$).

ROS Accumulation, and Activities and Expression of Antioxidant Systems After PSI Photoinhibition

To explore the relationship between PSI photoinhibition and accumulation of ROS, several markers of oxidative stress were evaluated in HL-treated leaves of WT and *pgr5* mutants. Membrane damage, estimated through electrolyte leakage, increased significantly after 1 h of HL treatment in both genotypes, compared to the GL controls; however, no difference was detected between WT and *pgr5* mutants in either condition (**Figure 4A**). Spectrophotometric measurements of H_2O_2 concentrations in leaf tissue showed no difference between GL and 1 h HL treatments or between genotypes (**Figure 4B**). Qualitative *in situ* assessments of H_2O_2 and superoxide ($O_2^{\bullet-}$) accumulation in HL-treated leaves by 3,3′-diaminobenzidine (DAB) and nitro-blue tetrazolium (NBT) staining, respectively, also showed no obvious differences between WT and *pgr5* in terms of accumulation of these ROS (**Figures 4C,D**).

Activities of SOD, CAT, APX, MDHAR, and DHAR were measured in leaves to assess any effects of PSI photoinhibition on ROS scavenging capacity. Overall, the results showed slightly higher enzyme activities in *pgr5*, in comparison to WT, in both light conditions (**Figure 5**). Total leaf CAT activity was significantly higher in *pgr5* than in WT under GL (**Figure 5B**), while total DHAR activity showed a significant increase in HL-treated *pgr5*, compared to GL-treated *pgr5*, which was not evident in WT (**Figure 5E**). Changes in the expression of genes involved in the Foyer–Halliwell–Asada cycle were assessed in WT and *pgr5* plants prior to HL treatment, as well as after 15 min and 1 h HL exposure. Most genes were upregulated by HL treatment in both WT and *pgr5* plants, with only minor differential expression between genotypes in most cases. Despite the similar trend of HL-induced expression in both genotypes, APX2, DHAR1 and the SOD enzymes CDS1, CDS2, and FSD2, were down-regulated in *pgr5* under HL relative to WT levels (**Figure 6**). Conversely,

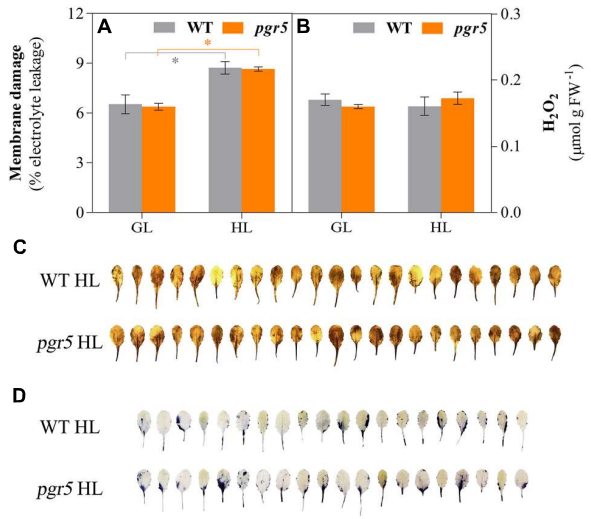

FIGURE 4 | Indicators of oxidative stress in WT and *pgr5* mutants under growth light or after high light treatment. Membrane damage **(A)** and H_2O_2 content **(B)** in leaves of WT and *pgr5* mutants treated with growth light (GL; 125 μmol m^{-2} s^{-1}) or high light (HL; 1,000 μmol m^{-2} s^{-1}) for 1 h. Error bars show standard error among replicates (n = 4). Significant differences between treatments and genotypes are indicated by asterisks (Student's t-test, $p < 0.05$). 3,3-diaminobenzidine (DAB, **C**) and nitro-blue tetrazolium (NBT, **D**) staining to assess the accumulation of H_2O_2 and superoxide accumulation, respectively, in detached leaves of HL-treated WT and *pgr5* plants.

APX1, CAT2 and FSD1 were upregulated in HL-treated *pgr5* compared to the WT.

Assessment of thiobarbituric acid-reactive substances (TBARS) content provides an indication of lipid peroxidation. TBARS detected in GL-treated *pgr5* did not differ significantly from GL-treated WT, while after 1 h HL treatment TBARS content in *pgr5* was markedly lower than GL and WT levels (**Figure 7A**). Autoluminescence imaging showed that levels of lipid oxidation in leaves and rosettes increased in WT after 1 h HL treatment, in comparison to GL-treated plants, but a corresponding increase was not detected in HL-treated *pgr5* (**Figures 7B,C**). In contrast, strong autoluminescence signals were detected in both genotypes after mechanical wounding of leaves (**Figure 7B**). Western blots showed increases in the abundance of chloroplast lipoxygenase (LOX2) in both WT and *pgr5* after 1 h HL treatment. However, substantially lower LOX2 abundance was detected in both GL- and HL-treated *pgr5* leaves, in comparison to WT controls (**Figure 7D**), corroborating the results of TBARS tests (**Figure 7A**).

DISCUSSION

Oxidative stress in plants is closely linked to photosynthetic activity, as the transfer of photosynthetic excitation or electrons to oxygen can lead to the overproduction of ROS (for a recent review, see Mullineaux et al., 2018). Excess ROS production resulting from disturbed photosynthetic redox homeostasis is the cause of photodamage to both PSII and PSI, although the mechanisms of damage and repair differ considerably between the two photosystems and distinct intersystem regulation is evident. For example, it has become well established that PSII damage can serve as a photoprotective mechanism by preventing over-reduction and inactivation of downstream factors, especially PSI (Tikkanen et al., 2014; Huang et al., 2016). The current work suggests that rapid PSI photoinhibition under severe photosynthetic imbalance can also prevent excessive ROS production and oxidative damage.

PSI photoinhibition under disturbed redox homeostasis is associated with insufficient stromal acceptor capacity and increased utilization of O_2 as an alternative electron acceptor, leading to formation of $O_2^{\bullet-}$ that can inactivate PSI iron-sulfur (FeS) clusters (reviewed in Sonoike, 2011). Protection from PSI photoinhibition is especially dependent on functional pH-dependent regulation of electron flow to PSI during increased irradiance (Suorsa et al., 2012; Kono et al., 2014; Tiwari et al., 2016; Gollan et al., 2017; Lima-Melo et al., 2019; Yamamoto and Shikanai, 2019). In the current work, a large decrease in P_m within the first minutes of exposure of *pgr5* mutants to HL shows that PSI photoinhibition occurs rapidly upon the onset of imbalance between the PSI donor and acceptor sides. This rapid inhibition suggests that the normal levels of antioxidant activity measured in *pgr5* (**Figure 5**) were not sufficient to mitigate ROS-induced PSI damage within the initial stages of imbalance. These results support other findings that showed that chloroplast antioxidant

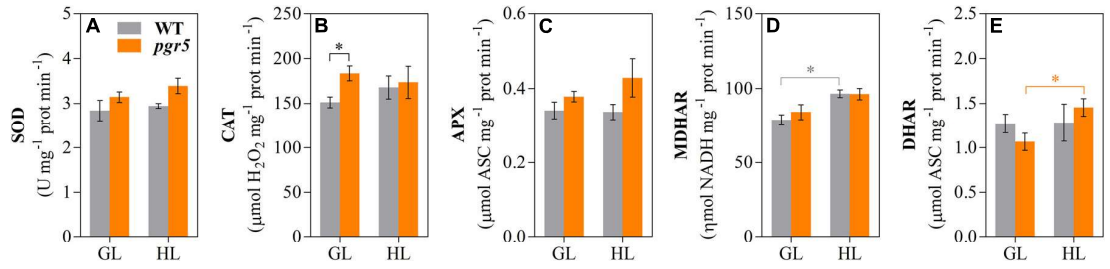

FIGURE 5 | Activities of Foyer–Halliwell–Asada cycle enzymes. Activities of superoxide dismutase (SOD, **A**); catalase (CAT, **B**); ascorbate peroxidase (APX, **C**); monodehydroascorbate reductase (MDHAR, **D**) and dehydroascorbate reductase (DHAR, **E**) were measured in total leaf extracts of WT and *pgr5* mutants treated with growth light (GL; 125 μmol m^{-2} s^{-1}) or high light (HL; 1,000 μmol m^{-2} s^{-1}) for 1 h. Activities are normalized to protein content. Error bars show standard error among replicates (n = 4). Significant differences between treatments and genotypes are indicated by asterisks (Student's t-test, $p < 0.05$).

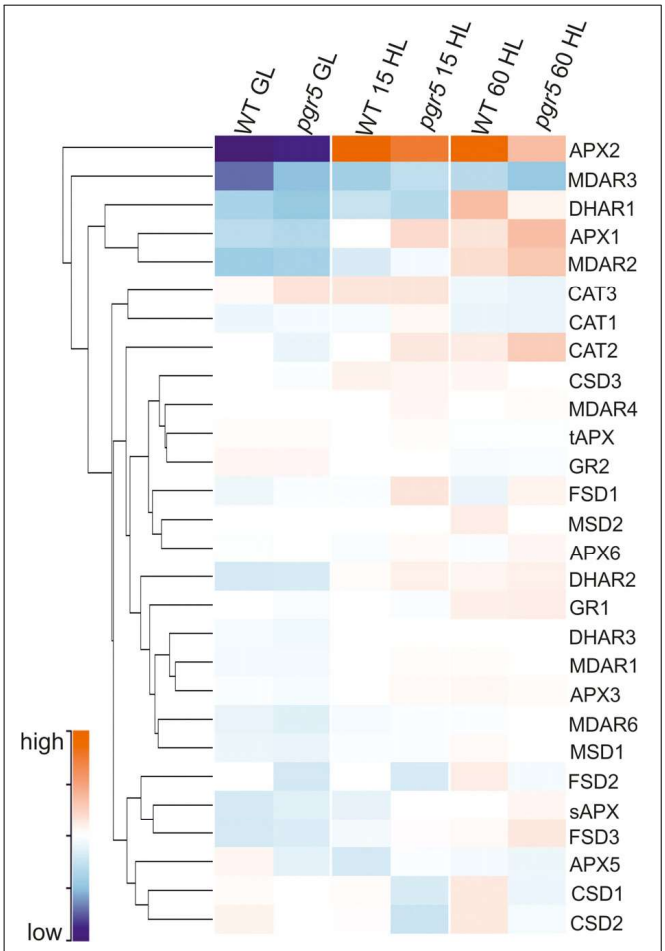

FIGURE 6 | Clustered heatmap showing normalized abundance of transcripts encoding enzymes in the Foyer–Halliwell–Asada cycle. Samples show gene expression in WT and *pgr5* mutant plants under growth light (GL; 125 μmol m^{-2} s^{-1}) and after 15 and 60 min in high light (HL; 1,000 μmol m^{-2} s^{-1}). Color intensities indicate transcript abundance, according to the key. APX, ascorbate peroxidase; MDAR, monodehydroascorbate reductase; DHAR, dehydroascorbate reductase; CAT, catalase; CSD, Cu/Zn-superoxide dismutase; tAPX, thylakoidal ascorbate peroxidase; GR, glutathione reductase; FSD, Fe-superoxide dismutase; MSD, Mn-superoxide dismutase; sAPX, stromal ascorbate peroxidase.

scavengers cannot prevent PSI photoinhibition under conditions of donor/acceptor side imbalance (Sejima et al., 2014; Zivcak et al., 2015a,b; Takagi et al., 2016).

A slower rate of P_m decline in *pgr5* after 30 min in HL, and the eventual stabilization of P_m after 2 h (**Figure 1**), indicated progressive decrease in ROS-induced PSI inactivation induced by decreasing intensity of stromal over-reduction. Again, this could not be attributed to any improvement in stromal ROS scavenging in *pgr5* (**Figure 5**) and was also not associated with decreased abundance of ROS after 1 h HL (**Figure 4**). Instead, a slower rate of PSI inhibition was likely directly related to alleviation of electron pressure on stromal acceptors caused by inactivation of PSI electron transport (described in **Figure 8**). This observation highlights the protective nature of PSI photoinhibition against over-production of ROS in the chloroplast stroma, which has been previously suggested (Tikkanen and Aro, 2014). Furthermore, in the absence of adequate pH-dependent photosynthetic control, as in the *pgr5* mutant, the extent of PSI inhibition appears to correlate to the level of imbalance between PSI donor and acceptor sides, which was high during the initial stages of HL and diminished as PSI inhibition progressed. In this way, PSI photoinhibition can be seen to support PSI donor side regulation in preventing oversupply of reductants to the stromal acceptor side. The idea that PSI photoinhibition is sensitive to the extent of photosynthetic imbalance was also evident in the changes in CO_2 assimilation in *pgr5* during the HL treatments. A rapid rate of decline during the first 15 min of HL (**Figure 2**) corresponded with rapid PSI photoinhibition (**Figure 1A**), while slower decline during the latter part of the HL treatment correlated with a slower decrease in P_m during this phase of treatment. During the second HL treatment, rapid A decline was not observed in *pgr5* (**Figure 2**, 150–180 min), presumably because PSI inhibition from the previous HL exposure had effectively "pre-set" PSI activity to suit the capacity of stromal acceptors at 1,000 μmol photons m^{-2} s^{-1}.

Although PSI inhibition can protect against over-production of stromal ROS during conditions of insufficient stromal acceptor capacity, PSI damage is a major impediment to carbon metabolism under normal growth conditions (Gollan et al., 2017; Lima-Melo et al., 2019). In the current study, this was especially

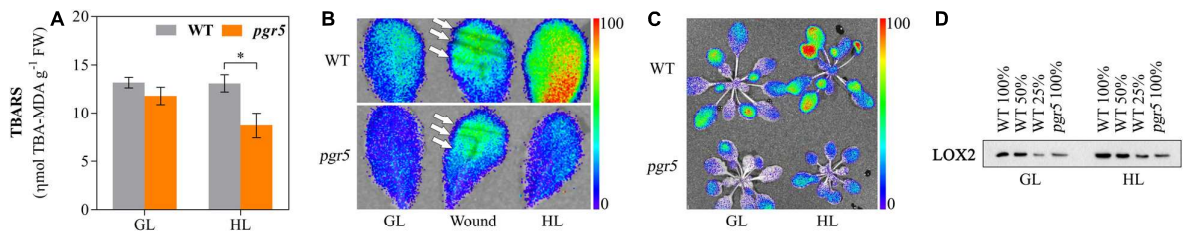

FIGURE 7 | Lipid oxidation in *pgr5* mutants after high light treatment. Content of thiobarbituric acid-reactive substances (TBARS; **A**), autoluminescence imaging **(B,C)**, and Western blotting detection of chloroplast lipoxygenase (LOX2) abundance **(D)** in WT and *pgr5* mutants treated with growth light (GL; 125 μmol m^{-2} s^{-1}) and high light (HL; 1,000 μmol m^{-2} s^{-1}) for 1 h. Luminescence intensities **(B,C)** correspond to color scales as shown. Luminescence images overlay photographs of the same leaf/rosette samples. Wounding of leaves is indicated by white arrows in **(B)**. Error bars show standard error among replicates (n = 4). Significant differences between treatments and genotypes are indicated by asterisks (Student's t-test, $p < 0.05$).

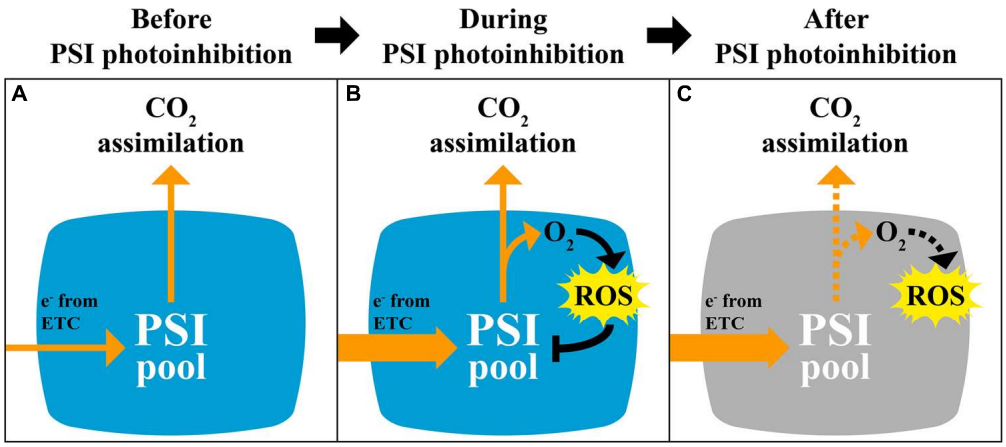

FIGURE 8 | Hypothetical scheme describing the mechanism and impact of PSI photoinhibition on CO_2 fixation and ROS production. **(A)** Under constant conditions, electron pressure at the donor and acceptor sides of PSI is balanced due to partially oxidized state of P700 and stromal electron carriers. Excess ROS production is minimal. **(B)** During the first minutes of electron imbalance between PSI donor and acceptor sides, such as during exposure of *pgr5* mutants to high light, or during low light and cold temperature (Sonoike and Terashima, 1994) or fluctuating light (Kono et al., 2014), limited stromal electron acceptor capacity leads to increased reduction of molecular oxygen. Increased ROS production leads to inactivation of PSI, presumably through oxidation of FeS clusters. **(C)** Partial inactivation of the PSI pool leads to decreased electron flow to the stroma, which limits the capacity for CO_2 fixation, especially under low light, and presumably decreases excess ROS production to protect downstream electron acceptors.

clear in the diminished CO_2 fixation in HL-treated *pgr5* plants under subsequent GL (**Figures 2**, **3A**). This phenomenon was not due to decreased availability of CO_2 in *pgr5* leaves, as internal CO_2 concentration (C_i) in *pgr5* plants was equivalent to WT levels, and higher in HL-treated *pgr5* plants. Instead, the light-dependent effect on *A* in PSI-inhibited plants reflects PSI quantum efficiency, where the highly reduced state of P700 under low light is exacerbated by PSI damage, while more $P700^+$ is formed under HL due to more active PSI electron transport, in combination with high light-activated electron transport regulation (Baker et al., 2007; Lima-Melo et al., 2019). Despite the positive effects of HL, CO_2 assimilation rates in PSI-inhibited plants remained lower than WT controls during the second HL treatment (**Figure 2**). Considering these results, we expect that the generation of $O_2^{\bullet-}$ during a subsequent HL treatment would also have been diminished in plants with inhibited PSI, although this was not specifically tested. Slightly higher stomatal conductance (g_s) in *pgr5* mutants compared to WT under GL correlated with higher transpiration rates (*E*) in the mutant under GL, while lower water use efficiency (WUE) in HL-treated *pgr5* reflected low levels of CO_2 fixation (**Figure 3**). Abnormal gas exchange in *pgr5* leaves may be related to the influence of plastoquinone (PQ) reduction state on stomatal opening and regulation of WUE in response to light (Busch, 2014; Głowacka et al., 2018), given that over-reduction of the PQ pool has been demonstrated in *pgr5* mutants, especially after HL-treatment (Nandha et al., 2007; Munekage et al., 2008; Suorsa et al., 2012; Kono et al., 2014; Gollan et al., 2017; Lima-Melo et al., 2019).

Decreased production $O_2^{\bullet-}$ and H_2O_2, generated from O_2 reduction and $O_2^{\bullet-}$ dismutation, respectively, was previously observed in *pgr5* mutant seedlings exposed to fluctuating light stress (Suorsa et al., 2012). In addition, H_2O_2-related gene expression was negatively affected in HL-stressed *pgr5* plants (Gollan et al., 2017). These results were attributed to increased antioxidant capacity in *pgr5* (Suorsa et al., 2012) and/or decreased O_2 reduction by inactivated PSI (Gollan et al., 2017). However, results of the current study demonstrated that ROS accumulation and oxidative stress after severe PSI photoinhibition was not substantially different from HL-stressed leaves with functional PSI, despite oxidative damage that was seen to occur in both genotypes by increases in electrolyte leakage after HL treatment (**Figure 4A**). Our results showing no apparent over-accumulation of H_2O_2 or $O_2^{\bullet-}$ in HL-treated *pgr5* leaves, compared to WT, may differ from previous results because we measured ROS levels after completion of HL treatments, rather than assaying accumulation of ROS during stress treatments (Suorsa et al., 2012). It is likely that foliar $O_2^{\bullet-}$ and H_2O_2 contents did increase during the first minutes under HL in both WT and *pgr5* plants, but were returned to basal levels during the 1 h treatment, as has been previously demonstrated (Galvez-Valdivieso et al., 2009; König et al., 2018). Efficient H_2O_2 scavenging during HL relies on the activity of the Foyer–Halliwell–Asada cycle for redox turnover of ascorbate and GSH (reviewed in Foyer and Shigeoka, 2011), which appeared to function normally in HL-treated *pgr5* plants according to similar transcript levels and activities of enzymes of the cycle (**Figures 5**, **6**). An exception was DHAR, which showed increased total activity in HL-treated *pgr5* leaves, despite the expression of the mitochondrial DHAR1 isoform being significantly down-regulated in this condition. DHAR converts DHA to ascorbate using electrons from the reduced form of GSH, suggesting a higher accumulation of DHA in *pgr5* during HL stress. Similarly, expression of APX2 was significantly down-regulated in *pgr5* after HL treatment, as previously reported (Gollan et al., 2017). Induction of Arabidopsis APX2 expression is dependent on the occurrence of photosynthetic electron transport (Karpiński et al., 1997, 1999; Chang et al., 2004; Galvez-Valdivieso et al., 2009),

which is lower in the case of severe PSI photoinhibition. Interestingly, the total activity of catalase (CAT) in *pgr5* leaves was higher under non-stress conditions than in WT leaves, correlating with increased expression of peroxisomal CAT3 in these conditions.

PSI photoinhibition in *pgr5* plants appeared to have a substantial negative effect on lipid oxidation, as measured by quantification of TBARS content and autoluminescence of leaves and rosettes. We previously detected no difference in lipid oxidation between WT and *pgr5* plants that were treated with severe high light stress that also caused chlorophyll bleaching in affected leaves of both genotypes (Gollan et al., 2017). In the current study, exposure to 1,000 μmol photons m^{-2} s^{-1} for 1 h did not bleach leaves, and this treatment revealed substantially lower levels of lipid oxidation in *pgr5* in comparison to WT. Lipid peroxides can be formed in the chloroplast either non-enzymatically, through the reaction between singlet oxygen ($^1O_2$) and unsaturated lipids (reviewed in Laloi and Havaux, 2015), or enzymatically through the activity of lipoxygenase (LOX) enzymes (reviewed in Wasternack and Hause, 2013). Non-enzymatic lipid peroxidation is associated with $^1O_2$ formation in PSII, especially under conditions of PSII over-reduction (Triantaphylidès et al., 2008). PSI photoinhibition is known to increase excitation pressure on PSII (Suorsa et al., 2012; Kono et al., 2014; Lima-Melo et al., 2019), suggesting that higher non-enzymatic lipid oxidation may be expected in HL-treated *pgr5*. On the contrary, decreases in HL-induced lipid oxidation observed in *pgr5* likely relate to the low abundance of chloroplast-localized lipoxygenase LOX2, which was evident in both GL- and HL-treated plants (**Figure 7C**). Down-regulation of LOX2 suggests disrupted chloroplast signaling in *pgr5*, which is in line with our previous detection of decreased oxylipin signaling in PSI-photoinhibited *pgr5* (Gollan et al., 2017). Indeed, LOX gene expression is induced by oxylipins (Porta et al., 2008; Sarde et al., 2018), while lipid peroxidation is an early step in enzymatic oxylipin synthesis (Wasternack and Hause, 2013), making it difficult to distinguish the cause of low lipid oxidation from the effect in this case. Equivalent luminescence signals were detected in both WT and *pgr5* after physical wounding of leaves (**Figure 7B**), indicating that wound-responsive lipid oxidation pathways were operational in *pgr5* plants.

CONCLUSION

This study shows that PSI photoinhibition is rapidly induced under conditions of imbalanced reduction pressure between PSI donor and acceptor sides, and that PSI photoinhibition is not associated with increases in HL-induced ROS accumulation at the whole leaf level. It should be noted that the donor/acceptor side imbalance in *pgr5* under HL is more severe than that induced by natural conditions like low temperatures or fluctuating light (Terashima et al., 1994; Kono et al., 2014; Lima-Melo et al., 2019). Therefore the extent, and probably the mechanism, of PSI photoinhibition in the *pgr5* system can be considered overly severe. Nonetheless, the current results can improve our understanding of PSI inhibition induced by natural stresses, while also underscoring the importance of PGR5-dependent protection of PSI. We present the notion that PSI inactivation prevents ROS over-production and oxidative stress in the chloroplast stroma and in the wider cell. This resembles the protective effect of PSII photodamage that prevents over-reduction of downstream components (Tikkanen et al., 2014; Huang et al., 2016), except that damaged PSII is replenished far more efficiently than damaged PSI (Aro et al., 1993; Scheller and Haldrup, 2005). In light of its slow recovery, PSI protection is often considered to be the main target of photosynthetic regulation mechanisms (Tikkanen et al., 2012; Larosa et al., 2018); however, the current work suggests that PSI is also expendable in the effort to mitigate stromal over-reduction. Considering our recent findings that a partially inhibited PSI pool can support normal CO_2 metabolism (Lima-Melo et al., 2019), inactivation of PSI may be more affordable than commonly thought.

DATA AVAILABILITY

The raw data supporting the conclusions of this manuscript will be made available by the authors, without undue reservation, to any qualified researcher.

AUTHOR CONTRIBUTIONS

YL-M, E-MA, and PG devised the work. YL-M, VA, AL, RS, and PG conducted the experiments. YL-M, MT, E-MA, JS, and PG analyzed the data. YL-M, E-MA, JS, and PG wrote the manuscript.

FUNDING

The authors acknowledge financial support from: CAPES (project BEX10758/14-3, YL-M); CIMO (project TM-16-10130, E-MA); CNPq (Proc. 154471/2018-6, AL; INCT Plant Stress Biotech, Proc. 465480/2014-4, JS); FCT-Portugal/FUNCAP-Brazil (FUNCAP – FCT AAC No. 02/SAICT/2017, JS); and Academy of Finland (projects 26080341, PG; and 307335 and 303757, E-MA).

REFERENCES

Apel, K., and Hirt, H. (2004). Reactive oxygen species: metabolism, oxidative stress, and signal transduction. *Annu. Rev. Plant Biol.* 55, 373–399. doi: 10.1146/annurev.arplant.55.031903.141701

Aro, E. M., Virgin, I., and Andersson, B. (1993). Photoinhibition of photosystem II. Inactivation, protein damage and turnover. *Biochim. Biophys. Acta* 1143, 113–134. doi: 10.1016/0005-2728(93)90134-2

Asada, K. (1999). The water-water cycle in chloroplasts: scavenging of active oxygens and dissipation of excess photons. *Annu. Rev. Plant Physiol. Plant Mol. Biol.* 50, 601–639. doi: 10.1146/annurev.arplant.50.1.601

Baker, N. R., Harbinson, J., and Kramer, D. M. (2007). Determining the limitations and regulation of photosynthetic energy transduction in leaves. *Plant Cell Environ.* 30, 1107–1125. doi: 10.1111/j.1365-3040.2007.01680.x

Barth, C., Krause, G. H., and Winter, K. (2001). Responses of photosystem I compared with photosystem II to high-light stress in tropical shade and sun leaves. *Plant Cell Environ.* 24, 163–176. doi: 10.1046/j.1365-3040.2001.00673.x

Beers, R. F., and Sizer, I. W. (1952). A spectrophotometric method for measuring the breakdown of hydrogen peroxide by catalase. *J. Biol. Chem.* 195, 133–140.

Birtic, S., Ksas, B., Genty, B., Mueller, M. J., Triantaphylidès, C., and Havaux, M. (2011). Using spontaneous photon emission to image lipid oxidation patterns in plant tissues. *Plant J.* 67, 1103–1115. doi: 10.1111/j.1365-313X.2011.04646.x

Blum, A., and Ebercon, A. (1981). Cell membrane stability as a measure of drought and heat tolerance in wheat. *Crop Sci.* 21, 43–47.

Bradford, M. M. (1976). A rapid and sensitive method for the quantification of microgram quantities of protein utilizing the principle of protein-dye binding. *Anal. Biochem.* 72, 248–254. doi: 10.1016/0003-2697(76)90527-3

Busch, F. A. (2014). Opinion: the red-light response of stomatal movement is sensed by the redox state of the photosynthetic electron transport chain. *Photosynth. Res.* 119, 131–140. doi: 10.1007/s11120-013-9805-6

Chang, C. C.-C., Ball, L., Fryer, M. J., Baker, N. R., Karpiński, S., and Mullineaux, P. M. (2004). Induction of ASCORBATE PEROXIDASE 2 expression in wounded Arabidopsis leaves does not involve known wound-signalling pathways but is associated with changes in photosynthesis. *Plant J.* 38, 499–511. doi: 10.1111/j.1365-313x.2004.02066.x

Czarnocka, W., and Karpiński, S. (2018). Friend or foe? Reactive oxygen species production, scavenging and signaling in plant response to environmental stresses. *Free Radic. Biol. Med.* 122, 4–20. doi: 10.1016/j.freeradbiomed.2018.01.011

de Souza, A., Wang, J.-Z., and Dehesh, K. (2017). Retrograde signals: integrators of interorganellar communication and orchestrators of plant development. *Annu. Rev. Plant Biol.* 68, 85–108. doi: 10.1146/annurev-arplant-042916-041007

Exposito-Rodriguez, M., Laissue, P. P., Yvon-Durocher, G., Smirnoff, N., and Mullineaux, P. M. (2017). Photosynthesis-dependent H2O2 transfer from chloroplasts to nuclei provides a high-light signalling mechanism. *Nat. Commun.* 8:49. doi: 10.1038/s41467-017-00074-w

Foyer, C. H., and Shigeoka, S. (2011). Understanding oxidative stress and antioxidant functions to enhance photosynthesis. *Plant Physiol.* 155, 93–100. doi: 10.1104/pp.110.166181

Galvez-Valdivieso, G., Fryer, M. J., Lawson, T., Slattery, K., Truman, W., Smirnoff, N., et al. (2009). The high light response in Arabidopsis involves ABA signaling between vascular and bundle sheath cells. *Plant Cell* 21, 2143–2162. doi: 10.1105/tpc.108.061507

Giannopolitis, C. N., and Reis, S. K. (1977). Superoxide dismutases. I. Occurrence in higher plants. *Plant Physiol.* 59, 309–314. doi: 10.1104/pp.59.2.309

Głowacka, K., Kromdijk, J., Kucera, K., Xie, J., Cavanagh, A. P., Leonelli, L., et al. (2018). Photosystem II subunit S overexpression increases the efficiency of water use in a field-grown crop. *Nat. Commun.* 9:868. doi: 10.1038/s41467-018-03231-x

Gollan, P. J., Lima-Melo, Y., Tiwari, A., and Tikkanen, M. (2017). Interaction between photosynthetic electron transport and chloroplast sinks triggers protection and signalling important for plant productivity. *Philos. Trans. R. Soc. B. Biol. Sci.* 372:20160390. doi: 10.1098/rstb.2016.0390

Gururani, M. A., Venkatesh, J., and Tran, L.-S. P. (2015). Regulation of photosynthesis during abiotic stress-induced photoinhibition. *Mol. Plant* 8, 1304–1320. doi: 10.1016/j.molp.2015.05.005

Havir, E. A., and McHale, N. A. (1987). Biochemical and developmental characterization of multiple forms of catalase in tobacco leaves. *Plant Physiol.* 84, 450–455. doi: 10.1104/pp.84.2.450

Heath, R. L., and Packer, L. (1968). Photoperoxidation in isolated chloroplasts. I. Kinects and stoichiometry of fatty acid peroxidation. *Arch. Biochem. Biophys.* 125, 189–198. doi: 10.1016/0003-9861(68)90654-1

Hossain, M. A., Nakano, Y., and Asada, K. (1984). Monodehydroascorbate reductase in spinach chloroplasts and its participation in regeneration of ascorbate for scavenging hydrogen peroxide. *Plant Cell Physiol.* 25, 385–395.

Huang, W., Yang, Y.-J., Hu, H., and Zhang, S.-B. (2016). Moderate photoinhibition of photosystem II protects photosystem I from photodamage at chilling stress in tobacco leaves. *Front. Plant Sci.* 7:182. doi: 10.3389/fpls.2016.00182

Huang, W., Zhang, S.-B., and Cao, K.-F. (2010). The different effects of chilling stress under moderate light intensity on photosystem II compared with photosystem I and subsequent recovery in tropical tree species. *Photosynth. Res.* 103, 175–182. doi: 10.1007/s11120-010-9539-7

Inoue, K., Sakurai, H., and Hiyama, T. (1986). Photoinactivation sites of photosystem I in isolated chloroplasts. *Plant Cell Physiol.* 27, 961–968.

Ivanov, A. G., Morgan, R. M., Gray, G. R., Velitchkova, M. Y., and Huner, N. P. A. (1998). Temperature/light dependent development of selective resistance to photoinhibition of photosystem I. *FEBS Lett.* 430, 288–292. doi: 10.1016/s0014-5793(98)00681-4

Ivanov, A. G., Rosso, D., Savitch, L. V., Stachula, P., Rosembert, M., Oquist, G., et al. (2012). Implications of alternative electron sinks in increased resistance of PSII and PSI photochemistry to high light stress in cold-acclimated *Arabidopsis thaliana*. *Photosynth. Res.* 113, 191–206. doi: 10.1007/s11120-012-9769-y

Karpiński, S., Escobar, C., Kaspinska, B., Creissen, G., and Mullineaux, P. M. (1997). Photosynthetic electron transport regulates the expression of cytosolic ascorbate peroxidase genes in Arabidopsis during excess light stress. *Plant Cell* 9, 627–640. doi: 10.1105/tpc.9.4.627

Karpiński, S., Reynolds, H., Karpinska, B., Wingsle, G., Creissen, G., and Mullineaux, P. (1999). Systemic signaling and acclimation in response to excess excitation energy in Arabidopsis. *Science* 284, 654–657. doi: 10.1126/science.284.5414.654

Kato, Y., Sun, X., Zhang, L., and Sakamoto, W. (2012). Cooperative D1 degradation in the photosystem II repair mediated by chloroplastic proteases in arabidopsis. *Plant Physiol.* 159, 1428–1439. doi: 10.1104/pp.112.199042

Klughammer, C., and Schreiber, U. (1998). "Measuring P700 absorbance changes in the near infrared spectral region with a dual wavelength pulse modulation system," in *Photosynth. Mech. Eff*, ed. G. Garab (Dordrecht: Springer), 4357–4360. doi: 10.1007/978-94-011-3953-3_1008

König, K., Vaseghi, M. J., Dreyer, A., and Dietz, K. J. (2018). The significance of glutathione and ascorbate in modulating the retrograde high light response in *Arabidopsis thaliana* leaves. *Physiol. Plant* 162, 262–273. doi: 10.1111/ppl.12644

Kono, M., Noguchi, K., and Terashima, I. (2014). Roles of the cyclic electron flow around PSI (CEF-PSI) and O2-dependent alternative pathways in regulation of the photosynthetic electron flow in short-term fluctuating light in *Arabidopsis thaliana*.pdf. *Plant Cell Physiol.* 55, 990–1004. doi: 10.1093/pcp/pcu033

Kudoh, H., and Sonoike, K. (2002). Irreversible damage to photosystem I by chilling in the light: cause of the degradation of chlorophyll after returning to normal growth temperature. *Planta* 215, 541–548. doi: 10.1007/s00425-002-0790-9

Laloi, C., and Havaux, M. (2015). Key players of singlet oxygen-induced cell death in plants. *Front. Plant Sci.* 6:39. doi: 10.3389/fpls.2015.00039

Larosa, V., Meneghesso, A., La Rocca, N., Steinbeck, J., Hippler, M., and Szabò, I. (2018). Mitochondria affects photosynthetic electron transport and photosensitivity in a green alga. *Plant Physiol.* 176, 2305–2314. doi: 10.1104/pp.17.01249

Li, L., Aro, E.-M., and Millar, A. H. (2018). Mechanisms of photodamage and protein turnover in photoinhibition. *Trends Plant Sci.* 23, 667–676. doi: 10.1016/j.tplants.2018.05.004

Lima-Melo, Y., Gollan, P. J., Tikkanen, M., Silveira, J. A. G., and Aro, E.-M. (2019). Consequences of photosystem-I damage and repair on photosynthesis and carbon use in *Arabidopsis thaliana*. *Plant J.* 97, 1061–1072. doi: 10.1111/tpj.14177

López, M. A., Vicente, J., Kulasekaran, S., Vellosillo, T., Martínez, M., Irigoyen, M. L., et al. (2011). Antagonistic role of 9-lipoxygenase-derived oxylipins and ethylene in the control of oxidative stress, lipid peroxidation and plant defence. *Plant J.* 67, 447–458. doi: 10.1111/j.1365-313X.2011.04608.x

McCord, J. M. (2000). The evolution of free radicals and oxidative stress. *Am. J. Med.* 108, 652–659.

Mittler, R. (2017). ROS are good. *Trends Plant Sci.* 22, 11–19. doi: 10.1016/j.tplants.2016.08.002

Mosblech, A., Feussner, I., and Heilmann, I. (2009). Oxylipins: structurally diverse metabolites from fatty acid oxidation. *Plant Physiol. Biochem.* 47, 511–517. doi: 10.1016/j.plaphy.2008.12.011

Mueller, S., Hilbert, B., Dueckershoff, K., Roitsch, T., Krischke, M., and Mueller, M. J. (2008). General detoxification and stress responses are mediated by oxidized lipids through TGA transcription factors in Arabidopsis. *Plant Cell* 20, 768–785. doi: 10.1105/tpc.107.054809

Mullineaux, P. M., Exposito-Rodriguez, M., Laissue, P. P., and Smirnoff, N. (2018). ROS-dependent signalling pathways in plants and algae exposed to high light: comparisons with other eukaryotes. *Free Radic. Biol. Med.* 122, 52–64. doi: 10.1016/j.freeradbiomed.2018.01.033

Munekage, Y., Hojo, M., Meurer, J., Endo, T., Tasaka, M., and Shikanai, T. (2002). PGR5 is involved in cyclic electron flow around photosystem I and is essential for photoprotection in Arabidopsis. *Cell* 110, 361–371. doi: 10.1016/s0092-8674(02)00867-x

Munekage, Y. N., Genty, B., and Peltier, G. (2008). Effect of PGR5 impairment on photosynthesis and growth in *Arabidopsis thaliana*. *Plant Cell Physiol.* 49, 1688–1698. doi: 10.1093/pcp/pcn140

Munns, R. (2005). Genes and salt tolerance: bringing them together. *New Phytol.* 167, 645–663. doi: 10.1111/j.1469-8137.2005.01487.x

Nakano, Y., and Asada, K. (1981). Hydrogen peroxide is scavenged by ascorbate-specific peroxidase in spinach chloroplasts. *Plant Cell Physiol.* 22, 867–880.

Nandha, B., Finazzi, G., Joliot, P., Hald, S., and Johnson, G. N. (2007). The role of PGR5 in the redox poising of photosynthetic electron transport. *Biochim. Biophys. Acta* 1767, 1252–1259. doi: 10.1016/j.bbabio.2007.07.007

Noctor, G., Reichheld, J. P., and Foyer, C. H. (2018). ROS-related redox regulation and signaling in plants. *Semin. Cell Dev. Biol.* 80, 3–12. doi: 10.1016/j.semcdb.2017.07.013

Ogawa, K., Kanematsu, S., and Asada, K. (1997). Generation of superoxide anion and localization of CuZn-superoxide dismutase in the vascular tissue of spinach hypocotyls: their association with lignification. *Plant Cell Physiol.* 38, 1118–1126. doi: 10.1093/oxfordjournals.pcp.a029096

Porta, H., Figueroa-Balderas, R. E., and Rocha-Sosa, M. (2008). Wounding and pathogen infection induce a chloroplast-targeted lipoxygenase in the common bean (*Phaseolus vulgaris* L.). *Planta* 227, 363–373. doi: 10.1007/s00425-007-0623-y

Ramel, F., Birtic, S., Ginies, C., Soubigou-Taconnat, L., Triantaphylidès, C., and Havaux, M. (2012). Carotenoid oxidation products are stress signals that mediate gene responses to singlet oxygen in plants. *Proc. Natl. Acad. Sci. U.S.A.* 109, 5535–5540. doi: 10.1073/pnas.1115982109

Sarde, S. J., Kumar, A., Remme, R. N., and Dicke, M. (2018). Genome-wide identification, classification and expression of lipoxygenase gene family in pepper. *Plant Mol. Biol.* 98, 375–387. doi: 10.1007/s11103-018-0785-y

Satoh, M., Tokaji, Y., Nagano, A. J., Hara-Nishimura, I., Hayashi, M., Nishimura, M., et al. (2014). Arabidopsis mutants affecting oxylipin signaling in photo-oxidative stress responses. *Plant Physiol. Biochem.* 81, 90–95. doi: 10.1016/j.plaphy.2013.11.023

Scheller, H. V., and Haldrup, A. (2005). Photoinhibition of photosystem I. *Planta* 221, 5–8.

Schreiber, U., Bilger, W., and Neubauer, C. (1995). "Chlorophyll fluorescence as a nonintrusive indicator for rapid assessment of in vivo photosynthesis," in *Ecophysiology of Photosynthesis*, 1st Edn, eds E.-D. Schulze and M. M. Caldwell (Berlin: Springer-Verlag), 49–70. doi: 10.1007/978-3-642-79354-7_3

Sejima, T., Takagi, D., Fukayama, H., Makino, A., and Miyake, C. (2014). Repetitive short-pulse light mainly inactivates photosystem I in sunflower leaves. *Plant Cell Physiol.* 55, 1184–1193. doi: 10.1093/pcp/pcu061

Sharma, P., Jha, A. B., Dubey, R. S., and Pessarakli, M. (2012). Reactive oxygen species, oxidative damage, and antioxidative defense mechanism in plants under stressful conditions. *J. Bot.* 2012, 1–26. doi: 10.1016/j.plaphy.2016.05.038

Simkin, A. J., McAusland, L., Lawson, T., and Raines, C. A. (2017). Over-expression of the RieskeFeS protein increases electron transport rates and biomass yield. *Plant Physiol.* 175, 134–145. doi: 10.1104/pp.17.00622

Sonoike, K. (1995). Selective photoinhibition of photosystem I in isolated thylakoid membranes from cucumber and spinach. *Plant Cell Physiol.* 36, 825–830. doi: 10.1093/oxfordjournals.pcp.a078827

Sonoike, K. (2011). Photoinhibition of photosystem I. *Physiol. Plant* 142, 56–64. doi: 10.1111/j.1399-3054.2010.01437.x

Sonoike, K., and Terashima, I. (1994). Mechanism of photosystem-I photoinhibition in leaves of *Cucumis sativus* L. *Planta* 194, 287–293. doi: 10.1007/bf01101690

Souza, P. V. L., Lima-Melo, Y., Carvalho, F. E., Reichheld, J.-P., Fernie, A. R., Silveira, J. A. G., et al. (2018). Function and compensatory mechanisms among the components of the chloroplastic redox network. *Crit. Rev. Plant Sci.* 38, 1–28. doi: 10.1080/07352689.2018.1528409

Suorsa, M., Järvi, S., Grieco, M., Nurmi, M., Pietrzykowska, M., Rantala, M., et al. (2012). PROTON GRADIENT REGULATION5 is essential for proper acclimation of Arabidopsis photosystem I to naturally and artificially fluctuating light conditions. *Plant Cell* 24, 2934–2948. doi: 10.1105/tpc.112.097162

Takagi, D., Takumi, S., Hashiguchi, M., Sejima, T., and Miyake, C. (2016). Superoxide and singlet oxygen produced within the thylakoid membranes both cause photosystem I photoinhibition. *Plant Physiol.* 171, 1626–1634. doi: 10.1104/pp.16.00246

Takahashi, S., and Murata, N. (2008). How do environmental stresses accelerate photoinhibition? *Trends Plant Sci.* 13, 178–182. doi: 10.1016/j.tplants.2008.01.005

Terashima, I., Funayama, S., and Sonoike, K. (1994). The site of photoinhibition in leaves of *Cucumis sativus* L. At low temperatures is photosystem I, not photosystem II. *Planta* 193, 300–306.

Thordal-Christensen, H., Zhang, Z., Wei, Y., and Collinge, D. B. (1997). Subcellular localization of H2O2 in plants. H2O2 accumulation in papillae and hypersensitive response during the barley-powdery mildew interaction. *Plant J.* 11, 1187–1194. doi: 10.1046/j.1365-313x.1997.11061187.x

Tikkanen, M., and Aro, E.-M. (2014). Integrative regulatory network of plant thylakoid energy transduction. *Trends Plant Sci.* 19, 10–17. doi: 10.1016/j.tplants.2013.09.003

Tikkanen, M., Grieco, M., Nurmi, M., Rantala, M., Suorsa, M., and Aro, E.-M. (2012). Regulation of the photosynthetic apparatus under fluctuating growth light. *Philos. Trans. R. Soc. B Biol. Sci.* 367, 3486–3493. doi: 10.1098/rstb.2012.0067

Tikkanen, M., Mekala, N. R., and Aro, E.-M. (2014). Photosystem II photoinhibition-repair cycle protects photosystem I from irreversible damage. *Biochim. Biophys. Acta* 1837, 210–215. doi: 10.1016/j.bbabio.2013.10.001

Tiwari, A., Mamedov, F., Grieco, M., Suorsa, M., Jajoo, A., Styring, S., et al. (2016). Photodamage of iron-sulphur clusters in photosystem I induces non-photochemical energy dissipation. *Nat. Plants* 2:16035. doi: 10.1038/nplants.2016.35

Tjus, S. E., Møller, B. L., and Scheller, H. V. (1998). Photosystem I is an early target of photoinhibition in barley illuminated at chilling temperatures. *Plant Physiol.* 116, 755–764. doi: 10.1104/pp.116.2.755

Triantaphylidès, C., Krischke, M., Hoeberichts, F. A., Ksas, B., Gresser, G., Havaux, M., et al. (2008). Singlet oxygen is the major reactive oxygen species involved in photooxidative damage to plants. *Plant Physiol.* 148, 960–968. doi: 10.1104/pp.108.125690

Wasternack, C., and Hause, B. (2013). Jasmonates: biosynthesis, perception, signal transduction and action in plant stress response, growth and development. An update to the 2007 review in Annals of Botany. *Ann. Bot.* 111, 1021–1058. doi: 10.1093/aob/mct067

Yamamoto, H., and Shikanai, T. (2019). PGR5-dependent cyclic electron flow protects photosystem I under fluctuating light at donor and acceptor sides. *Plant Physiol.* 179, 588–600. doi: 10.1104/pp.18.01343

Yamori, W. (2016). Photosynthetic response to fluctuating environments and photoprotective strategies under abiotic stress. *J. Plant Res.* 129, 379–395. doi: 10.1007/s10265-016-0816-1

Zhang, S., and Scheller, H. V. (2004). Photoinhibition of photosystem I at chilling temperature and subsequent recovery in *Arabidopsis thaliana*. *Plant Cell Physiol.* 45, 1595–1602. doi: 10.1093/pcp/pch180

Zhou, M., Diwu, Z., Panchuk-Voloshina, N., and Haugland, R. P. (1997). A stable nonfluorescent derivative of resorufin for the fluorometric determination of trace hydrogen peroxide: applications in detecting the activity of phagocyte

NADPH oxidase and other oxidases. *Anal. Biochem.* 253, 162–168. doi: 10.1006/abio.1997.2391

Zivcak, M., Brestic, M., Kunderlikova, K., Olsovska, K., and Allakhverdiev, S. I. (2015a). Effect of photosystem I inactivation on chlorophyll a fluorescence induction in wheat leaves: does activity of photosystem I play any role in OJIP rise? *J. Photochem. Photobiol. B Biol.* 152, 318–324. doi: 10.1016/j.jphotobiol.2015.08.024

Zivcak, M., Brestic, M., Kunderlikova, K., Sytar, O., and Allakhverdiev, S. I. (2015b). Repetitive light pulse-induced photoinhibition of photosystem I severely affects CO2 assimilation and photoprotection in wheat leaves. *Photosynth. Res.* 126, 449–463. doi: 10.1007/s11120-015-0121-1

Conflict of Interest Statement: The authors declare that the research was conducted in the absence of any commercial or financial relationships that could be construed as a potential conflict of interest.